DNA damage checkpoint pathways and the maintenance of genome stability in *C. elegans*

Dissertation
der Fakultät für Biologie
der Ludwig-Maximilians-Universität
München

vorgelegt von

Arno Alpi

München 2004

1. Gutachter: Prof. Erich Nigg

2. Gutachter: Prof. Charles David

Tag der mündlichen Prüfung: 11. Juni 2004-08-03

1. Table of content

1. Table of content ----------2
2. Statement ----------6
3. Abstract ----------7
4. List of Abbreviations ----------9
5. Introduction ---------- 11
5.1 DNA damage response pathways ---------- 11
5.2 Why using *C. elegans* for studying DNA damage response? ---------- 16
5.3 The *C. elegans* germ line ---------- 17
5.4 Genetic analysis of programmed cell death in *C. elegans* ---------- 19
5.5 Studying DNA damage response in *C. elegans* ---------- 22
6. Aim of the thesis ---------- 25
6.1 DNA damage checkpoint genes and genome integrity in *C. elegans* ---------- 25
7. Results and Discussion ---------- 28
***7.1* "*C. elegans* RAD-5/CLK-2 defines a new DNA damage checkpoint protein" 28**
7.1.1 Introduction ---------- 28
7.1.2.1 Results ---------- 31
7.1.2.1 *rad-5(mn159)* is allelic to *clk-2(qm37)* ---------- 31
7.1.2 2 *clk-2* is the only clock gene required for the DNA damage checkpoint ----- 34
7.1.2.3 Epistasis between *rad-5/clk-2* and other checkpoint mutants ---------- 35
7.1.2.4 *rad-5/clk-2* mutants are defective for the S-phase replication checkpoint -- 40
7.1.2.6 Telomere behaviour in *C. elegans* DNA damage checkpoint mutants **Fehler! Textmarke nicht definiert.**
7.1.2.7 Checkpoint phenotypes of S. cerevisiae *TEL-2* ---------- 47
7.1.3 Discussion ---------- 47
7.1.4 Analysis of the essential function of *rad-5/clk-2* ---------- 52
7.1.4.1 Lineage defect in *rad-5/clk-2* mutants at restrictive temperature ---------- 52
7.1.4.3 Accumulation of RAD-51 foci in mitotic germ cells of *rad-5/clk-2* mutants57
7.1.5 Analysis of the molecular function of RAD-5/CLK-2 ---------- 60
7.1.5.1. *cdc-7(RNAi)* causes synthetic lethality in *rad-5/clk-2* mutants ---------- 61
7.1.6 Future perspective ---------- 66

7.2. "Genetic and cytological characterization of the recombination protein RAD-51 in *Caenorhabditis elegans*" ---------- 69
7.2.1 Introduction ---------- 69
7.2.2 Results ---------- 73
7.2.2.2 Phenotypic analysis of the *rad-51* mutant ---------- 73
7.2.2.3 Meiosis in a *rad-51* mutant ---------- 75
7.2.2.4 Immunolocalization of RAD-51 in meiotic cells of wild-type and mutant worms ---------- 78
7.2.3 Discussion ---------- **Fehler! Textmarke nicht definiert.**
7.3 "Multiple genetic pathways involving the *C. elegans* Bloom's syndrome gene *him-6, mre-11, rad-51* and *top-3* are needed to maintain genome stability in the germ line." ---------- 93
7.3.1 Introduction ---------- 93
7.3.2 Results ---------- 96
7.3.2.1 *him-6* encodes the *C. elegans* homolog of the human Bloom's syndrome protein ---------- 96
7.3.2.2 *him-6* is required for normal levels of recombination during meiosis ------- 99
7.3.2.3 *him-6* has defects in response to DNA damage ---------- 102
7.3.2.4 Combined depletion of HIM-6 and TOP-3 leads to mitotic catastrophe, which is suppressed by the loss-of-function of *rad-51* ---------- 105
7.3.2.5 *mre-11* acts downstream or in parallel of *rad-51* in the processing of double strand breaks ---------- 107
7.3.2.6 Topoisomerase IIIα also acts at a late stage of meiotic recombination ----- 109
7.3.3 Discussion ---------- 111
8. Materials and methods ---------- 120
8.1 Worm strains ---------- 120
8.2. DNA damage response assays ---------- 122
8.3 Determination of the telomere length ---------- 124
8.4 RNAi ---------- 124
8.5 Production of anti-RAD-51 antibodies ---------- 125
8.6 Cytology ---------- 126

8.7 Recombination analysis ----------129
8.8 *cdc-7(RNAi)* and *rad-5(RNAi)* ----------130
8.9 4D Microscopy ----------131
8.10 Far Western Blot ----------131
8.11 Yeast two-hybrid interaction ----------132
8.12 Cell cycle profiling ----------133
9. List of Publications ----------135
10. Curriculum Vitae ----------137
***Scientific Education* ----------137**
***Teaching activity:* ----------138**
***Meeting abstracts:* ----------138**
11. Acknowledge ----------140
12. Bibliography ----------141

2. Statement

I have written this thesis independently, without the help of others. The content of this thesis is mainly based on experiments I performed by myself, but also includes data which we published and which where done in close collaboration with other labs. Part 7.1 and 7.2 have been published recently (Ahmed et al., 2001; Alpi et al., 2003). For Part 7.1 slight modifications were made (were updates were available) and very recent experiments performed by myself were included. Content of Part 7.3 is based on experiments done in collaboration with Chantal Wicky and Fritz Müller, University Fribourg, Switzerland. I performed all of the immunofluorescence studies and the DNA damage assays. Part 5 contains sections that have been published in Gartner A, Alpi A, Schumacher B, "Programmed cell death in *C. elegans*" in Genetics of Apoptosis, Grimm S (ed.), BIOS Scientific Publishers Limited, 2003, 155-175.

3. Abstract

The germ line of the nematode *C. elegans* has been successfully used as a model system to study the cellular responses to genotoxic stress. Genotoxic stress induces DNA damage checkpoint signals that trigger mitotic germ cells to transiently halt cell cycle progression and that elicit apoptosis of meiotic germ cells.

As part of previous genetic studies on DNA damage response pathways in *C. elegans*, two allelic mutants *rad-5* and *clk-2* had been isolated. These mutantes are severely defective in radiation induced cell death and cell cycle arrest. *rad-5/clk-2* maps to a chromosome location where no obvious *C. elegans* homologue of a known checkpoint gene had been identified. We identified the corresponding *rad-5/clk-2* checkpoint gene by positional cloning. *rad-5/clk-2* is a novel, evolutionary conserved DNA damage checkpoint gene. The *S. cerevisiae* homologue RAD-5/CLK-2, Tel2p, is implicated in telomere length regulation. However, no significant alteration of telomeric length was observed in *rad-5/clk-2* mutants. Based on double mutant analysis we could show that *rad-5/clk-2* acts in a genetic pathway that is distinct from *S. pombe rad-1/C.e.mrt-2/S. pombe hus-1/C.e.hus-1* pathway. Furthermore, *rad-5/clk-2* is essential for early embryonic survival. We aimed to analyse the terminal phenotype of *rad-5/clk-2* temperature sensitive embryos shifted to the restrictive temperature and observed embryonic lethality as a consequence of a distinct lineage defect during early embryogenesis. In addition, *rad-5/clk*-2 loss of function led to an accumulation of RAD-51 foci, which mark sites of double stranded breaks in germ cell nuclei. This elevated number of DSB is indicative for genome instability. Taken together, *rad-5/clk-2*

represents a novel DNA damage checkpoint gene with an additional function for early embryogenesis.

As part of the second focus of my thesis we aimed to better understand the Bloom´s syndrome gene and therefore analysed the *C. elegans* orthologue of the *him-6/blm*. Bloom's syndrome is an autosomal recessive human disorder associated with loss of genome integrity. Mutations in *him-6/blm* resulted in enhanced radiation sensitivity and partially defective DNA damage checkpoints. Double and triple mutant analysis revealed that, in contrast to the situation in yeast, *him-6/blm* acts redundantly with *topoisomerase IIIα* and downstream of *rad-51* to maintain genome integrity in mitotically proliferating germ cells.

Furthermore, in the third part of my thesis we used the *C. elegans* germ line for the combined genetic and cytological analysis of the meiotic prophase, which includes the various stages of pairing of homologous chromosomes and meiotic recombination. We investigated the correlation and interdependence of homologous recombination and the various stages of chromosome pairing during meiosis. We could show that homologous pairing and the formation of the synaptonemal complex (SC, which is a proteinaceous complex that holds meiotic chromosomes in tight association) is independent of the recombination protein RAD-51. Furthermore, we could show that the formation of RAD-51 foci is dependent on the initial presynaptic alignment of meiotic chromosomes, whereas the proper removal of RAD-51 foci is dependent on the formation of the SC.

4. List of Abbreviations

C. elegans: Caenorhabditis elegans

ced: cell death abnormal

egl: egg lying defective

mrt: mortal germ line

hus: hydroxyurea sensitive

rad: radiation sensitive

him: high incidence of males

clk: clock

gro: growth defective

top. topo-isomerase

chk: checkpoint kinase

mre: meiotic recombination defective

RNAi: RNA interference

gf: gain of function

lf: loss of function

DSB: double strand break

HR: homologous recombination repair

NHEJ: non-homologous end joining

Gy: Gray

HU: hydroxyurea

MBP: maltose binding protein

GST: gluthathion S transferase

SC: synaptonemal complex

IR: ionising radiation

NLS: nuclear localisation sequence

DAPI: 4´,6-diamidino-2-phenylindole

FISH: fluorescence in situ hybridisation

5. Introduction

5.1 DNA damage response pathways

Several mechanisms have evolved to maintain genome stability during cell cycle progression (for review see (van Gent et al., 2001; Zhou and Elledge, 2000; Osborn et al., 2002)). One of the key processes in the cell cycle is the transmission of genetic information to the daughter cells. The accurate transmission of genetic information relies mainly on the high fidelity of DNA replication, and the precise separation and equal distribution of chromosomes to the daughter cells. Besides that, cells have to deal with a wide variety of spontaneous DNA damage (for instance caused by reactive oxidative species) and induced DNA damage (by exposure with UV and ionising irradiation, and genotoxic compounds). To achieve this high fidelity of transmitting genetic information, cells have evolved a complex regulatory network of so called DNA damage checkpoint pathways, which are activated in the presence of DNA lesions as they may occur during DNA replication. The presence of a DNA lesion has to be recognized by a sensor, which transmits a signal via a network of signal transduction pathways to a series of down-stream effectors molecules. Dependent on the origin of the DNA lesion, the cell type and the cell cycle stage, where the damage occurs, cells can respond to DNA lesions in different ways: (1) they trigger DNA repair to remove the damage (2) they transiently halt cell cycle progression or (3) if the damage is irreversible they induce cell death which leads to the removal of the harmed cell. Inherited or acquired deficiencies in DNA damage checkpoint pathways lead to genomic instability, which contributes significantly to the onset and progression of cancer.

DNA damage checkpoint pathways can be described as signal transduction pathways (or as a network of interacting pathways) consisting of sensors, transducers and effectors. Currently it is not exactly clear how DNA damage can be sensed. However a group of four conserved proteins are potential candidates for DNA damage sensors because they interact with DNA and they are essential for the activation of the DNA damage response pathways (reviewed in (O'Connell et al., 2000). In *S. pombe* three of them, Rad9, Hus1, and Rad1 form a heterotrimeric complex (9-1-1 complex) that shares homology with the sliding clamp protein proliferating cell nuclear antigen (PCNA). PCNA forms a ring wide enough to slide over double stranded DNA. In analogy to PCNA, it has been suggested that the 9-1-1 complex slides over DNA and continuously scans the genome for DNA damage (Figure 0-1). The fourth conserved checkpoint component is Rad17 (again using *S. pombe* nomenclature), which shares homology with subunits of the replication factor C (RFC). Rad17 acts upstream of the 9-1-1 complex and is thought to mediate the loading of the 1-1-9 complex onto DNA as it has been proposed for RFC that assembles PCNA on DNA (Figure 0-1). In addition, a repair complex is implicated in the sensing and signalling of DNA lesions. In *S. pombe* the repair complex Mre11-Rad50-Xrc2 (Human MRE11-RAD50-NBS1) is tethered to DNA ends of double strand breaks (Figure 0-1).

As part of an early DNA damage response two members of the large phosphatidylinositol-3-OH kinase family (PI3-K), *S. pombe Rad3/*hATR and *S. pombe Tel1/*hATM, are activated and recruited to sites of DNA damage (Figure 0-1). These DNA damage checkpoint kinase are thought to be the primary transducers of the DNA damage signal (reviewed in (Abraham, 2001)). In the presence of DNA damage PI3-K

are activated and trigger a signal transduction pathway by the phosphorylation of multiple DNA repair and DNA damage checkpoint proteins. Among these are the "downstream" protein kinases Cds1/hCHK2 and Chk1/hCHK1 (*S pombe*/human nomenclature) that

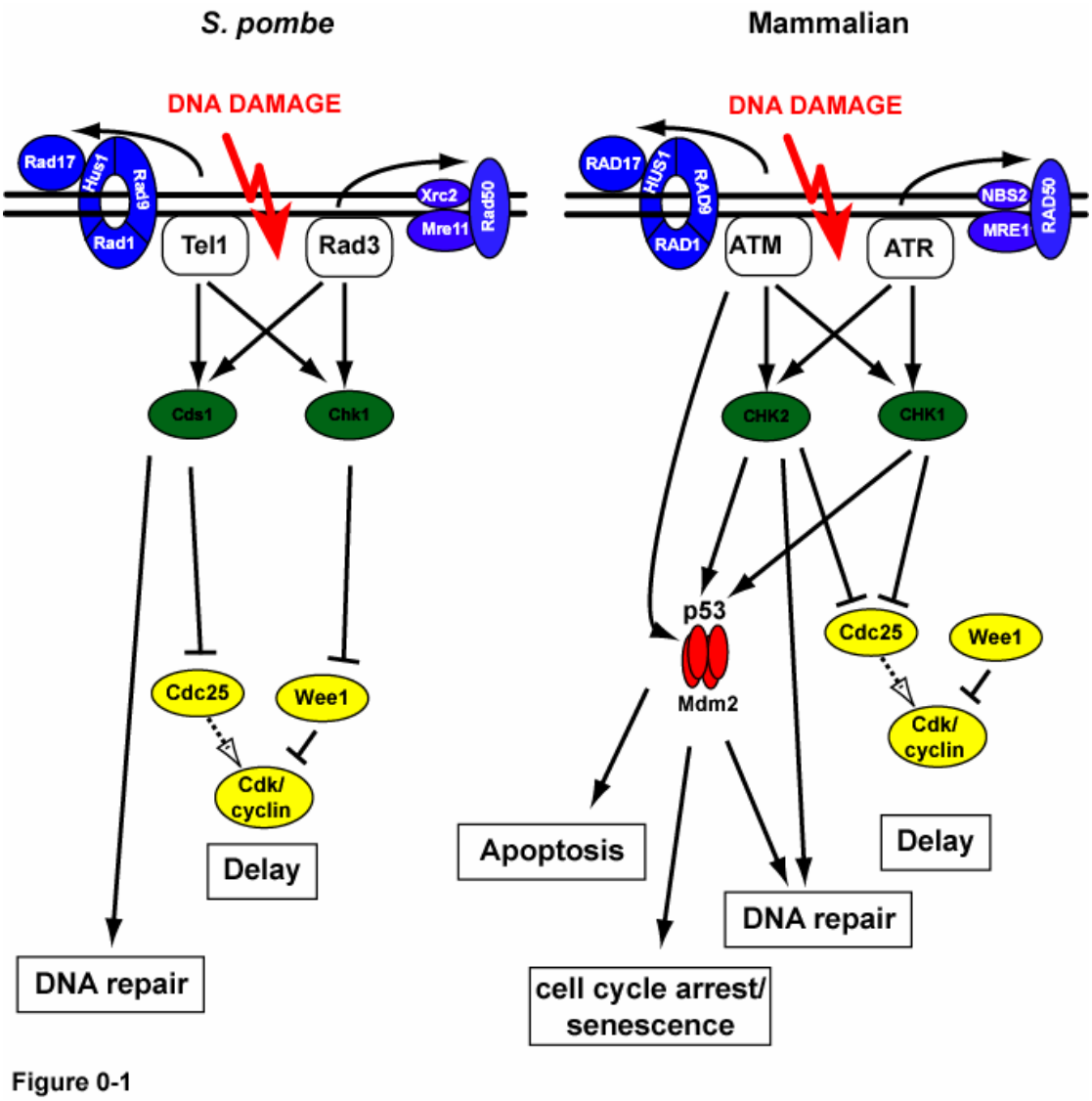

Figure 0-1

Figure 0-1 A schematic representation of the pathway in *S. pombe* and mammalian cells. See text for details.

influence cell cycle progression differently dependent on the point in the cell cycle where the damage occurs (Matsuoka et al., 1998; Brown et al., 1999; Chaturvedi et al., 1999). Cell cycle delay in response to DNA damage is mainly regulated by the maintenance of the inhibitory phosphorylation of Cdk kinases. Cdks have to be dephosphorylated by the phosphatase Cdc25 to be active and to trigger cell cycle progression (Nurse, 1997; Morgan, 1995). Upon DNA damage Cdc25 become inactivated. This inactivation is in part mediated by a Cds1/CHK2 and Chk1/CHK1 dependent phosphorylation of Cdc25 and its subsequent binding to 14-3-3 that lead to the retension of Cdc25 in the cytoplasm (Peng et al., 1997; Dalal et al., 1999; Yang et al., 1999). Beside a Cdc25 dependent cell cycle progression delay, mammalian cells induce a prolonged G1 arrest by the activity of the tumour suppressor protein p53 (Levine, 1997; Wahl et al., 1997). p53 is a sequence specific transcriptional regulator and induces the transcription of a variety of genes that are involved in cell cycle progression and apoptosis (Gottifredi et al., 2000). The transcriptional activity of p53 is mainly regulated by its turn over rate (reviewed in (Vogelstein et al., 2000; Kastan et al., 1991)). The ring-finger ubiquitin ligase MDM2 is one of the key regulators of p53 stability (Chen et al., 1994). MDM2 mediated polyubiquitination of p53 is required for the proteasome-dependent degradation of p53. In the presence of DNA damage p53 degradation is controlled by ATM/CHK2 dependent mechanisms that regulate the ability of MDM2 to bind to p53, and by mechanisms that regulate the ubiquitin ligase function of MDM2 (Maya et al., 2001). In addition, ATM phosphorylates p53 on Ser15 that interferes with MDM2 binding. Moreover, ATM activates CHK2 by phosphorylation (Matsuoka et al., 1998). Activated CHK2 in turn phosphorylates Ser20 on p53, which is within the MDM2 binding domain and therefore

directly interferes with MDM2/p53 association (Hirao et al., 2000). DNA damage checkpoint activation induces increased p53 stability that leads to a transcriptional upregulation of cell cycle progression inhibitors (e.g. p21) that act by inhibiting Cdk kinase activity. Beside the regulation of cell cycle progression, p53 is involved in the apoptotic response and induces the transcription of a variety of pro-apoptotic genes such as: BH3 only domain proteins like PUMA, and Noxa and the multidomain cell death trigger Bax (Rich et al., 2000; Yu et al., 2001).

Response to DNA damage is not limited to cell cycle delay or apoptosis, but further involves control of DNA repair. Most DNA repair pathways are constitutively active, but a number of regulatory connections between DNA damage response pathways and DNA repair have been described (reviewed in (Lee and Kim, 2002; D'Amours and Jackson, 2002b; Venkitaraman, 2002; Bartek et al., 2001). For example, the p48 gene, which is involved in nucleotide excision repair, is transcriptionally upregulated by p53 (Hwang et al., 1999). Another example of regulation of DNA repair comes from studies of the Nijmegen breakage syndrome gene (NBS). The NBS1 protein forms a complex with hMRE11 and hRAD50 (see above), that is implicated in both DNA double strand break repair pathways; non homologous end joining (NHEJ) and homologous recombination (HR) (Carney et al., 1998). ATM can directly phosphorylate NBS1 and phosphorylation is needed for its function within the repair hMRE11/hRAD50 complex (Gatei et al., 2000; Lim et al., 2000; Zhao et al., 2000). In addition, ATM and the NBS1/MRE11/RAD50 complex have been found in a large protein complex BASC that also contains the breast cancer susceptibility protein BRCA1 (Wang et al., 2000). Like NBS1, BRCA1 is a substrate for ATM dependent phosphorylation and it is required for

DNA double strand break repair (Moynahan et al., 1999). Taken together, DNA damage activates complex signal transduction pathways that trigger cell cycle delay, apoptosis, and DNA repair.

5.2 Why using *C. elegans* for studying DNA damage response?

Our present knowledge about DNA damage checkpoint pathways originates to a large extent from the genetic analysis of the unicellular model organisms *S. cerevisiae* and S. *pombe* (reviewed in (Weiss et al., 2000; Caspari et al., 2000b; Weinert et al., 2000; Rhind et al., 2000). Upon DNA damage, yeast cells respond with cell cycle arrest and repair of the DNA lesion. In metazoan animals DNA damage can lead to the induction of programmed cell death.

During the past years our knowledge about DNA damage induced apoptosis has been based on studies with human cell lines derived from patients with hereditary diseases effecting genomic stability (e.g.:Ataxia telangiectasia, Blooms syndrome, Li-Fraumeni syndrome, Xeroderma pigmentosum) (van Gent et al., 2001). In addition, mouse and chicken DT-40 knockout cell lines have further expanded our knowledge of DNA repair and checkpoint function in higher eukaryotes. However, the limited availability of genetic techniques to study these cell lines makes a more detailed genetic analysis that focuses on the interplay between different DNA damage responses hard to address. The availability of a suitable genetic model system might be very useful to dissect these various pathways and to identify their components. The nematode *Caenorhabditis elegans* is a powerful genetic system for the isolation and identification of novel genes by forward genetic screens. In particular, *C. elegans* was successfully used

to elucidate the genetics of the core apoptotic pathway (Hengartner and Horvitz, 1994b; Horvitz et al., 1994; Liu and Hengartner, 1999). Recently, it has been shown by my thesis advisor Anton Gartner that DNA damage induced checkpoint pathways can be studied in *C. elegans* (Gartner et al., 2000; Hofmann et al., 2000). The aim of my PhD thesis was to expand these studies, and to continue to use *C. elegans* as a model system for DNA damage induced cell death.

5.3 The *C. elegans* germ line

The DNA damage response in *C. elegans* is restricted to the female germ line which is the only proliferating tissue in the adult animal (Gartner et al., 2000). Therefore, the anatomy and cellular features of the hermaphrodite germ line will be described in more detail (see Figure 0-2). The germ line consists of two U-shaped tubes, which are channelled in a common uterus. All the mitotic and the early meiotic germ cells are in a syncytium, which is partially enclosed by a plasma membrane, but joined together by a common cytoplasmic core (Hall et al., 1999; Seydoux and Schedl, 2001). The distal tip cell (DTC) caps the distal-most end of the gonad arm and induces germ cells to proliferate mitotically (Berry et al., 1997). Germ cells move further proximally and out of the Notch signalling gradient that represses entry into meiosis. This section of the gonad is called the transition zone (TZ). In the TZ germ cells enter meiosis and their nuclei can be recognized as dense half-moon shaped chromatin structures after staining with the DNA dye 4´,6-diamidino-2-phenylindole (DAPI) (Seydoux and Schedl, 2001; Zetka and Rose, 1995a). Germ cell nuclei are preceding their proximal migration and go through all

stages of meiotic prophase. At the bend of the gonad mainly late pachytene nuclei are found (Seydoux and Schedl, 2001). Right after the bend oogenesis occurs which is characterized by a marked increase of the cell volume and the complete cellularisation. Mature oozytes arrest at diakinesis until they become fertilized when they slip through the spermateca.

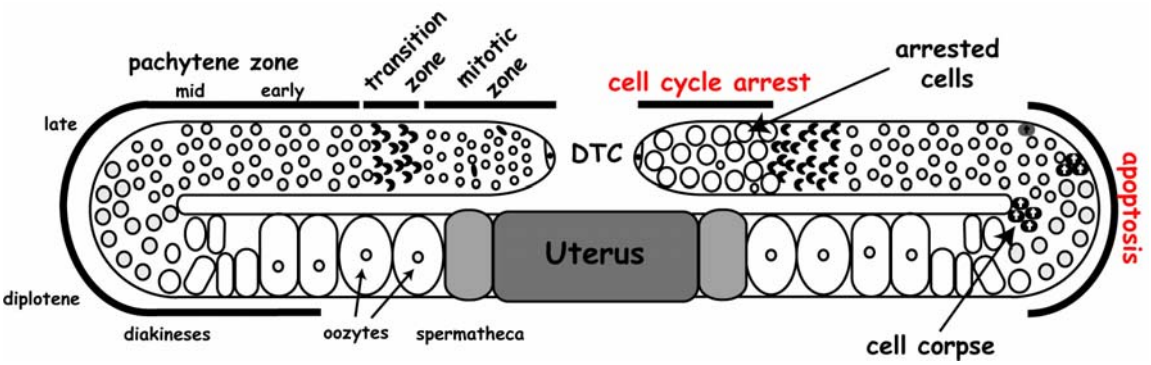

Figure 0-2 The *C. elegans* germ line: The gonad is organised in two U-shaped tubes, which are channelled in a common uterus. In the left gonad arm the different germ cell compartments are indicated. The localization of DNA damage induced responses is illustrated in the right gonad arm. Cell cycle arrest, which is indicated by enlarged germ cells, can be observed in the mitotic zone. The apoptotic response can be monitored near the gonad bend region where cell corpses appear as dense disk like structures.

Gumienny et al. first observed that programmed cell death in *C. elegans* occurs not only as part of invariant somatic development but also in the female germ line of the hermaphrodite worms (Gumienny et al., 1999). Using Nomarski optics, a steady state level of zero to four apoptotic cells can be observed in the bend region (germ cells in late pachytene, Figure 0-2) of the gonad arm (Gumienny et al., 1999). Germ cell death seems to be correlated with age as the number of cell corpse increases with the age of the worm.

As a consequence, under normal growth conditions about 50% of female germ cells (approximately 300 germ cells in total) are fated to die by programmed cell death. These apoptotic deaths are termed “physiological germ cell deaths” (Gumienny et al., 1999). The physiological function of this germ cell death is still elusive but a role in maintaining tissue homeostasis has been suggested.

5.4 Genetic analysis of programmed cell death in *C. elegans*

The genetics of apoptosis and the identification of primary components implicated in the cell death machinery have been mainly defined by studies done in *C. elegans*. Lineage analysis of embryonic and post-embryonic cell division patterns revealed that during somatic development of the hermaphrodite worm, 131 out of the total of 1090 cells, which are born, undergo programmed cell death (Kimble and Hirsh, 1979; Sulston and Horvitz, 1977; Sulston, 1983). Programmed cell death of somatic cells mostly occurs during embryonic development but also to a lesser extent, during the transition through the four larval stages (Kimble and Hirsh, 1979; Sulston and Horvitz, 1977; Sulston, 1983). Genetic analysis has led to the identification of over 100 different mutations that affect programmed cell death. These mutations define more than 15 genes that affect all programmed cell death and a small number of genes that are needed to commit specific cells to the apoptotic fate (Ellis and Horvitz, 1986; Ellis et al., 1991; Ellis and Horvitz, 1991; Hedgecock et al., 1983; Hengartner et al., 1992).

Apoptosis can be separated into four steps, each of which is defined by the analysis of various mutants. (1) Initially, specific cell types are committed to the

apoptotic fate. (2) Subsequently, the general apoptotic machinery, which is used in all dying cells, is activated. (3) Later, the recognition and engulfment of dying cells by neighbouring cell proceeds. (4) Finally, the remnants of engulfed cells are degraded. In several genetic screens four genes, *egl-1, ced-3, ced-4* and *ced-9* have been identified, which define a genetic pathway needed for almost all programmed cell deaths (Ellis and Horvitz, 1986; Hengartner et al., 1992; Conradt and Horvitz, 1998). All these *C. elegans* genes have homologues in mammals that perform similar functions in the control of apoptosis. *ced-9* encodes a protein sharing 24% overall sequence identity with the mammalian Bcl-2 oncogene, which, like *ced-9*, negatively regulates cell death (Hengartner and Horvitz, 1994a). *ced-3* encodes a protein with similarity to a family of death inducing proteases called caspases (Yuan et al., 1993). *ced-4* is related to mammalian Apaf-1, which in mammals acts together with caspase-9, caspase-3, and cytochrome c in the core apoptotic program (Li et al., 1997; Yuan and Horvitz, 1992; Zou et al., 1997). Finally, EGL-1 is related to the mammalian BH-3-only-domain proteins, such as Bid, Bad, Bim or Puma, all of which are implicated in pro-apoptotic signalling. Based on the finding that *C. elegans* has only one component of the core apoptotic pathway, *C. elegans* might contain the evolutionary most simple cell death pathway (Conradt and Horvitz, 1998; Nakano and Vousden, 2001; O'Connor et al., 1998; Wang et al., 1998; Wu and Deng, 2002; Yang et al., 1995; Yu et al., 2001; Yuan and Horvitz, 1992).

Several biochemical studies suggest that apoptosis in *C. elegans* is initiated by the processing of CED-3 from its inactive zymogen form into active caspase. Autocatalytic activation of CED-3 requires association of the zymogen with oligomerized CED-4

(Yang et al., 1998). In cells fated to survive, CED-4 is bound to and sequestered by CED-9 to mitochondrial membranes, thereby preventing oligomerization and CED-3 activation (Chen et al., 2000). The CED-9/CED-4 interaction is stable in living cells, but is disrupted in cells committed to die. Upon apoptotic signals, *egl-1* is transcriptionally upregulated. Subsequently, EGL-1 interferes with the CED-9/CED-4 complex by binding to CED-9 and thereby releasing CED-4 into the cytoplasm (Conradt and Horvitz, 1998; del Peso et al., 2000; Parrish et al., 2000). Oligomerized cytoplasmic CED-4 is then able to activate CED-3 (Yang et al., 1998).

Based on genetic analysis, cell death in the germ line, namely physiological cell death (see above) and DNA damage induced cell death, is dependent on the same core apoptotic machinery CED-9/CED-4/CED-3, which has been defined in somatic cell death. Loss of function (lf) alleles of *ced-3(n717)* or *ced-4(n1162)* completely abolishes germ cell death (Gumienny et al., 1999). Moreover, germ cell death is strongly suppressed in the gain of function allele *ced-9(n1950)*. In contrast to the "physiological germ cell death", which seems to be independent of *egl-1(Gumienny et al., 1999)*, DNA damage induced cell death is reduced but not abolished in *egl-1(n3082lf)* indicating that *egl-1* participates in DNA damage induced cell death (Gartner et al., 2000). Taken together, these observations suggest that germ cell death is, beside the requirement of the components of the core apoptotic pathway CED-9/CED-4/CED-3, genetically distinct from somatic cell death. Different upstream signals seem to act on the core apoptotic pathway specifying cell death.

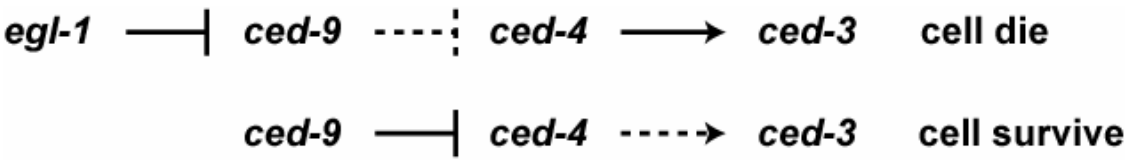

Figure 0-3 Genetic core-pathway for programmed cell death: The upper lane shows the status of cell death signaling as a consequence *egl-1* activation. The lower panel indicates the status of signaling in living cells. Solid arrows and solid T-bars indicate activation and repression, respectively. Dotted arrows and T-bars indicate that activation and repression do not occur.

5.5 Studying DNA damage response in *C. elegans*

Programmed cell death does not only occur during *C. elegans* development and germ cell maturation. Germ cells, but not somatic cells, can also undergo apoptosis in response to genotoxic stress (Gartner et al., 2000). When worms at the fourth larval stage (at L4 stage female germ cells begin to proliferate) are exposed to ionising irradiation the apoptotic response can be monitored in a time-window of 12-36 hrs post irradiation under Nomarski optics in anaesthetised animals (Gartner et al., 2000). Apoptotic germ cells can easily be distinguished from other germ cells by their typical morphology. The first sign of programmed cell death is a decrease in the refractivity of the nucleus. Soon afterwards, both nucleus and cytoplasm become increasingly refractile until they resemble a flat disk, termed as “cell corpse”. Finally, the disk starts to disappear and the nucleus begins to appear crumpled and vanishes within less an hour. The number of cell corpses can be used to quantify the apoptotic DNA damage response (Gartner et al., 2000).

The induction of apoptosis is very quick, as shown in an alternative experimental set up. Here, a synchronous population of adult wild-type animals is irradiated and the

apoptotic response is scored in a 60 minutes interval (Gartner et al., 2000). The number of cell corpse significantly increases after 4 hr post irradiation, which is in correlation to the apoptotic kinetic of irradiated mammalian thymocytes (Lowe et al., 1993). Other assays have been set up to detect apoptotic cells. In living animals, cell corpses can also be specifically stained with a fluorescent dye Acridine Orange and monitored with a Fluorescence Microscope set up (Gartner et al., 2000). The direct staining of apoptotic corpse in living animals was successfully used for high throughput genetic screens for mutants that affect the apoptotic DNA damage response (Anton Gartner personal communication).

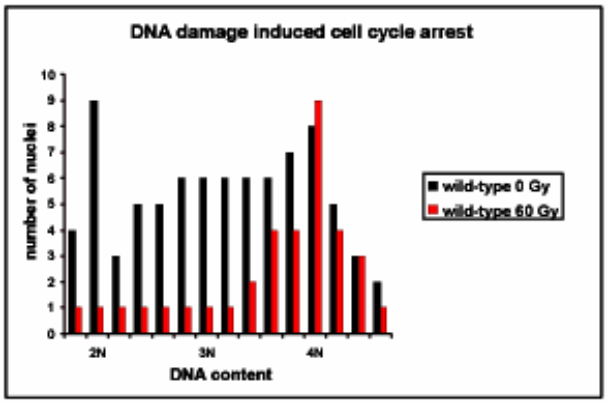

Figure 0-5 DNA damage induced cell cycle arrest. The number of germ cell nuclei within a given mitotic region is blotted against their DNA content. Two peaks at 2N (G1 phase) and 4N (G2/M phase) are characteristic for the histogram of mitotically proliferating germ cells. Ionising irradiation (60 Gy) leads to an accumulation of germ cell nuclei with 4N DNA content, which is an indication for a G2 cell cycle arrest.

Besides DNA damage induced apoptosis, a cell cycle arrest response to DNA damage is observed in mitotically proliferating germ cells. Upon DNA damage (ionising

irradiation and hydroxyurea) the number of germ cells is significantly decreased. In addition the volume of mitotic germ cell nuclei as well as their surrounding cytoplasm is enlarged, because cellular and nuclear growth continues during radiation-induced cell proliferation arrest (Gartner et al., 2000). The cell cycle arrest is transient as cells resume cell cycle progression 24 hours after irradiation (Gartner et al., 2000).

Cell cycle stages of germ cells can be determined by monitoring their DNA content. DNA of germ cells nuclei of isolated gonads was stained with the fluorescence dye Propidiumiodide (PI) and the DNA content was determined by measuring the intensity of the fluorescent PI signal within individual nuclei (Feng et al., 1999). Using this method germ cells with 2N DNA content (cells in the G1 phase) can be distinguished from cells with 4N DNA content (cells in the G2/M phase). The histogram of an asynchronous population of proliferating germ cells ((Feng et al., 1999) and Figure 0-5, black bars) shows two peaks one with 2N and a second with 4N DNA content. Measurement of the DNA content of irradiated (60 Gy) versus unirradiated germ cells revealed a significant accumulation of germ cells with 4N DNA content (Figure 0-5, compare black bars with red bars). This experiment indicates an accumulation of germ cells in G2/M after ionising irradiation. Taken together, germ cells respond to DNA damage in to ways: (1) mitotic germ cells undergo transient cell cycle arrest, whereas (2) meiotic pachytene cells induce the apoptosis.

6. Aim of the thesis

6.1 DNA damage checkpoint genes and genome integrity in *C. elegans*

The main aim of my PhD thesis is a better understanding of DNA damage checkpoint pathways in higher eukaryotes. We therefore used the nematode *C. elegans* as an experimental system. Recently Gartner et al. described specific cellular responses of germ cells (Gartner et al., 2000) after treatment of worms with genotoxic agents. Upon ionising radiation, mitotic germ cells transiently halt cell cycle whereas meiotic pachytene cells undergo programmed cell death.

Characterization of the DNA damage checkpoint mutant *rad-5*. A mutant, *rad-5(mn159),* which showed severe defects in these DNA damage checkpoint pathways was previously isolated (Gartner et al., 2000). Initial three-factor crosses revealed a map position to the middle of chromosome III. In that particular chromosome location no obvious *C. elegans* homologue of a known DNA damage checkpoint gene could be identified. We, therefore, assumed that *rad-5* might be a potential candidate for a new checkpoint gene and aimed to clone the *rad-5* gene by positional cloning. After cloning *rad-5,* we aimed to perform an epistasis analysis of *rad-5* with known checkpoint genes. These experiments should elucidate if *rad-5* is part of a known DNA damage checkpoint pathway or if *rad-5* defines a novel pathway. Besides its checkpoint function, *rad-5* has an additional function essential for embryogenesis (Hartman and Herman, 1982) as non-functional RAD-5 leads to embryonic lethality. Using 4D-microscopy imaging we aimed to determine the terminal phenotype of *rad-5* mutants during early embryogenesis.

Homologous recombination and chromosome pairing during meiosis. In a second

project we aimed to study the correlation of homologous recombination and various stages of homologous pairing during meiosis. In yeast, fungi, plants, and mammals pairing of homologous chromosomes in meiosis is dependent on the formation of double strand breaks, which initiate recombination. In contrast, initiation of recombination is not required for homologous pairing in *D. melanogaster* and *C. elegans*. Meiotic chromosome pairing is initiated by a process referred to as presynaptic alignment, which is followed by the formation of a tight protein complex between fully paired chromosomes, which is referred to as the synaptonemal complex (SC). We generated an antibody specific for RAD-51, a key enzyme in homologous recombination, and showed that RAD-51 foci specifically mark sites of ongoing meiotic recombination. Via the analysis of *rad-51* mutants worms, and the analysis of the pattern of RAD-51 foci formation in several mutants defective in various stages of meiotic chromosome pairing and recombination we aimed to elucidate the correlation between recombination and homologous pairing.

The *C. elegans* RecQ like orthologue of the Bloom´s syndrome gene. In the third aim of my thesis we focused on the *him-6* gene, which encodes for a *C. elegans* RecQ like helicase and which is the orthologue of the human Bloom´s syndrome gene. Bloom's syndrome is an autosomal recessive human disease associated with predisposition to cancer. To better understand the *in vivo* function of the Bloom's syndrome gene, and in particular its genetic interaction with *top-3, mre-11,* and *rad*-51, we wanted to undertake a comprehensive analysis of *him-6/blm* in genome stability and meiosis. Genome instability is characterized by an elevated number of double strand breaks. Using the number of RAD-51 foci as a cytological marker for DSBs we aimed to analyze the state

of genome stability in various single and double mutants combinations. Furthermore, using the pattern of RAD-51 foci in several stages of the meiotic prophase we aimed to pin down the role of *him-6/blm* in the process of meiotic recombination (see also aim 2).

7. Results and Discussion

7.1 "*C. elegans* RAD-5/CLK-2 defines a new DNA damage checkpoint protein"

7.1.1 Introduction

DNA damage checkpoint genes encode a group of proteins whose function is (1) to physically detect DNA damage, (2) to transmit a signal that DNA damage is present, and then either (3) to elicit cell cycle arrest and DNA repair (which removes the DNA damage), or (4) to elicit programmed cell death (which removes the compromised cell). The apoptotic response to DNA damage is found only in higher eukaryotes, including worms, flies, and mammals (Fraser and James, 1998). Proteins required for the DNA damage checkpoints are evolutionary conserved and have primarily been identified through genetic analysis in yeast and biochemical studies in mammalian cells (Rich et al., 2000)

Of the DNA damage checkpoint proteins identified thus far, it is unclear which protein actually senses DNA damage, although several candidates that interact with DNA are known. ScDdc1p (*Saccharomyces cerevisiae* Ddc1p), scRad17p, and scMec3p form a complex that structurally resembles a PCNA sliding DNA clamp (Burtelow et al., 2001; Caspari et al., 2000a; Kondo et al., 1999; Rauen et al., 2000; Venclovas and Thelen, 2000) and has recently been shown to associate to DNA close to double strand breaks *in vivo*, in a scRad24p-dependent manner (Kondo et al., 2001; Melo et al., 2001). However, these proteins are not required for DNA damage-induced activation of the checkpoint

protein kinase spRad3p, which is the *S. pombe* homologue of scMec1p and mammalian ATR (Edwards et al., 1999). Furthermore, the *in vivo* association of the scMec1p kinase with damaged DNA does not require scDdc1p, scRad17p, and scMec3p (Kondo et al., 2001). Together these results suggest that the PCNA-like checkpoint protein complex is not required for sensing DNA damage (Green et al., 2000; Kim and Brill, 2001; Krause et al., 2001; Naiki et al., 2000; Shimada et al., 1999). Furthermore, although complexes of the PCNA- and RFC-like checkpoint proteins are likely to interact with DNA in response to DNA damage, purified complexes containing these proteins fail to bind to DNA *in vitro*, suggesting that they may be downstream of the initial DNA damage checkpoint signal (Lindsey-Boltz et al., 2001). Other DNA damage checkpoint proteins that are likely to interact with DNA include the MRE11/RAD50/NBS1 nuclease complex (D'Amours and Jackson, 2001; Grenon et al., 2001; Usui et al., 2001). In addition to the above checkpoint proteins, studies in *S. cerevisiae* have also implicated DNA polymerase ε as an upstream component of checkpoint signalling that potentially acts as a sensor of DNA damage during S phase (Navas et al., 1995; Navas et al., 1996). It is unclear, however, whether DNA polymerase ε, scMec1p/spRad3p/ATM/ATR, the MRE11/RAD50/NBS1 nuclease, some other checkpoint protein, or some combination thereof might be the primary sensor(s) of DNA damage. The DNA damage signal is relayed via the scMec1p/spRad3p/ATM/ATR kinases to CHK1 and CHK2 kinases, which cause cell cycle arrest via phosphorylation of key cell cycle proteins (Dasika et al., 1999). How DNA damage-induced apoptosis and DNA repair is regulated is less well understood.

We have recently shown that DNA damage-induced checkpoints occur in the *C.*

elegans germ line (Gartner et al., 2000). When wild-type *C. elegans* worms are irradiated, one observes programmed cell death of meiotic pachytene cells as well as a transient cell proliferation arrest of mitotic germ cells (Gartner et al., 2000). Radiation-induced germ cell death is dependent on the general cell death regulators *ced-3* and *ced-4* and is negatively regulated by *ced-9*. Moreover *egl-1* partially contributes to radiation-induced apoptosis (Gartner et al., 2000). Importantly, three DNA damage checkpoint mutants have been identified, *op241, rad-5(mn159),* and *mrt-2(e2663),* and these mutants are defective for radiation induced cell death and cell cycle arrest (Gartner et al., 2000). *mrt-2* encodes the *C. elegans* homologue of budding yeast *RAD17*/fission yeast *rad1*(+) (Ahmed and Hodgkin, 2000).

rad-5(mn159) is a *C. elegans* DNA damage checkpoint mutant that was identified in a screen for radiation hypersensitive animals (Hartman and Herman, 1982). *rad-5(mn159)* worms are viable at 20°C but show maternal-effected embryonic lethality at 25°C. *rad-5* is thus either an essential gene or is required for life at 25°C (Hartman and Herman, 1982). When grown on permissive temperatures, the *rad-5(mn159)* mutant has reduced brood sizes and is hypersensitive to agents like UV, X-rays, and ethyl methan sulphonate, all of which damage DNA (Hartman and Herman, 1982). Since DNA damage fails to induce either cell cycle arrest or apoptosis in the germ line of *rad-5(mn159),* the RAD-5 protein is required for the DNA damage checkpoint in *C. elegans* (Gartner et al., 2000).

Here we show that the *C. elegans rad-5(mn159)* is allelic with *clk-2(qm37),* a *C. elegans* gene that affects both biological rhythms and life span (Lakowski and Hekimi, 1996). By epistasis analysis, we show that *rad-5/clk-2* mutants are defective for the *mrt-2*

and *hus-1* DNA damage checkpoint pathway but that *rad-5/clk-2* mutants are also defective for the S phase replication checkpoint. Cloning of *C. elegans rad-5/clk-2* reveals that it is structurally related to budding yeast Tel2p, a protein that has been shown to bind DNA *in vitro* (Kota and Runge, 1999; Kota and Runge, 1998; Runge and Zakian, 1996).

7.1.2.1 Results

7.1.2.1 *rad-5(mn159)* is allelic to *clk-2(qm37)*

To further characterize *rad-5(mn159),* we refined its map position to the middle of chromosome III by a series of three-factor crosses (Figure 1-1a). *rad-5(mn159)* displays a weak maternal-effected slow growth (Gro) phenotype, such that *rad-5m+z-* homozygotes (m, maternal genotype; z, zygotic genotype) develop at wilt type rates, whereas *rad-5(mn159)m-z-* worms have slightly slower growth rates (Figure 1-1b) (Hartman and Herman, 1982). A maternal effected Gro phenotype is rare in *C. elegans* and has been described for mutations in four other genes: *clk-1, clk-2, clk-3* and *gro-1* (Lakowski and Hekimi, 1996). We noticed that *clk-2* and *rad-5* genes had similar map positions. In addition, the only *clk-2* mutant allele that has been identified, *qm37*, displays a maternal-effected embryonic lethal phenotype at 25°C, as seen with *rad-5(mn159)* (Lakowski and Hekimi, 1996). To test the possibility that *rad-5(mn159)* and *clk-2(qm37)* might be allelic, we generated *rad-5(mn159)/clk-2(qm37)* trans-heterozygotes and found that they showed embryonic lethality at 25°C (Figure 1-1c). In addition *rad-5(mn159)/clk-2(qm37)* heterozygotes grown at 20°C had a slow growth phenotype that was intermediate between that of *rad-5(mn159)* (weak Gro) and that of *clk-2(qm37)* (strong Gro) (Figure

(a)

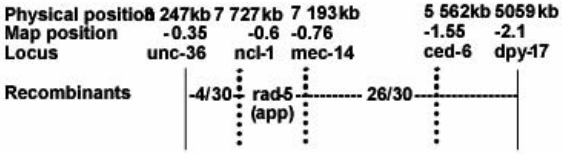

(b)

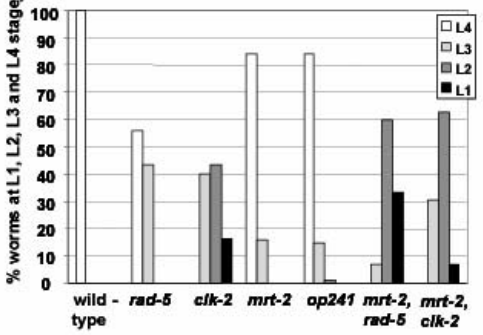

(c)

Strain	% survival (60Gy)	slowgrowth	ts
N2	75±1	wildtype	no
rad-5	29±5	slight	yes
rad-5/clk-2	12±7	moderate	yes
clk-2	13±3	strong	yes

(d)

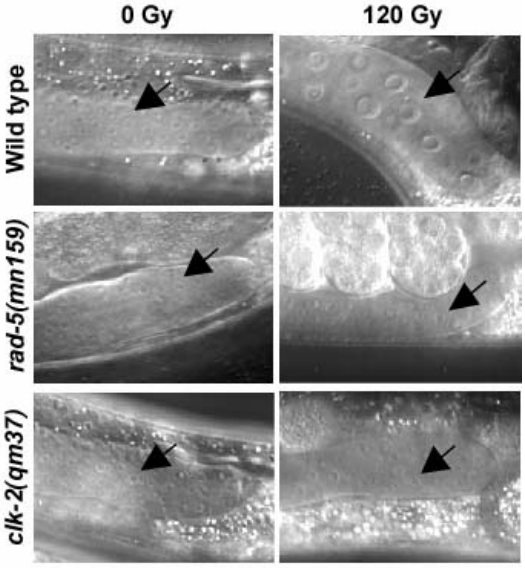

(e)

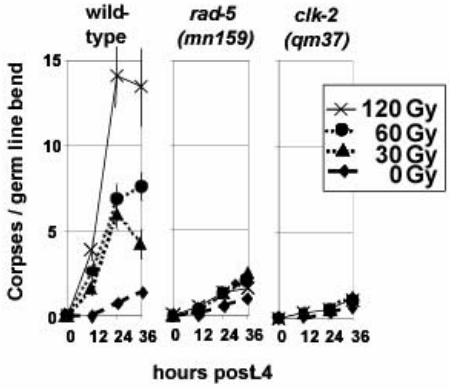

(f)

60 Gy survival

wild-type	65±6%
clk1(e2519)	76±10%
clk1(qm30)	61±9%
clk3(qm38)	69±14%
gro-1(e2400)	67±11%

(g)

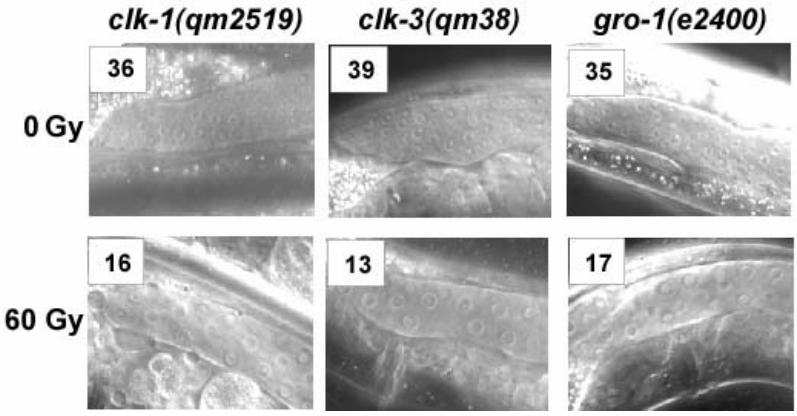

Figure 1-1 *rad-5(mn159)*is allelic with *clk-2(qm37).* (a) *rad-5(mn159),* whose map position was previously reported near -2 on chromosome III, was mapped more precisely using a multi-factor cross with the strain WS 711 *dpy-17(e164) ced-6(n1813) mec-14(u55) ncl-1(e1865) unc36(e251)*. Dpy-non-Unc and Unc-non Dpy animals were picked in the F2 generation and scored for the temperature-sensitive lethality associated with *rad-5(mn159)*. The number of recombinants and the approximate map position of *rad-5(mn159)* are indicted. **(b)** Growth rates of various single and double checkpoint mutants: Adult animals were allowed to lay embryos for 4 hours. After 48 h at 20°C, 100% of wild type animals are in the L4 larval stage. To estimate growth retardation, the proportion of various single and double mutants in the four larval stages L1, L2, L3 and L4 was determined. Based on these data, we estimate that *rad-5(mn159)* reaches the L4 stage 6h later than wild type whereas *clk-2(qm37)* is retarded by approximately 18h. **(c)** Complementation analysis: Embryonic survival was scored as the percentage of surviving embryos laid after irradiation of mothers with 60 Gy of radiation. **(d)** Radiation-induced cell cycle arrest was determined as described previously. In brief, worms were irradiated at the L4 stage and checkpoint-induced cell cycle arrest defects were scored as a lack of mitotic germ cell enlargement. **(e)** To assay for radiation induced germ cell death, worms were irradiated at the L4 stage with the indicated doses of X-irradiation and apoptotic corpses were determined 12, 24 and 36 h after irradiation using Nomarski optics. **(f,g)** *clk-2(qm37)* is the only checkpoint defective *clock* mutant. **(g)** Radiation-induced cell cycle arrest. **(f)** Radiation sensitivity of *clk* mutants (determined as described in (c) and (d)).

1-1b and c). Thus, *rad-5(mn159)* fails to complement *clk-2(qm37)* both for slow growth and for embryonic lethality at 25°C.

We next tested whether the *clk-2(qm37)* mutant displayed the DNA damage checkpoint defects seen with *rad-5(mn159).* To measure radiation sensitivity, worms were irradiated at the L4 larval stage, and the survival rate of F1 embryos was determined by counting F1 larvae and dead eggs (Gartner et al., 2000). Indeed, *clk-2(qm37)* mutants showed reduced survival following irradiation, as did *rad-5(mn159)/clk-2(qm37)*

heterozygotes (Figure 1-2c). In addition, *clk-2(qm37)* was defective for DNA damage induced cell cycle arrest (Figure 1-1d). In wild-type worms, mitotic cells in the distal arm of the *C. elegans* germ line transiently halt cell proliferation after irradiation but continue to growth, as indicated by a decrease in the cell number and enlargement of cellular and nuclear size. Checkpoint mutants such as *mrt-2(e2663)* and *rad-5(mn159)* are defective in this response. We observed that both *rad-5* and *clk-2* mitotic germ lines continue to proliferate following ionising irradiation (many small nuclei) (Figure 1-1d), as seen in *mrt-2(e2663)* checkpoint mutants (data not shown). To further corroborate that *clk-2(qm37)* is checkpoint defective, we examined radiation induced germ cell death in the meiotic part of the germ line by scoring morphologically distinct apoptotic corpses under Normarski optics as described previously (Gartner et al., 2000). Radiation induced germ cell death is completely abrogated in *clk-2(qm37)* mutants (Figure 1-1e). Thus, the *clk-2(qm37)* mutant is defective for the DNA damage checkpoint and is allelic with *rad-5(mn159)*. Since both *rad-5* and *clk-2* mutant names have been published, we designate this gene *rad-5/clk-2* (*rad-5* being the first mutant published) (Hartman and Herman, 1982; Lakowski and Hekimi, 1996)

7.1.2 2 *clk-2* is the only clock gene required for the DNA damage checkpoint

clk-2(qm37) mutants have a maternal effect clock phenotype, which is defined by slow growth, slow defecation, slow pharyngeal pumping, and slow movement (Lakowski and Hekimi, 1996). Mutations in three other genes, *clk-1, clk-3* and *gro-1*, also result in clock phenotypes (Lakowski and Hekimi, 1996). In addition, all known *clk* mutants have extended life spans (Lakowski and Hekimi, 1996). We were curious to know if the

checkpoint phenotype of *clk-2(qm37)* might be due to slow growth, and all *clk* mutants were tested for DNA damage checkpoint defects. We found that the germ lines of *clk-1(e2519), clk-3(qm38),* and *gro-1(e2400)* all responded to radiation-induced DNA damage by inducing wild-type levels of cell cycle arrest in the mitotic germ line and apoptosis in the meiotic germ line. Furthermore, the radiation sensitivity of *clk-1, clk-3,* and *gro-1* mutations is similar to that of wild-type (Figure 1-1f). Thus, the abnormal DNA damage checkpoint phenotypes of *rad-5(mn159)* and of *clk-2(qm37)* are not simply a consequence of the slow growth phenotype of these mutants.

7.1.2.3 Epistasis between *rad-5/clk-2* and other checkpoint mutants

Three *C. elegans* DNA damage checkpoint mutants have been previously identified: *mrt-2(e2663), op241,* and *rad-5(mn159)*. MRT-2 is a conserved DNA damage checkpoint protein and is homologous to *S. pombe* Rad1p and to *S. cerevisiae* Rad17p (Ahmed and Hodgkin, 2000). The *mrt-2(e2663)* splice junction mutation is likely to represent a severe allele of *mrt-2 (Ahmed and Hodgkin, 2000)*. In contrast, *rad-5(mn159)* and *clk-2(qm37)* are likely to be partial loss-of-function mutations, since they both cause temperature-sensitive embryonic lethality and are missense mutations. Finally, *hus-1(op241)* is a mutation in a conserved gene which is homologous to the DNA damage checkpoint gene *S. pombe* Hus1p and *S. cerevisiae* Mec3p (Hofmann et al., 2002). Neither *mrt-2(e2663)* nor *hus-1(op241)* is temperature sensitive.

To establish the epistatic relationship between these DNA damage checkpoint mutants, we generated all double mutant combinations and assayed for embryonic lethality and for extend of DNA damage-induced cell cycle arrest and apoptosis

following ionising radiation. Prior to construction of the double mutants, mutant strains were carefully out-crossed to eliminate the possibility of secondary mutations that could potentially affect radiation sensitivity. We found that *mrt-2(e2663), hus-1(op241), rad-5(mn159),* and *clk-2(qm37)* single mutants displayed little embryonic lethality at 20°C and neither did the *hus-1(op241);mrt-2(e2663)* double mutant (Figure 1-2a). In contrast, all double mutant combinations with either *rad-5(mn159)* or *clk-2(qm37)* showed an increase in embryonic lethality that was greater than the predicted additive lethality for both single mutants (Figure 1-2a). In addition, the growth rates of all *rad-5(mn159)* or *clk-2(qm37)* double mutants were retarded in comparison with the respective single mutants (Figure 1-1b). The synergistic lethality of *rad-5/clk-2* mutations with the *mrt-2(e2663)* and *hus-1(op241)* DNA damage checkpoint mutations suggests that mutations of the *rad-5/clk-2* DNA damage checkpoint gene may result in endogenous DNA damage whose repair requires the *mrt-2* and *hus-1* gene product or vice versa.

The radiation sensitivity of germ lines of single checkpoint mutants was examined by irradiation L4 larvae that have proliferating germ lines and by then scoring for the survival of embryos that are generated from the irradiated germ lines. Note that although *rad-5(mn159)* and *clk-2(qm37*) normally produce fewer eggs than wild-type, the total number of eggs laid by irradiated worms drops to about half that of unirradiated controls for all strains examined (Figure 1-2b). In contrast, the amount of lethality among the eggs of irradiated strains varied significantly. When single mutants were examined for X-ray sensitivity, *mrt-2(e2663)* was the most sensitive, *hus-1(op241)* was moderately sensitive, *clk-2(qm37)* was less sensitive, and *rad-5(mn159)* was the least sensitive (Figure 1-2c). The extensively out-crossed *rad-5(mn159)* strain used in this study was less sensitive to

irradiation than previously reported, because the original strain contains a second mutation that enhances radiation sensitivity (Gartner et al., 2000). These results agree with the possibility that *mrt-2(e2663)* is likely to be a strong allele and that *rad-5(mn159)* and *clk-2(qm37)* is temperature sensitive and therefore likely to be partial loss-of-function mutations.

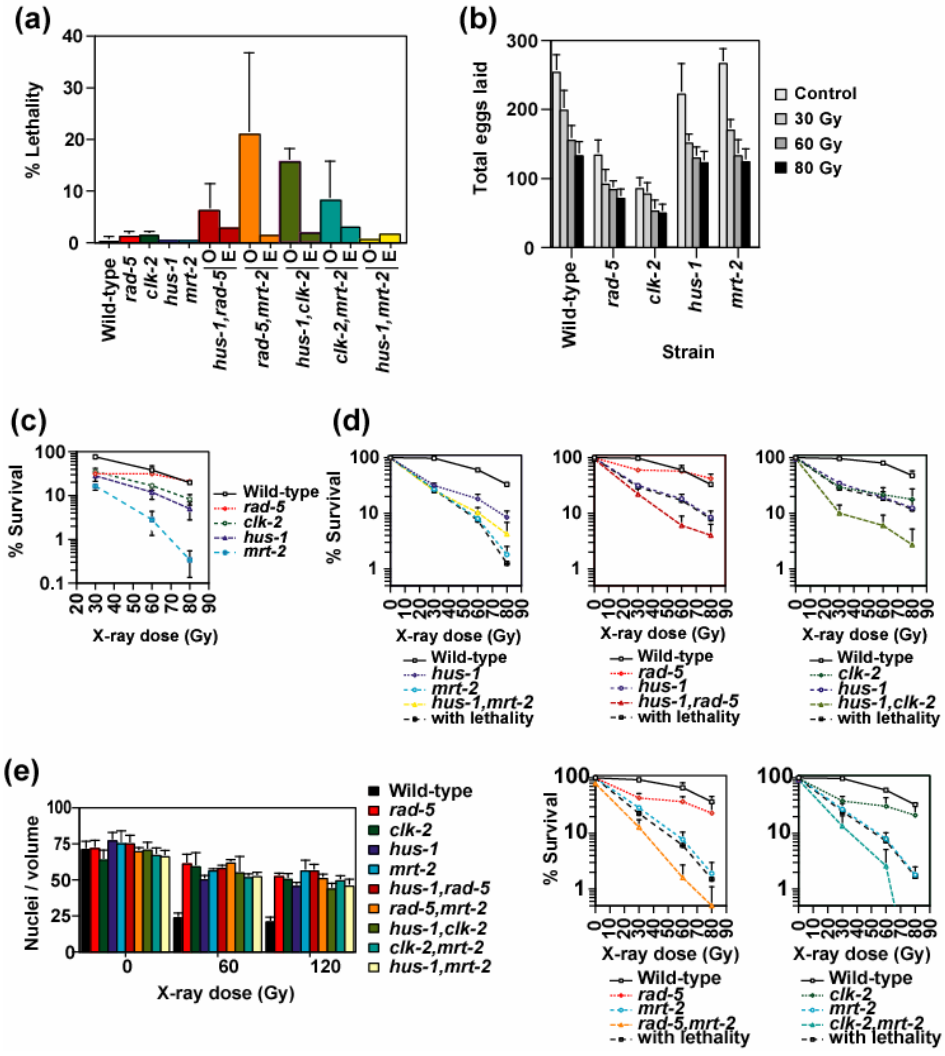

Figure 1-2 Epistasis analysis of *rad-5/clk-2* with *mrt-2* and *hus-1*. (a) Synthetic lethality is observed in *rad-5* or *clk-2* double mutants. In double mutants, the expected lethality (based on adding the lethality of single mutants) is indicated by 'E', whereas the observed lethality is indicated by 'O'. **(b)** Brood size drops by about 50% for all strains examined following high doses of irradiation. **(c)** X-ray hypersensitivity of single

checkpoint mutants. **(d)** X-ray hypersensitivity of various double mutant combinations. Although the same single mutant controls are used in several panels, these controls were part of a large experiment, and different graphs are used for clarity. **(e)** radiation-induced cell cycle arrest was determined by scoring for the number of mitotic germ cell nuclei in a volume of 54000μm^3, 12 h after irradiation at the L4 stage. For each experiment at least 5 germ lines were scored.

When the various double mutants were examined for their sensitivity to X-ray, the *hus-1(op241);mrt-2(e2663)* double mutant was no more sensitive than either single mutant, indicating that these two mutations affect a single DNA damage checkpoint pathway. In contrast, germ line of double mutants that contain either *rad-5(mn159)* or *clk-2(qm37)* were always more sensitive to irradiation than the most sensitive single mutant, even when the added lethality of two single mutants was taken into consideration (Figure 1-2d). The enhanced sensitivity of *rad-5* and *clk-2* double mutants suggest that *rad-5/clk-2* might act in a pathway parallel to that of *mrt-2* and *hus-1*, thus helping to repair DNA damage independently of the *mrt-2* and *hus-1* checkpoint genes.

The radiation sensitivity experiments described above (Figure 1-2c and d) measured the survival of embryos generated from irradiated, proliferating germ line nuclei. This assay is probably the most sensitive measurement of DNA damage checkpoint regulation, according for the combined effects of the DNA damage checkpoint response, namely, cell cycle arrest, apoptosis, and DNA repair. To assess which of these factors might be responsible for the enhanced radiation sensitivity of *rad-5/clk-2* double mutants, radiation induced cell cycle arrest was examined by scoring the number of mitotic germ cell nuclei in a defined volume 12 hr after irradiation at the L4

stage (Figure 1-2e). Our experiments indicate that the cell cycle arrest response is equally

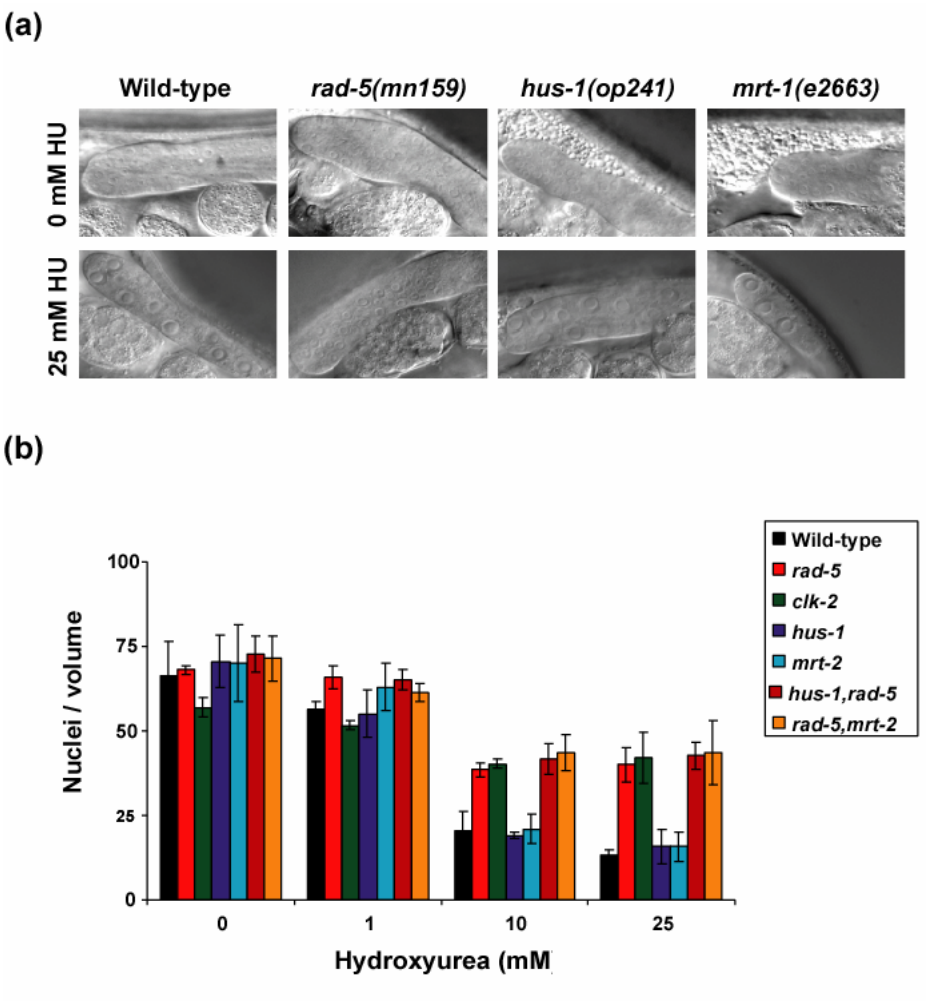

Figure 1-3 . *rad-5/clk-2* is defective in the S-phase checkpoint. (a) Mitotic germ cells of HU treated worms are shown. HU-induced cell cycle arrest was determined as described by MacQueen and Villeneuve. In brief, worms at the L4 stage were plated on NGM plates containing 25 mM HU and pictures of the mitotic part of the germ line were taken as described in (Figure 1-1d) after 14h incubation on HU plates at 25°C. Similar results were obtained when the assay was performed at 20°C (data not shown). **(b)** Quantification of S-phase defects. Worms were grown on NGM plates containing the indicated concentrations of HU starting from the L4 stage at 25°C. After 14h the extent of HU-induced cell cycle arrest was determined as described for IR induced cell cycle arrest (Figure 1-2e) by scoring for the number of mitotic germ cell nuclei in a volume of 54000μm^3.

strong in all single and double mutants. Given that *rad-5(mn159), clk-2(qm37),* and the various double mutants are as defective as *mrt-2(e2663)* for DNA damage-induced cell cycle arrest (Figure 1-2e) and apoptosis (data not shown) (Gartner et al., 2000), we concluded that this classical checkpoint responses do not fully account for the wild-type level of resistance of the germ line to DNA damage. Thus, although *rad-5/clk-2* and *mrt-2* appear to function in two parallel checkpoint pathways in terms of total irradiation sensitivity, the enhanced sensitivity is not due to enhanced defects in either cell cycle arrest or apoptosis but rather to defects in at least one additional parameter, possible DNA repair. In addition, our data indicate that *rad-5/clk-2* and *mrt-2* also function in a common pathway that regulates cell cycle arrest and apoptosis in response to DNA damage.

7.1.2.4 *rad-5/clk-2* mutants are defective for the S-phase replication checkpoint

The S phase replication checkpoint is defined by hydroxyurea (HU), a drug that causes DNA replication arrest through inhibition of ribonucleotide reductase and the consequent depletion of dNTP pools (Enoch et al., 1993). A recent study demonstrated that HU treatment of *C. elegans* L4 larvae causes mitotic germ cell arrest and results in enlarged mitotic germ cell nuclei. In addition, the *chk-2* DNA damage checkpoint protein was not required for this response (MacQueen and Villeneuve, 2001). Given that our double mutant analysis indicated that *rad-5/clk-2* functions in at least one checkpoint pathway that is independent of *mrt-2*, we tested to see if *rad-5/clk-2* might be involved in the S phase replication checkpoint (Figure 1-3a). We found that the HU-sensitive replication checkpoint is normal in *mrt-2* and *hus-1* animals but is severely compromised in the *rad-*

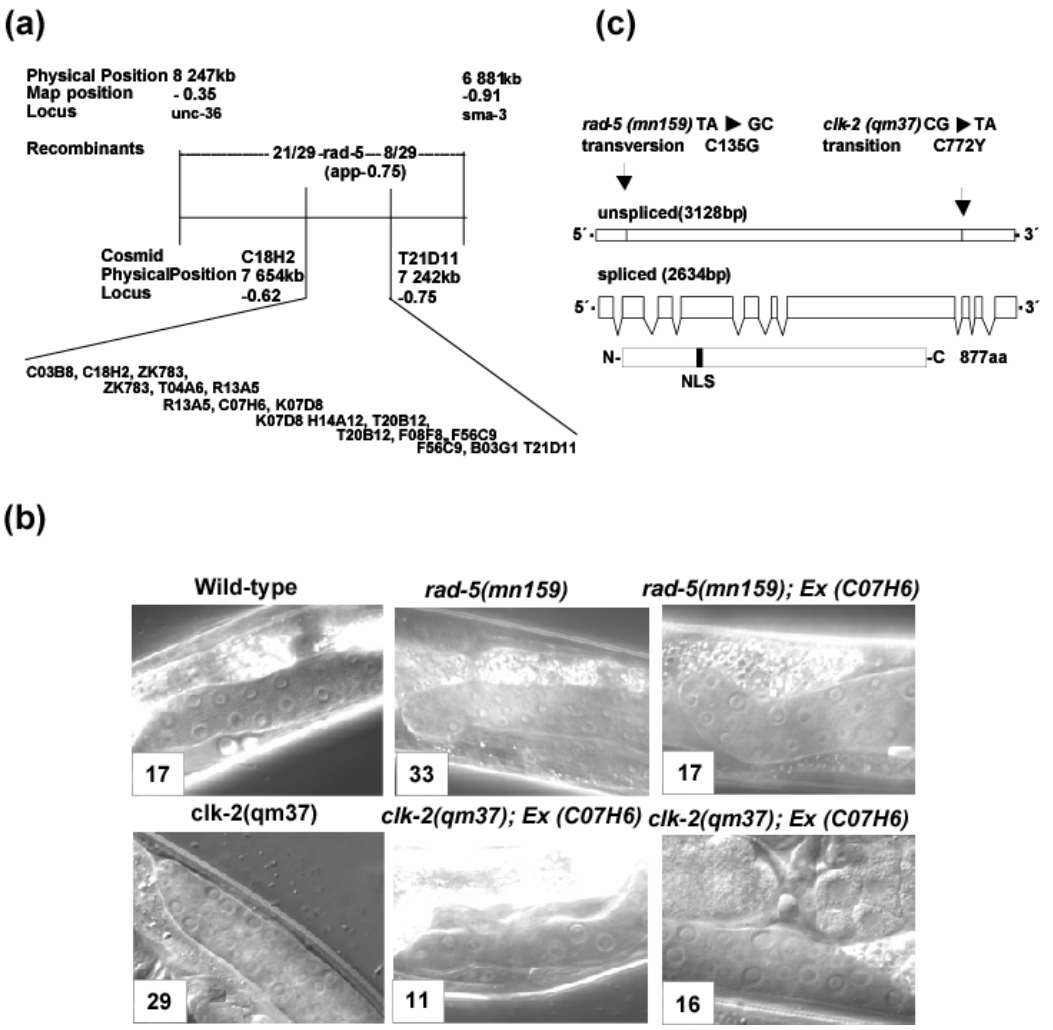

Figure 1-4 ***rad-5/clk-2*** **is encoded by C07H6.6. (a)** To more precisely map *rad-5(mn159)*, three-factor mapping was done with an *unc-36 rad-5 sma-3* strain, which was crossed with the polymorphic CB4854 strain. Recombinant animals were picked and the *rad-5(mn159)* map position was refined by analysis of single nucleotide polymorphisms between N2 and CB4854. **(b)** Rescue of *rad-5(mn159)* and *clk-2(qm37)* checkpoint phenotypes by cosmid C07H6. N2 wild type, mutant and transgenic worms were irradiated and the status of the mitotic germ line was scored after 12 h. The number of mitotic germ cell nuclei is indicated. **(c)** Sequence analysis revealed a single point mutation in C07H6.6 in *rad-5(mn159)* and in *clk-2(qm37)*. The *rad-5*/clk-2 cDNA sequence was determined by analysing the apparently full-length EST yk447b4 (data not shown). A putative NLS (aa 290-307) was found using used InterPro search software.

5 and *clk-2* animals (Figure 1-3a and b). *rad-5* double mutants are equally resistant to HU as *rad-5* single mutants (Figure 1-3b). Thus, our data indicate that the RAD-5/CLK-2 DNA damage checkpoint protein is required in *C. elegans* both for the S phase replication checkpoint and for ionising radiation induced checkpoints that are specific for *mrt-2* and *hus-1* and are likely to occur at G1 and G2/M.

7.1.2.5 RAD-5/CLK-2 defines a new evolutionary conserved protein

rad-5(mn159) mapped to an interval of 420 kb that is covered by 12 overlapping cosmids (Figure 1-4a). To determine the molecular identity of *rad-5/clk-2*, cosmid pools were injected. One cosmid pool stably rescued the *rad-5* ts lethality at 25°C. Injections of individual cosmids from this pool restricted the rescuing activity to a region unique to cosmid CO7H6, which contains four genes (Figure 1-4c). We obtained five C07H6 transgenic lines that complemented the ts lethality of *rad-5(mn159)* and *clk-2(qm37),* three of which also complemented the associated DNA damage checkpoint defect (Figure 1-4b). We were unable to phenocopy *rad-5* defects by either RNAi injection or by RNAi feeding, so we sequenced four genes in the middle of cosmid C07H6 in both *rad-5(mn159)* and *clk-2(qm37)* and found missense mutations only in C07H6.6. These mutations result in a G135C change in *rad-5(mn159)* and in a C772Y change in *clk-2(qm37)* (Figure 1-4c). C07H6.6 and C07H6.8 are likely to be part of an operon (data not shown). Thus, a DNA fragment containing both genes was PCR amplified and used to rescue the ts lethality of both *rad-5(mn159)* and *clk-2(qm37),* thus confirming the molecular identity of *rad-5/clk-2* (data not shown). Out of the four transgenic lines that rescued the temperature sensitivity of *clk-2(qm37*), one line also rescued the checkpoint

phenotype (Figure 1-4b). Rescue of the checkpoint phenotype was expected to be difficult, as this is a germ line phenotype, and injected, extrachromosomal DNA is often silenced in the germ line of *C. elegans* (Dernburg et al., 2000; Ketting and Plasterk, 2000). We thus conclude that *rad-5/clk-2* is encoded by C07H6.6. *rad-5/clk-2* is expressed throughout all developmental stages (data not shown) (Hill et al., 2000).

To determine whether *rad-5/clk-2* is evolutionary conserved, PSI Blast (NCBI) was performed using the RAD-5/CLK-2 protein family with a single homologue in vertebrates, Arabidopsis, Drosophila, budding and fission yeast (Figure 1-5). After five rounds of PSI Blast, probability scores for *rad-5/clk-2* family members ranged from 1e-178 to 1e-71, whereas the highest score for an unrelated protein was 0.92. Equally, PSI Blast searches with partial RAD-5/CLK-2 sequences detected the same proteins (data not shown). RAD-5/CLK-2 is homologous to the *S. cerevisiae* Tel2p protein, which was identified in a genetic screen for budding yeast mutants with short telomeres. Telomeres of the *tel2-1* mutant shorten progressively for about 100 cell divisions and then stabilize (Lustig and Petes, 1986). In addition, Tel2p has been reported to bind to single-stranded, double stranded, and four-stranded yeast telomeric DNA *in vitro (Kota and Runge, 1999; Kota and Runge, 1998)*. We therefore decided to examine telomere length in *rad-5(mn159)* and *clk-2(qm37)*

7.1.2.6 Telomere behaviour in *C. elegans* DNA damage checkpoint mutants

The MRT2 checkpoint protein is thought to be required for telomere replication, because *mrt-2(e2663)* mutants display progressively shortened telomeres, late-onset end-to-end chromosome fusions, and late-onset sterility – phenotypes typical of telomerase-defective

mutants in yeast and mouse (Ahmed and Hodgkin, 2000). In comparison with telomeres of N2 wild-type strains, telomeres of *rad-5(mn159)* and *clk-2(qm37)* strains tended to be slightly elongated, often containing a long telomeric restriction fragment found in *rad-5/clk-2* parental strains. However, telomere length varies considerably in *C. elegans*

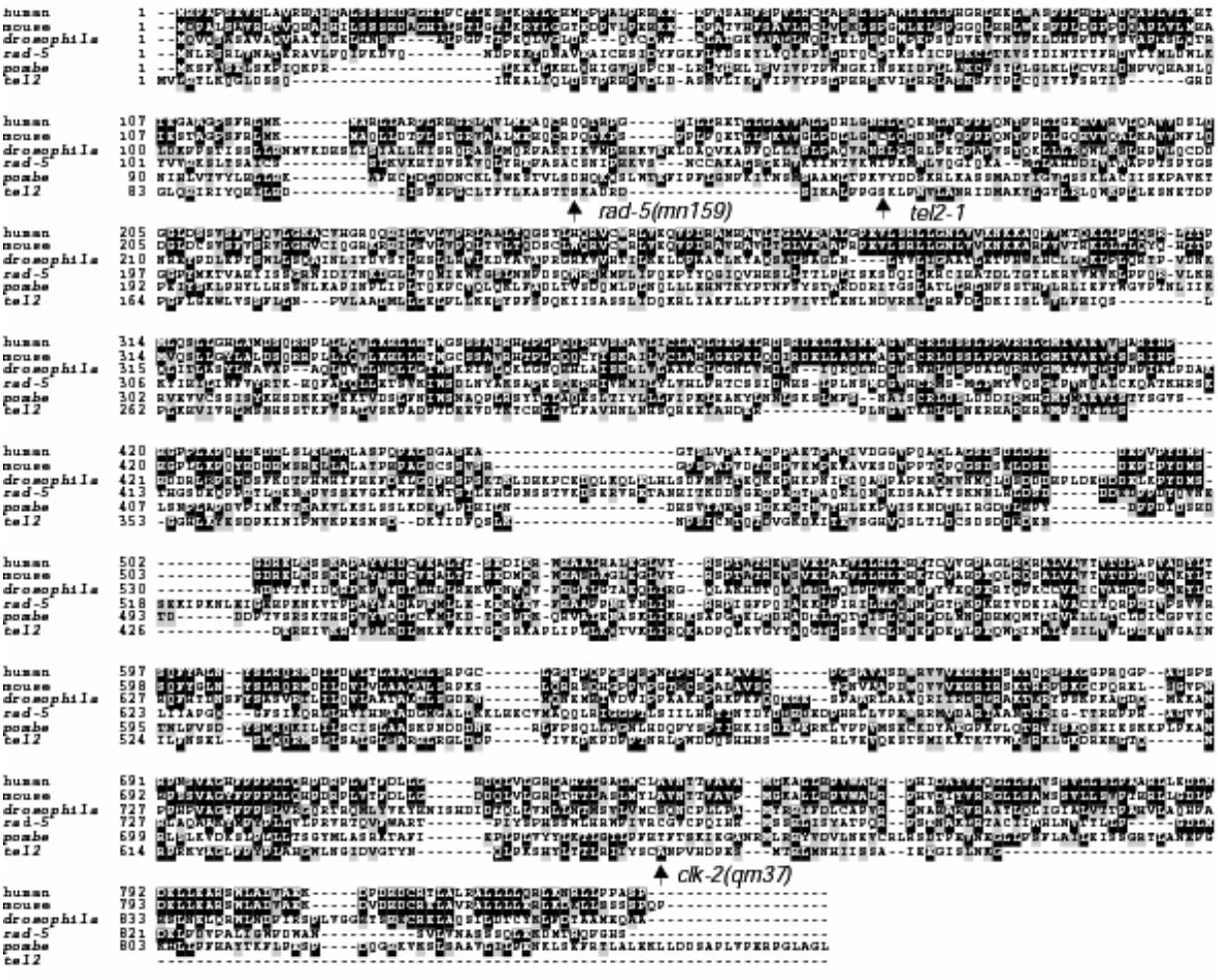

Figure 1-5

Figure1-5: RAD-5/CLK-2 has unique homologs in mammals, flies, and yeast and is related to budding yeast Tel2p. The multiple protein alignment was performed using Clustal W 1.8.

strains and can fluctuate within single isogenic lines (data not shown). Thus, crosses were performed between wild-type and *rad-5/clk-2* mutant worms, homozygous mutant and wild-type F2 progeny were picked from the same F1 heterozygotes, and independent F2 lines from the same F1 parents were analysed in order to determine if *rad-5* or *clk-2* mutations affect telomere length (Figure 1-6a). Wild-type F2 lines from these crosses (*clk-2*+/+ sibs) had telomere length that were similar to those of their *rad-5/clk-2* mutant siblings, indicating that the *rad-5(mn159)* and *clk-2(qm37)* missense mutations have no immediate effect on telomere length (Figure 1-6a). In contrast, F2 lines of *mrt-2* all have discrete telomeric bands, suggesting tight regulation of telomeric length in the absence of telomere elongation, a phenotype that is also seen in *Arabidopsis* telomerase-defective mutants (Riha et al., 2001).

When telomere length of checkpoint-defective *C. elegans* strains was examined over several generations, N2 wild-type telomeres either stayed fairly constant in length (Figure 1-6b) or elongated slightly (in 3/6 experiments each) (data not shown), whereas *rad-5* and *clk-2* lines usually displayed slightly telomere lengthening (in 5/6 experiments) (Figure 1-6b; data not shown). Note that the example shown in Figure 1-6b is misleading in the absence of further trials, as it suggests that wild-types telomeres remain the same length, whereas *rad-5* and *clk-2* telomeres elongate slightly with time. Wild-type telomeres often elongate as well (data not shown). *hus-1* telomeres showed little change in telomere length over time, whereas *mrt-2* telomeres shortened progressively (Figure 1-6b), as previously described (Ahmed and Hodgkin, 2000). We thus conclude that mutations of *rad-5/clk-2* have no significant effect on telomere length, which is in

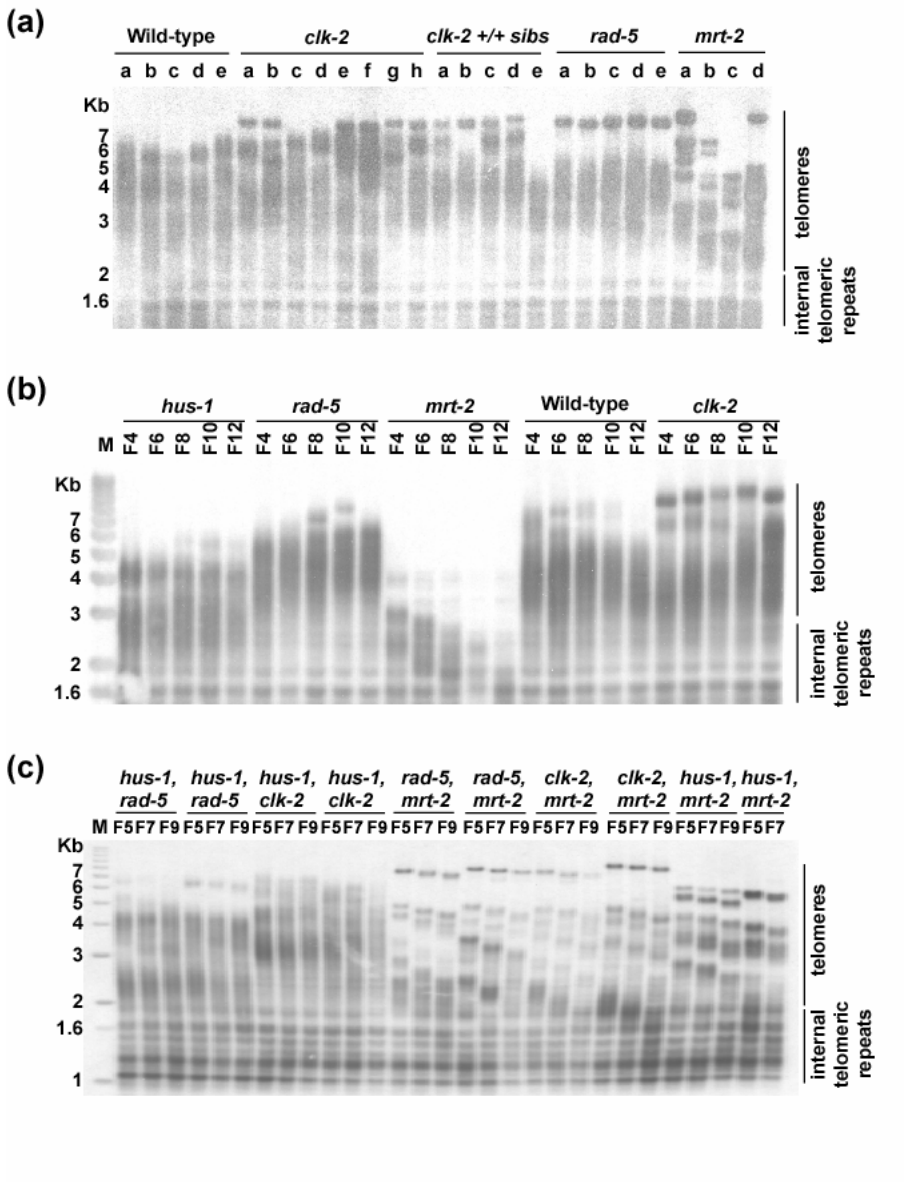

Figure 1-6: Telomere length of *C. elegans* checkpoint mutants. (a) Telomere length of a number of different freshly outcrossed F2 plates of *rad-5(mn159)*, *clk-2(qm37)*, *mrt-2(e2663)*, *hus-1*(*op241)*, and of *clk-2 (+/+)* wild-type siblings. (b) Telomere length of various *C. elegans* checkpoint mutant strains over the course of several generations. Since telomere length can fluctuate even in wild-type *C. elegans* strains, 6 independent experiments were conducted, an example of which is shown. (c) Telomere length of various *C. elegans* checkpoint double mutants. Positions of telomeric and internal non-telomeric restriction fragments are indicated (Wicky et al., 1996)**.**

contrast to the telomere shortening observed in S. cerevisiae *tel2-1* mutants. Telomere length was also examined in the various double mutant combinations and shown to drift slightly in *hus-1(op241),rad-5(mn159)* or *hus-1(op241),clk-2(qm37)* strains (Figure 1-6c). Notably, telomeres *of hus-1,rad-5* double mutants shortened progressively (Figure 1-6c), although these double mutants did not display the discrete telomeric bands or mortal germ line senescence that are seen for *mrt-2* telomerase-deficient mutants (data not shown). All double mutant combinations with *mrt-2* displayed progressive telomere shortening and mortal germ line phenotypes, as is typical of *mrt-2* mutants (Figure 1-6c and data not shown) (Ahmed and Hodgkin, 2000).

7.1.2.7 Checkpoint phenotypes of S. cerevisiae *TEL-2*

Since *rad-5/clk-2* and *TEL-2* are related by sequence, we were curious to know if Tel2p might be required for the DNA damage checkpoint in *S. cerevisiae*. We analysed the single reported viable *tel2* allele, *tel2-1 (Lustig and Petes, 1986)*, but did not observe enhanced sensitivity to X-ray irradiation, to MMS, or to HU, as we observed with a control DNA damage checkpoint mutant, *mec1-1* (data not shown). We conclude that this partial loss-of-function *tel2-1* allele, which has a rather mild telomere shortening phenotype (Lustig and Petes, 1986)does not display defects that might be expected for a yeast DNA damage checkpoint mutant.

7.1.3 Discussion

Using *C. elegans* as an experimental system, we have identified a novel DNA damage checkpoint protein that is structurally related to budding yeast Tel2p. Both *C. elegans*

rad-5(mn159) and *clk-2(qm37)* alleles affect DNA damage checkpoint responses, have little effect on telomere length, and display a maternal-effect Gro phenotype. *clk-2(qm37)* displays stronger Gro and radiation sensitivity phenotypes than does *rad-5(mn159)* (Figure 1-1b), and *clk-2(qm37)* is also more sensitive to radiation (Figure 1-2d), indicating that it is a stronger allele. The two identified alleles are both missense mutations, and both of these are temperature-sensitive embryonic lethal. Both alleles of *rad-5/clk-2* are therefore likely to be partial loss-of-function, suggesting that *rad-5/clk-2* is an essential gene. Since *rad-5/clk-2* is a DNA damage checkpoint gene, it seemed possible that the temperature sensitive phenotype of *rad-5/clk-2* mutant worms might be due to an S-phase defect at 25°C. However, developmental recordings of *rad-5(mn159)* or *clk-2(qm3)* embryos raised at 25°C failed to reveal any cell cycle defects in the first two cell divisions (data not shown) (Benard et al., 2001; Gonczy et al., 2000). In addition, telomere length in *rad-5(mn159)* and *clk-2(qm37)* animals grown to adulthood at 25°C was not different from that of wild-type controls (data not shown). It is possible that a subtle kind of lethal DNA damage accumulates at 25°C in these mutants. Alternatively, RAD-5/CLK-2 may be needed to organize late embryonic development (Hartman and Herman, 1982) or may have another essential function.

Two recent papers report the cloning of *clk-2* (Benard et al., 2001; Lim et al., 2001). Given that *rad-5/clk-2* is related to budding yeast *TEL2,* a gene that regulates telomere length, these reports have each tested telomere length in single *clk-2(qm37)* strains and have observed either elongated (Benard et al., 2001) or shortened telomeres (Lim et al., 2001) in comparison with wild-type. Given that telomere length is generally variable in *C. elegans* strains (Shawn Ahmed, unpublished data), it is not surprising that

differences in telomere length might be observed between single *clk-2/qm37)* and wild type strains from different laboratories. Furthermore, rescue of an elongated *clk-2* telomere phenotype by one laboratory resulted in telomeres that were shorter than normal (Benard et al., 2001)suggesting that cosuppression silencing of *rad-5/clk-2* may have occurred as a consequence of the rescuing extrachromosomal array (Benard et al., 2001). Our analysis of wild-type and long-lived *clk-2(qm37)* F2 siblings that were derived from the same F1 parent revealed telomeres of similar lengths (Figure 1-6a), indicating that *clk-2(qm37)* does not have an immediate effect on telomere length and that *clk-2* worms do not have extended life span as a consequence of either long or short telomeres. Furthermore, we have followed telomere length of *clk-2(qm37)* and *rad-5(mn159)* mutant worms for many generations, and our data indicate that the *clk-2(qm37)* and *rad-5(mn159)* mutations do not significantly affect telomere length. If telomere length fluctuates slightly in these mutant strains over time, it also does so in wild-type strains.

Given that *rad-5/clk-2* is a DNA damage checkpoint gene, we decided to examine the single reported viable allele of the budding yeast homologue, *tel2-1* , but could not detect the enhanced sensitivity to DNA damaging agents (data not shown). However, as both *rad-5/clk-2* and *TEL2* are essential genes, the partial loss-of-function missense mutations that are available may not reveal all functions of these genes, such as checkpoint defects in *tel2* mutant or telomere defects in a *rad-5/clk-2* mutants. Several previous observations indicate that budding yeast Tel2p may have a checkpoint function. Tel2p has been shown to act in the same telomere length regulation pathway as that of Tel1p checkpoint protein, which is related to the human ataxia telangiectasia-mutated DNA damage checkpoint protein (Runge and Zakian, 1996). In addition, the *tel2-1*

mutant displays a weak chromosome loss phenotype, which is often seen with yeast DNA damage checkpoint mutants (Klein, 2001). It is possible that a checkpoint defect for *tel2-1* may be revealed when combined with other yeast checkpoint mutants, as seen with *tel-1* mutations (Greenwell et al., 1995; Morrow et al., 1995). However, it is also possible that the *C. elegans* homologue of *TEL-2, rad-5/clk-2,* may have acquired its checkpoint function during the evolution of multicellular organisms.

Our study reveals several DNA damage checkpoint functions for the conserved *rad-5/clk-2* checkpoint gene. Analysis of *rad-5/clk-2* double mutants using a variety of assays demonstrated synthetic effects with the *mrt-2* and *hus-1* checkpoint mutants. The enhanced radiation sensitivity of *rad-5/clk-2* double mutants may be solely due to an additional defect in the S-phase replication checkpoint (Figure 1-3). Further, the failure to observe an S phase checkpoint defect in *mrt-2* mutants (MacQueen and Villeneuve, 2001) indicates that *mrt-2/scRAD-1/sprad17* family members may not be required for the S phase checkpoint in multicellular organisms. Similarly, *scrad17/sprad1* mutations are only weakly HU sensitive in fission and budding yeast (Lydall and Weinert, 1997; Paulovich et al., 1997).

Budding yeast Tel2p has been shown to bind a variety of nucleic acid structures *in vitro*, including single-stranded and unusual four-stranded DNA structures, which may resemble damaged DNA (Kota and Runge, 1999; Kota and Runge, 1998). Thus the RAD-5/CLK-2 checkpoint protein may act at sites of DNA damage, either early in the pathway, as a primary sensor of DNA damage, or later in the pathway, to help repair of damaged DNA. It is curious that DNA polymerase ε has been identified in yeast as an S phase checkpoint protein that may be a sensor of DNA damage. Double mutants between

polymerase ε and canonical DNA damage checkpoint mutants show synthetic lethality and enhanced sensitivity to radiation (Feng and D'Urso, 2001; Navas et al., 1995; Navas et al., 1996), and we have observed similar synthetic phenotypes for *rad-5/clk-2*. However, DNA polymerase ε has only been shown to affect the S phase checkpoint, whereas *rad-5/clk-2* affects both the DNA damage checkpoint and the s phase replication checkpoint (Figure 1-2 and 1-3)

This study demonstrates that *C. elegans* genetics is useful for identifying novel DNA damage checkpoint proteins – proteins that are likely to have significance in mammals and, possibly, in oncogenesis. Further studies will be required to reveal the precise molecular function of RAD-5/CLK-2 and its homologues.

In the following chapters we will present data on RAD-5/CLK-2 that are not part of the recent publication by Ahmed et al. (Ahmed et al., 2001).

7.1.4 Analysis of the essential function of *rad-5/clk-2*

In addition to its checkpoint function, *rad-5/clk-2* has also an essential function needed for embryogenesis (Hartman and Herman, 1982). While the two alleles of *rad-5/clk-2*, *mn159* and *qm37*, are defective in the DNA damage checkpoint signalling at 20°C to the same extend as we observed for *mrt-2* and *hus-1* mutants (Gartner et al., 2000)(Figure 1-2e), they are, in contrast to *mrt-2* and *hus-1,* temperature sensitive for embryonic viability. Embryos survive at 20°C, but embryonic development is halted at the restrictive temperature of 25°C. We postulated, that the essential function of *rad-5/clk-2* could be explained by two models: (1) *rad-5/clk-2* might be required for a distinct, DNA repair and checkpoint independent step during embryonic development. (2) Alternatively, the embryonic lethality of *rad-5/clk-2* mutants might be explained by a failure to maintain genome stability that ultimately results in dead embryos. If this hypothesis is correct one might expect a non-uniform terminal phenotype of *rad-5/clk-2* embryos as genome instability is expected to occur stochastically.

7.1.4.1 Lineage defect in *rad-5/clk-2* mutants at restrictive temperature

During *C. elegans* embryonic development cell division patterns – also referred to as cell lineages – are invariant (Figure 1-7). This characteristic provides a unique experimental system as abnormalities in cell migration and cell cleavages during development can be

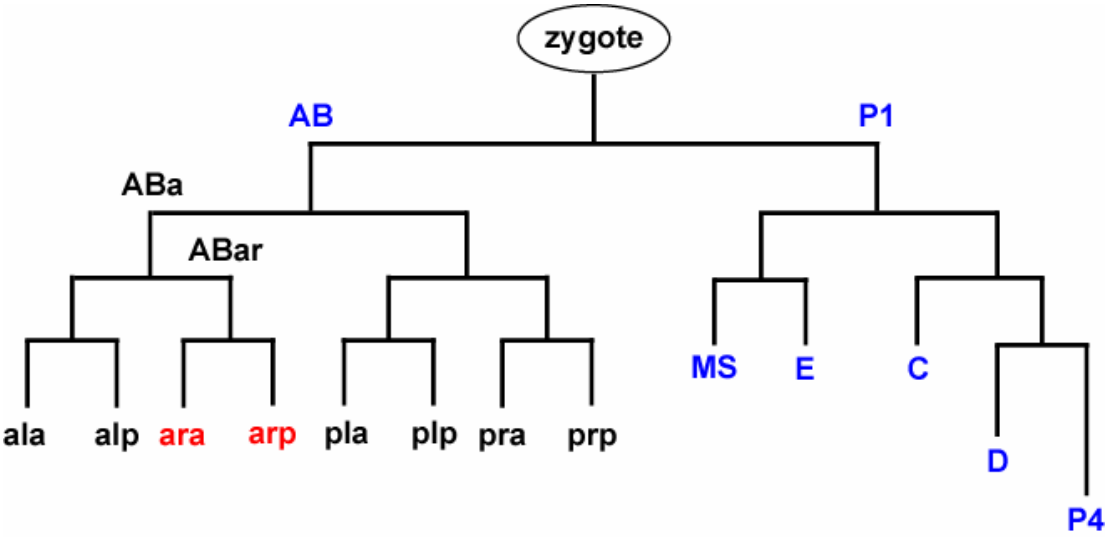

Figure 1-7 The early *C. elegans cell* lineage: The first eight AB great granddaughter cells are abbreviated using their last three letters (a: anterior, p: posterior, l: left, r: right). The two great granddaughters, which are abnormal in *rad-5/clk-2* mutants are highlighted in red. Founder cells are indicated by AB, MS, E, C, D and P4 in blue.

observed easily. (Sulston and Horvitz, 1977; Sulston, 1983). Early embryogenesis consists of five asymmetric and asynchronous cell divisions. These early cleavages produce six "founder " cells called AB, MS, E, C D, and P_4 (Sulston and Horvitz, 1977; Sulston, 1983)(Figure 1-7).

Recently it has been shown that defects in DNA replication cause a delay in cell divisions and an enhanced asynchrony of early cleavages in *C. elegans* (Encalada et al., 2000). Furthermore, Brauchle at al. showed that the cell cycle delay caused by defects in DNA replication is dependent on the DNA damage checkpoint genes *atl-1* and *chk-1* (Brauchle et al., 2003; Schumacher et al., 2003). Strikingly, if the *atl-1/chk-1* checkpoint was abrogated even in the absence of DNA replication defects, the cell cycle progression of the P1 cell was accelerated and the gap between the completion of AB and P1

divisions was shortened (Brauchle et al., 2003). Given that *rad-5/clk-2* might have a function in S-phase we wanted to know if *rad-5/clk-2* mutants have a defect similar to *atr-1/chk-2* mutants in cell cycle timing of the first embryonic cell divisions. Moreover, we addressed the question if *rad-5/clk-2* has a distinct role during embryonic development.

To monitor abnormalities in the embryonic cell divisions we used a 4D-microscope equipped with a multifocal-plane, time-lapse video recording system (Schnabel et al., 1997). Briefly described, a stack of twenty DIC-images, viewing different focal planes of the embryo, are taken every 30 seconds over the whole period of embryogenesis (~18 hrs). The "Biocell" program was used to document and illustrate the position of each cell and their descendants at different times (Schnabel et al., 1997). This technique allows to analyse abnormalities in cell lineages, cell migrations, timing of cell divisions and terminal fates. In comparison to wild-type we observed in both *rad-5(mn159)* (4 out of 5 analysed embryos) and *clk-2(qm37)* (3 out of 4 analysed embryos) mutant embryos at restrictive temperature (25°C) a slightly slower cell cycle progression of all monitored cell cycles (data not shown). In addition, cell lineages were normal up to the 12-cell stage. However, at the 12-cell stage we monitored an abnormal migration/rotation of the ABar (granddaughter cell of the AB founder cell; a: anterior, r: right, Figure 1-7) daughter cells ABarp and ABara. Subsequently the ABarp daughter cell, and not the ABara came in contact to the MS blastomer (Figure 1-8). In this abnormal context the ABarp cell (and not the ABara cell as in wild-type) got an abnormal left-right induction signal (arrow in 3D-model of Figure 1-8) from the MS blastomere (Wood, 1991). As a consequence, cell fates of the ABarp (mainly forming the epidermis)

and ABara (mainly forming the pharynx) lineages were exchanged and no viable embryo could develop.

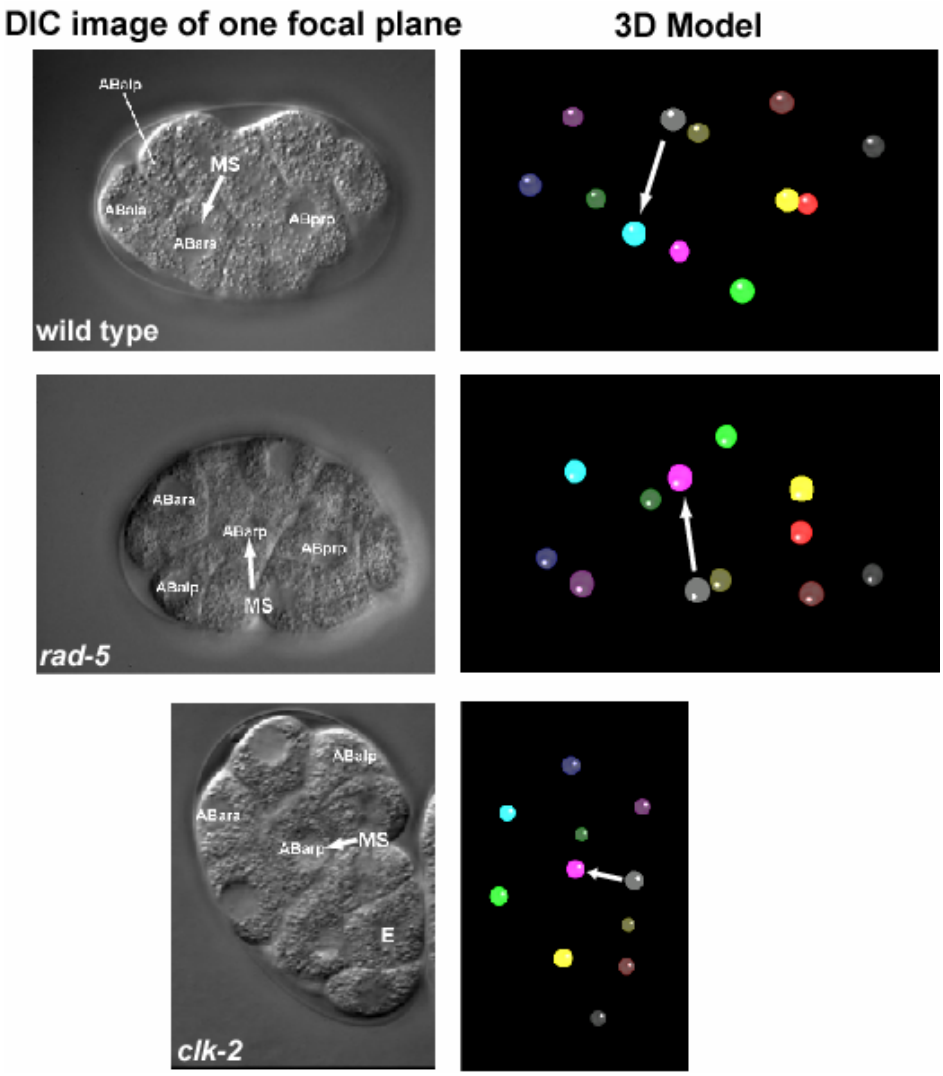

Figure 1-8 early embryonic lineage defect in rad-5/clk-2 mutants. The left panel shows DIC images of representative focal planes of the 12-cell stage embryos. Daughter cells from ABar, ABal, and MS blostomere cell are indicated. The right panel visualizes the 12 embryonic cells in a 3D-model. Furthermore, the inductive signal (arrow) from MS (gray ball) to ABara, turquoise ball (in the wild type situation) and ABarp, pink ball (in the *rad-5/clk-2* mutants) is indicated. (AB, MS founder cells, a:anterior, p:posterior, l:left, r:right)

Given that very defined defect at the 12-cell stage, the checkpoint/repair gene *rad-5/clk-2* might be also responsible for a distinct, DNA repair independent step during early embryonic development. Future studies will be needed to define the molecular function of *rad-5/clk-2* at the 12-cell stage.

7.1.4.2 *rad-5/clk-2* has a distinct function in early embryonic development

We analysed the role of the putative RAD-5/CHK-2 checkpoint protein using 4D-microscopy and found a very defined early defect at the 12-cell stage (Figure 1-8). Defects in the first embryonic cell divisions of *C. elegans* have also been published for DNA replication genes (Encalada et al., 2000) and the *atl-1/chk-1* checkpoint pathway. *atl-1* and *chk-1* regulate in part the asynchrony between the cell cycle timing of AB and P1 cell divisions (Brauchle et al., 2003). Our results indicate that RAD-5/CLK-2 might also act as a replication checkpoint gene in the timing of cell divisions at the 12-cell stage. In particular the timing of the ABar cell division by RAD-5/CLK-2 might be important for the further embryonic development. However, we consider it more likely that RAD-5/CLK-2 might be involved in a second distinct function in embryogenesis that is DNA damage checkpoint and DNA repair independent.

An early developmental defect has been described for *Drosophila melanogaster* embryos that are deficient in *D.m*.Mei41/ATL or *D.m*.Grapes/CHK1 checkpoint kinases (Sibon et al., 1999; Sibon et al., 1997). Early *Drosophila* embryogenesis consists of 13 rapid syncytial mitotic cell divisions. The 14^{th} cell division is then slowed down and nuclei migrate to the periphery and cellularize to form an epithelial mono-layer. This stage, which also correlates with the onset of zygotic transcription, is also called the mid-

blastula transition. Inactivation of the Mei-41/Grapes checkpoint terminates the mid-blastula transition. More than 14 syncytial divisions occur and embryos die without forming cells (Sibon et al., 1999; Sibon et al., 1997).

In vertebrates, several DNA damage checkpoint genes like ATR and CHK1 DNA damage checkpoint kinases are also essential for embryonic viability. Knockouts of these two mouse DNA damage checkpoint genes cause early embryonic lethality. The analysis of ES cells derived from these mice revealed an essential cell cycle function (Liu et al., 2000; Brown and Baltimore, 2000). It has been suggested that the embryonic lethality is caused by massive genome instability, which eventually triggers apoptosis (Liu et al., 2000; Brown and Baltimore, 2000). However, a developmental specific function for ATR or CHK1 cannot be excluded.

7.1.4.3 Accumulation of RAD-51 foci in mitotic germ cells of *rad-5/clk-2* mutants

Defects in DNA damage checkpoints and in DNA repair are often associated with genome instability (reviewed in (van Gent et al., 2001)). When *rad-5(mn159)* animals are cultivated at 20°C they display a mutator phaenotype as they accumulate mutations, in particular, small deletions (mutator phenotype; (Hartman and Herman, 1982)and Shawn Ahmed, unpublished observation).

To analyse genome instability we monitored double strand breaks by immunofluorescence studies using an antiRAD-51 antibody. RAD-51 is key protein involved in homologous recombination and cytological detection of RAD-51 reveals bright nuclear foci, which have been shown to localize to sites near double strand breaks by immunofluorescence staining (West, 2003) (see also 7.2.1).

(a)

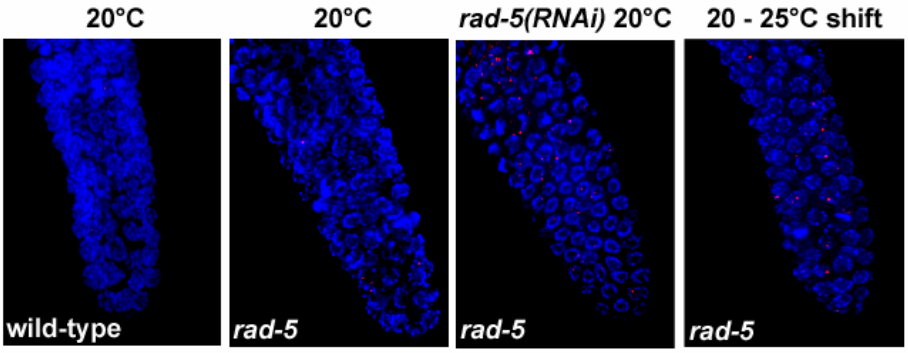

(b)

phenotype	*cdc-7(RNAi) inj.*	*rad-5,cdc-7(RNAi) inj.*	*rad-5,cdc7(RNAi) feed*	*clk-2,cdc-7(RNAi) inj.*
embryonic lethality	0-2%	61,20%	97,80%	63,50%
sterility	0%	7%	n.a.	32%
L1 growth arrest	0%	53,30%	n.a.	40,90%
analysed animals	n=30	n=45	n=20	n=44

phenotype	*mrt-2,cdc-7(RNAi) inj.*	*clk-1,cdc-7(RNAi) inj.*	*him-6*	*him-6,cdc-7(RNAi) inj.*
embryonic lethality	2,10%	0,50%	45%	50%
sterility	0%	0%	0%	0%
L1 growth arrest	0%	0%	0%	0%
analysed animals	n=38	n=22	n=50	n=16

(c)

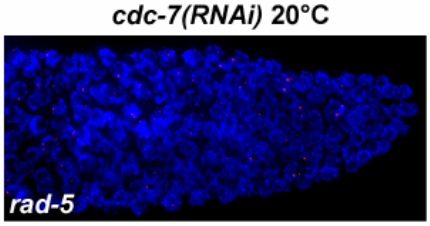

Figure 1-9 (a) Wild type and *rad-5* mutant worms were incubated at the indicated temperatures and/or depleted for RAD-5/CLK-2 by RNAi as indicated. Gonads of these animals were prepared for immunofluorescence staining with polyclonal antiRAD-51 antibody. The distal tip of a representative gonad is shown. RAD-51 forms bright nuclear foci, which were counted and their numbers normalized to the number of germ cells (see 7.1.4.1). (b) Summary of phenotypes of CDC-7 RNAi in different mutant backgrounds (for detail see 7.1.4.2 and Material and Methods). (c) *rad-5* mutants animals were depleted for CDC-7 at 20°C. Immunofluorescence staining was performed as described in (a).

We determined the number of RAD-51 foci in the distal tip of dissected wild-type gonads. We observed an average of 2+/-1.0 RAD-51 foci (normalized to 100 mitotic germ cells), which indicated the presence of spontaneous double strand breaks in proliferating germ cells. This observation is consistent with recent findings in human fibroblast cell lines describing the formation of RAD-51 foci particularly during S-phase (Tashiro 1996). At 20°C gonads from *rad-5(mn159)* and *clk-2(qm37)* animals showed already a slightly elevated number of RAD-51 foci with an average number of 5.7+/-2.5 and 4.5+/-1.8 foci, respectively. After the temperature shift to 25°C the number of RAD-51 foci dramatically increased to 43.1+/-13.6 foci for *rad-5(mn159)* and to 20.0+/-8.0 foci for *clk-2(qm37)* mutants (Figure 1-9a). To confirm that the accumulation of RAD-51 foci is due to the loss of functional RAD-5/CLK-2 at 25°C, we knocked down *rad-5/clk-2* in the *rad-5(mn159)* animals at 20°C by RNAi (see Material and Methods). Indeed, RAD-5/CLK-2 depletion led to an accumulation of RAD-51 foci (44.3+/-13.6 foci) in mitotic germ cells (Figure 1-9a).

The elevated numbers of RAD-51 foci in *rad-5/clk-2* mutants can be explained in two different ways. One obvious explanation is that RAD-5/CLK-2 is required for homologous recombination repair of spontaneous DNA lesions, which occur in proliferating germ cells. In this case loss of RAD-5/CLK-2 might lead to an accumulation of unprocessed DNA repair intermediates that are associated with RAD-51. In addition, the mutator phenotype of *rad-5(mn159)* at 20°C could be explained by a weak genome instability caused by the presence of a few unprocessed DNA repair intermediates. Alternatively, *rad-5/clk-2* mutants are not defective in DNA repair but are partially defective in some aspect of S-phase progression (see model Figure 1-11). A partial defect

in S-phase progression might still allow germ cell divisions to occur but the number of stalled or collapsed replication forks, that ultimately lead double strand breaks, might be increased. Double strand breaks are repaired by homologous recombination in a *rad-51* dependent manner. Thus the accumulation of RAD-51 foci is due to the presence of an increased number of double strand breaks. The elevated steady state level of double strand breaks might then lead to severe genome instability. This hypothesis also favours the model that RAD-5/CLK-2 is needed to maintain genome stability during germ cell proliferation (Figure 1-11).

7.1.5 Analysis of the molecular function of RAD-5/CLK-2

We have described several lines of evidence that RAD-5/CLK-2 has a DNA damage checkpoint function and an essential function in maintaining genome stability and/or during early embryonic development. The molecular function of RAD-5/CLK-2 is still speculative. The first hint as to the molecular function of RAD-5/CLK-2 came from studies with the *S. cerevisiae* homologue Tel2p. *tel-2-1* mutants show a progressive shortening of telomere ends. Moreover, biochemical studies reveal that Tel2p can bind telomeric DNA sequences *in vitro* (Runge and Zakian, 1996). In contradiction to the finding that Tel2p is a telomere binding protein, a GFP-tagged RAD-5/CLK-2 protein localizes to the cytoplasmic compartment (Benard et al., 2001). Subcellular fractionating of human cell lysates revealed a distribution of the human RAD5/CLK2 homologue in a nuclear, cytoplasmatic and membrane bound fraction (Jiang et al., 2003). More recently it has been reported that Tel2p interacts with the protein kinase Cdc7p in a large-scale yeast two-hybrid screen (Uetz et al., 2000). Cdc7p is essential for efficient initiation of DNA

replication in particular the firing of late origins of replication (Bousset and Diffley, 1998; Donaldson et al., 1998; Jiang et al., 1999). Moreover, Cdc7p might have a role in the DNA replication checkpoint, which is activated upon replication stress induced by HU(Costanzo et al., 2003; Takeda et al., 1999; Tercero et al., 2003; Weinreich and Stillman, 1999). In response to HU the DNA damage checkpoint kinase *S.c.Rad53p/*hCHK2 phosphorylates Dbf4p, which is associated with Cdc7p and required for Dbf4p kinase activity (Jackson et al., 1993; Weinreich and Stillman, 1999; Yoon et al., 1993). Hyperphosphorylated Dbf4p attenuates Cdc7p kinase activity thereby slowing down S-phase progression. Given that *C. elegans* CDC-7 is a potential interactor for RAD-5/CLK-2 we aimed to analyse the DNA damage checkpoint function of *cdc-7* and the genetic interaction of *cdc*-7 with *rad-5/clk-2*. Moreover, we wanted to confirm the Tel2p/Cdc7p yeast two-hybrid interaction with the respective *C. elegans* proteins using yeast two-hybrid analysis and *in vitro* binding assays.

7.1.5.1. *cdc-7(RNAi)* causes synthetic lethality in *rad-5/clk-2* mutants

To test a possible DNA damage checkpoint function for the *C. elegans* homologue of *cdc-7*, we inactivated *cdc-7* in wild-type and various checkpoint defective worms using two different RNAi techniques. First, we injected *in vitro* synthesized dRNA corresponding to *cdc-7* into wild type animals. The injected animals (P0 generation) and their offspring (F1 generation) behave like wild-type animals (non-injected control worms) when assayed for embryonic lethality, radiation sensitivity, irradiation induced cell cycle arrest, and apoptosis (Figure 1-9b, and data not shown). Secondly, we confirmed these data by using the RNAi feeding technique (Fire et al., 1998). For this

technique worms are fed with *E. coli,* which synthesize double stranded RNA corresponding to *cdc-7*. No obvious DNA damage checkpoint defects were observed in *cdc-7(RNAi)* F1 and F2 animals (data not shown).

We were not able to detect any checkpoint defects in *cdc-7(RNAi)* animals. It might well be that RNAi was not efficient to fully deplete CDC-7. An alternative possibility is that *cdc-7* has no checkpoint function or *cdc-7* acts in a redundant pathway. Surprisingly, however, when we depleted CDC-7 (by *cdc-7*(dRNA) injection) in the *rad-5(mn159)* and *clk-2(qm37)* worms at 20°C a synthetic embryonic lethality that affects 61.2% and 63.5% of the progeny, respectively, was observed (Figure 1-9b). The synthetic lethality was even more prominent when *rad-5(mn159)* animals were fed with *cdc-7(RNAi)* (97.8% embryonic lethality) (Figure 1-9b). Furthermore, we often observed that some of the hatched embryos arrested in the first larval stage L1 and did not develop to adult animals (Figure 1-9b). We are confident to suggest that the synthetic lethality we observed is specific for *rad-5/clk-2* and *cdc-7* as *cdc-7(RNAi)* RNAi in the DNA damage checkpoint mutants *mrt-2(e2663)*, the DNA replication checkpoint mutant *him-6(e1423)*, and the slow growing mutant *clk-1(e2519)* did not cause synthetic lethality. We further analysed gonads of *rad-5(mn159)cdc-7(RNAi)* animals in immunofluorescence studies. These gonads accumulate RAD-51 foci in germ cells to a comparable level as we observed in *rad-5(mn159)* at 25°C, and *rad-5(mn159)rad-5(RNAi)* at 20°C germ cells (Figure 1-9a and c). Taken together *cdc-7 (RNAi)* knock down in *rad-5(mn159)* mimics the phenotype of *rad-5(mn159)rad-5(RNAi)* and *rad-5(mn159)(25°C)*. Therefore, we assume that *cdc-7* and *rad-5/clk-2* might prevent the accumulation of DNA lesions (most likely double strand breaks), which are repaired by homologous recombination. It would

be of great interest to analyse *rad-5(mn159)cdc-7(RNAi)* embryos for lineage defects such as we described for *rad-5/clk-2* mutants at 25°C.

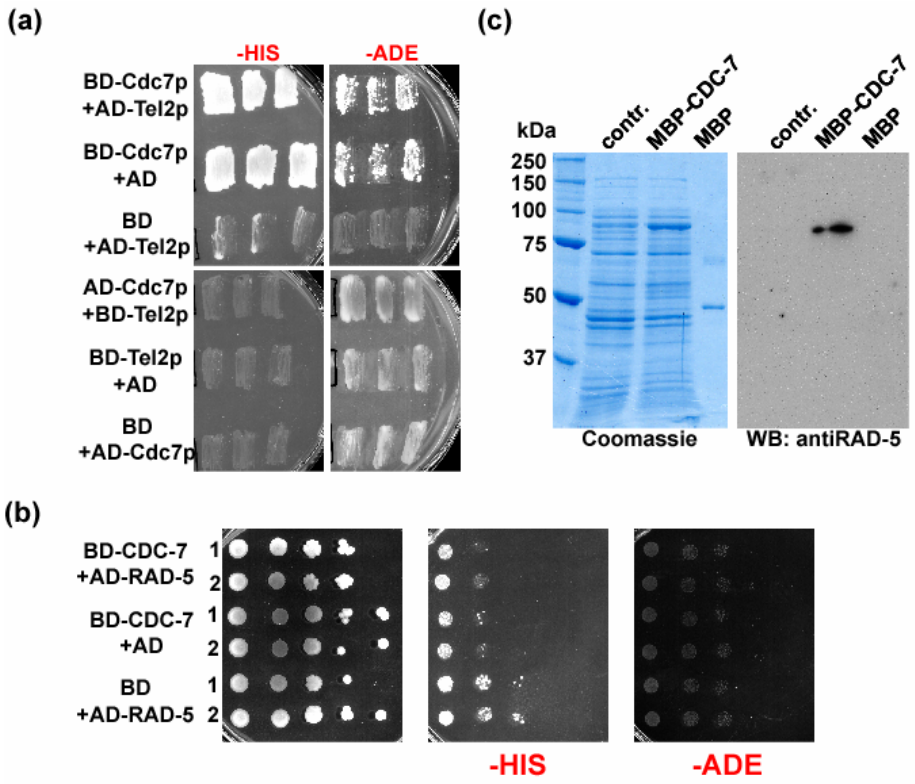

Figure 1-10 Interaction studies between RAD-5/CLK-2 and CDC-7. (a) The yeast two-hybrid system was used to test for protein interaction between CDC-7 GAL4 DNA binding domain (BD) fusions and CDC-7 GAL4 activation domain (AD) fusions with AD-TEL-2 and BD-TEL-2, respectively, by growth on –ADE and –HIS autotrophic plates. **(b)** The yeast two-hybrid system was again used to test the interaction of the *C. elegans* orthologues CDC-7 and RAD-5/CLK-2. No interaction was detected between BD-CDC-7 and AD-RAD-5/Clk-2 fusion proteins **(c)** Far Western Blot analysis. Cell lysate of *E. coli* cells expressing MBP-CDC-7 were separated on a SDS-PAGE gels and transferred to nitrocellulose membrane. This membrane was incubated with purified recombinant RAD-5 protein. Bound RAD-5 protein was detected by Western Blot analysis using a polyclonal antiRAD-5 antibody. As a negative control we used purified MBP-tag and uninduced *E. coli* cell lysate. RAD-5 specifically bound to MBP-CDC-7(line 2). Note, that no RAD-5 could be detected on the negative control samples (line 1 and 3).

After we found a genetic interaction of *rad-5/clk-2* with *cdc-7* we wanted to know if there is a physical interaction between RAD-5/CLK-2 and CDC-7. Uetz et al. published the yeast two hybrid interaction of budding yeast Tel2p with Cdc7p (Uetz et al., 2000). This finding resulted from a large-scale interaction screen. We were not able to confirm the Tel2p/Cdcp7 interaction in our Y2H experimental set up. In fact, in the control experiment Tel2p fused to the activation domain (AD) alone gave a positive signal for an interaction (Figure 1-10a, and see Material and Methods for details). Therefore, it might well be that the published Tel2p/Cdc7p interaction is a false positive. In addition, the *C. elegans* homologues RAD-5/CLK-2 and CDC-7 did not interact in our yeast two-hybrid assay (Figure 1-10b).

We used a second approach to test a RAD-5/CLK-2 interaction with CDC-7. Recombinant CDC-7 fused at its N-terminal end with a maltose-binding-protein tag (MBP) was expressed in *E. coli*, total cell lysate was separated on a SDS-PAGE, and transferred to nitrocellulose. For a Far Western Blot assay, RAD-5/CLK-2 was expressed as a N-terminal GST-fusion protein in *E. coli* and affinity purified under native conditions (see Material and Methods for detail). A nitrocellulose membrane with immobilized MBP-CDC-7 cell lysates was incubated with purified RAD-5/CLK-2 recombinant protein. After several washing steps bound RAD-5/CLK-2 protein was detected by using a polyclonal antibody specific for RAD-5/CLK-2 (Figure 1-10c). Note, that no RAD-5/CLK-2 could be detected in an uninduced *E. coli* cell lysate (Figure 1-10c first line) and purified MBP-tag alone (Figure 1-10c line 3).

These data indicate a possible physical interaction between RAD-5/CLK-2 and CDC-7 *in vitro*. Although, interaction analysis using yeast two-hybrid assays failed to confirm the CDC-7/RAD-5/CLK-2 interaction by Far Western blotting. One explanation

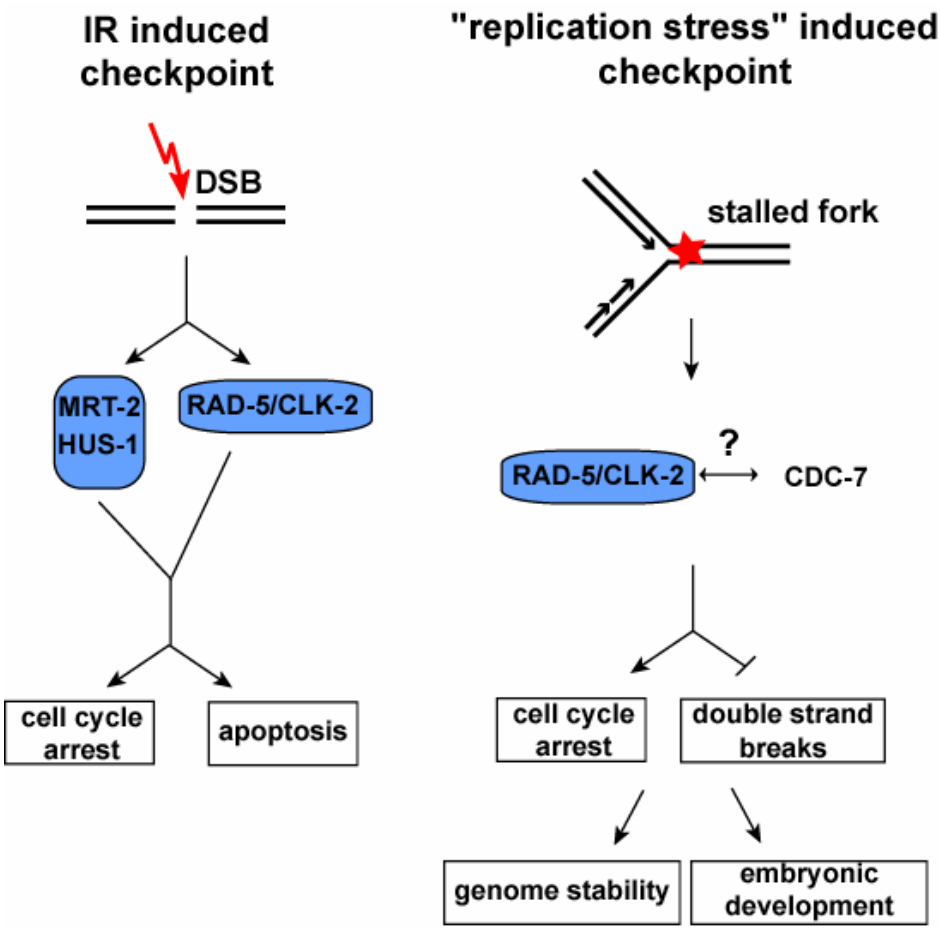

Figure 1-11: Model for RAD-5/CLK-2 checkpoint function: See text for detail

is that the two hybrid fusion proteins of RAD-5/CLK-2 and CDC-7 are not functional and are therefore not able to bind to each other. However, a RAD-5/CLK-2-CDC-7 interaction would support the result of the genetic interaction between *cdc-7* and *rad-5/clk-2*.

To summarize, we have several lines of evidence indicating that there might be an interaction between CDC-7 and RAD-5/CLK-2. Nevertheless data on the genetic and physical interaction of RAD-5/CLK-2 with CDC-7 are very preliminary and a direct role of RAD-5/CLK-2 in a replication checkpoint is only speculative (Figure 1-11). Future experiments will be performed to elucidate the molecular function of RAD-5/CLK-2 in DNA replication and/or replication checkpoint signalling.

7.1.6 Future perspective

An initial bioinformatic analysis of RAD-5/CLK-2 by conventional PSI blast analysis revealed a single homologue of RAD-5/CLK-2 in all eukaryotic species analysed. (Ahmed et al., 2001). Subsequent, more careful protein sequence analysis of RAD-5/CLK-2 and its orthologues in other species, similarly did not reveal any homology to known sequence motives or functional domains that would indicate a molecular function for RAD-5/CLK-2 (Alex Schleifer, IMP Vienna, personal communication). Interestingly, however, structure predictions for secondary structures revealed that RAD-5/CLK-2 is likely to be built up of a tandem array of alpha helical domains. This structural pattern is reminiscent to Armadillo/HEAT repeat proteins (Alex Schleifer, personal communication). Helical repeat proteins like Armadillo/β-catenin or Pds5 often function as a docking station for other regulatory proteins. In the case of Pds5, Pds5 is tethered to the Esp1, a protease involved in the cell cycle specific cleavage of cohesin, which is needed to break chromatid cohesion at the onset of anaphase (for review see (Nasmyth et al., 2000)). Armadillo/β-catenin has been shown to be involved in the regulation of segmental patterns by the Wingless signalling pathway. (for review see (Peifer, 1995;

Peifer, 1993)). Activation of the Wingless signalling pathway leads to the stabilisation and subsequent nuclear transfer of Armadillo/β-catenin protein, which provides a transactivation domain when complexed with the HMG box transcription factor dTCF/LEF-1 and thereby activates expression of epithelial cell proliferation and differentiation genes (Dierick and Bejsovec, 1999).

Given the structural relation between RAD-5/CLK-2 and Armadillo/HEAT repeat proteins we propose a scaffold/adapter function for RAD-5/CLK-2. RAD-5/CLK-2 might dock as a scaffold protein to DNA damage checkpoint and/or DNA repair proteins to facilitate the formation of checkpoint and repair complexes. The identification of *in vivo* composition of RAD-5/CLK-2 complexes under different DNA damage responses might elucidate the molecular function of RAD-5/CLK-2. Experimental tools for the generation of stable worm lines expressing tagged versions of RAD-5/CLK-2 are already available. These worm lines will be used for co-immunoprecipitation experiments and interaction partners of RAD-5/CLK-2 will be identified by mass-spectroscopy. The biological relevance of a putative interaction of a candidate protein with RAD-5/CLK-2 in DNA damage responses can be analysed by RNAi depletion of the candidate protein using DNA damage assays, which have been set up in our lab for cell cycle arrest, apoptosis, and DNA repair. Moreover, the generation of Green Fluorescence Protein (GFP) tagged versions of RAD-5/CLK-2 and its putative interaction partners should allow us to analyse their *in vivo* subcellular localisation, in particular after DNA damage checkpoint activation. Furthermore, these localization studies can be done in different DNA damage checkpoint mutants to analyse the dependence of RAD-5/CLK-2 complex formation on these checkpoint genes. Taken together, *C. elegans* will be a powerful model organism to

identify RAD-5/CLK-2 protein complexes and, more important, to study the *in vivo* function of these complexes in DNA damage response pathways.

RAD-5/CLK-2 is highly conserved with eukaryotes and therefore studies shall not be limited to *C. elegans* but be expanded to other model organisms including yeast vertebrates. Accumulating findings from studies in different model organisms will lead to a better understanding of the molecular function of RAD-5/CLK-2 in future.

7.2. "Genetic and cytological characterization of the recombination protein RAD-51 in *Caenorhabditis elegans*"

7.2.1 Introduction

Meiosis is a specialized cell division that leads to the reduction of the diploid chromosome complement and results in the production of haploid gametes. Compared with mitotic division, the first meiotic division is unique as homologous parental chromosomes associate with each other to enable the reciprocal exchange of corresponding portions and the orderly disjunction of chromosomes.

During meiotic recombination, double-stranded DNA breaks (DSBs) are deliberately generated by the type II topoisomerase-like Spo11p nuclease in order to trigger the exchange of sequences between chromosomes (Bergerat et al., 1997; Cervantes et al., 2000; Dernburg et al., 1998; Keeney et al., 1997; Keeney et al., 1999; Mahadevaiah et al., 2001). In addition to *spo-11*, studies in budding yeast also implicated further genes including the *mre-11* nuclease, which is involved both in DSB generation and processing. Meiotic DSBs are repaired by recombinational DNA repair, which may result in reciprocal recombination (=crossing over). Crossing over produces chiasmata that, in combination with sister chromatid cohesion, allow the formation of stable bivalents. Moreover, crossing over contributes to the genetic variability that underlies evolution.

One of the key enzymatic activities needed for recombinational repair is DNA strand exchange conferred by Rad51p, a homologue of the bacterial RecA protein (Paques and Haber, 1999; Shinohara et al., 1992).To allow for strand exchange, DSBs are

resected such that extended single-stranded 3` overhangs are produced. These single-stranded DNA tracks are loaded with Rad51p and form a nucleoprotein filament (Ogawa et al., 1993) in which single-stranded DNA assumes a stretched configuration that makes it competent to search for and invade a homologous double-stranded DNA sequence to initiate strand exchange. As a consequence of recombinational repair, genetic information is transferred from the template molecule to the repaired DNA molecule.

Meiotic recombination requires the recognition and pairing of homologous chromosomes. In meiotic prophase, two axes representing the two homologous chromosomes start to align at a distance (presynaptic alignment) before they associate intimately via the synaptonemal complex (SC) (Loidl, 1990; Roeder, 1997; Zickler and Kleckner, 1999). In the budding yeast, mouse and *Arabidopsis*, meiotic DSBs were found to precede and to be required for chromosome synapsis (Grelon et al., 2001; Hunter and Kleckner, 2001; Mahadevaiah et al., 2001; Romanienko and Camerini-Otero, 2000). The sites of initial chromosome association are thought to be sites where DSBs are generated. Based on these cytological data it was thus postulated that a RAD-51 nucleofilament invades a complementary DNA sequence on the homologous chromosome, leading to subsequent synapsis. In *Caenorhabditis elegans*, however, DSBs are not a precondition for SC formation (Dernburg et al., 1998)

Several features of the nematode worm *C. elegans* make it a particularly useful model to study the mechanisms underlying DNA damage response, meiotic recombination and meiotic chromosome pairing. Within the gonad cells are organized in a highly polarized way with the most distal end of the ovotestes containing a mitotic stem cell compartment that is followed by cells in different stages of meiotic prophase. Two

states of meiotic chromosome pairing, namely synapsis-independent association (which we refer to as presynaptic alignment throughout the text) and synapsis can be separated by mutational analysis (MacQueen et al., 2002), allowing the assignment of biochemical and genetic events of recombination and pairing to processes at the cytological level by immunolocalization of the respective proteins. In addition, *C. elegans* is a multicellular system that circumvents the intrinsic complication of mammalian systems where deletion of genes involved in meiotic recombination or chromosome pairing results in early embryonic lethality or tends to elicit programmed cell death, which confounds detailed cytological analysis in the respective mutants (Hirao et al., 2000; Lim and Hasty, 1996; Luo et al., 1999; Tsuzuki et al., 1996; Yamaguchi-Iwai et al., 1999)

The *C. elegans* genome project revealed that *C. elegans* has two *RecA* homologues, one of which, Y43C5A.6, is closely related to *rad-51* and termed both *Ce-rad-51* and *Ce-rdh1* (Rinaldo et al., 1998; Takanami et al., 1998).The other *RecA* homolog (C30A5.2), the inactivation of which by RNA interference (RNAi) or by transgene cosuppression did not show a distinct phenotype, is related to mammalian *rad-51C* and was shown to interact with RAD-51 in a two-hybrid (Boulton et al., 2002)Anton Gartner, unpublished). Initial, RNAi-based studies on *Ce-rad-51* suggested that RNAi depletion resulted in low viability of the offspring of worms, in bivalents that appeared not properly condensed, in a meiotic chromosome segregation defect, and in the activation of the DNA damage checkpoint pathway (Gartner et al., 2000; Rinaldo et al., 2002; Rinaldo et al., 1998; Takanami et al., 1998). However, the cytological localization of meiotic recombination enzymes like RAD-51 has not been described in *C. elegans.* To further our understanding of meiosis-associated roles of *rad-51* and their correlation with

meiotic chromosome pairing we embarked on a genetic and cytological analysis of the *C. elegans rad-51* ortholog.

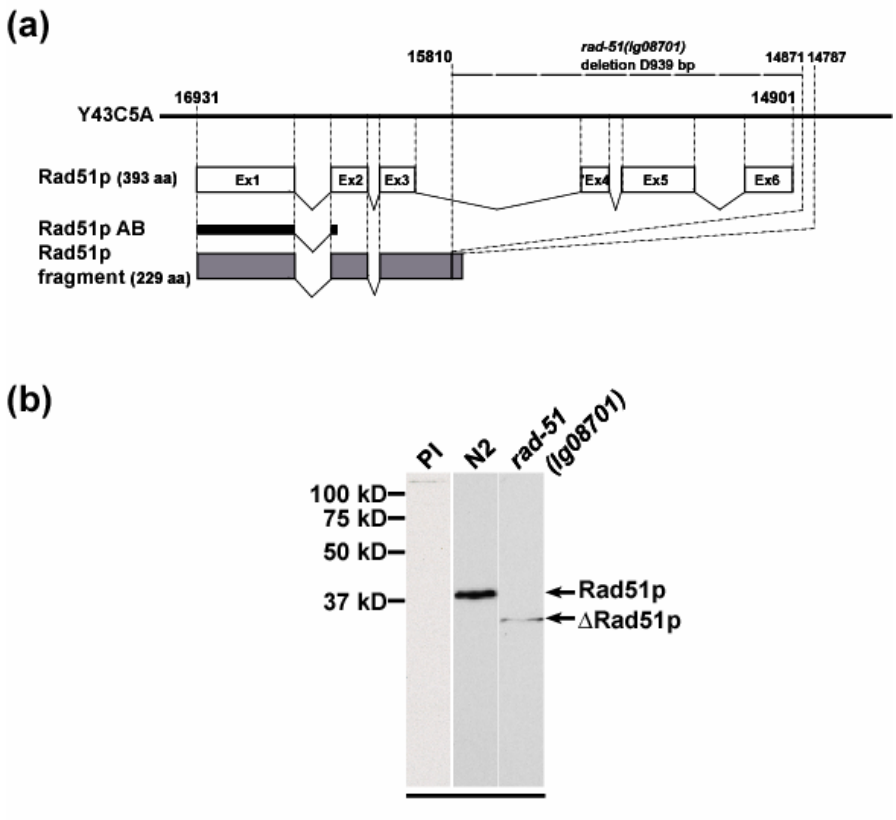

Figure 2-1 (a) Map of the sequence region Y43C5A.6, which encodes RAD-51, with six exons. Also shown are the truncated protein of the *rad-51(lg08701)* allele and the region against which the antibody (*AB*) was raised. The mutation *rad-51(lg08701*) is a 939 bp deletion of the last three exons of rad-51, which contain the conserved domain for ATP-dependent strand exchange activity. **(b)** Immunoblot of *Caenorhabditis elegant* protein extracts. Affinity-purified RAD-51 antibody was used for immunoblot analysis on total worm lysates (protein equivalent of ~50 worms loaded) of wild-type (*N2*) and *rad-51(lg08701)*. With preimmune serum (*PI*) no band is detected. The antibody recognizes a band of M_r 39,000 corresponding to *RAD-51* in wild-type worms (*N2*) and the truncated protein in the mutant

7.2.2 Results

7.2.2.1 Isolation of a *rad-51* mutant

To study the role of *C. elegant* RAD-51 in meiosis we isolated a deletion mutant of the *rad-51* gene using a *C. elegant* deletion library. One 939bp deletion was recovered *(lg08701)* that ablates the last three exons of *rad-51* and includes conserved catalytic domains needed for ATP hydrolysis and DNA strand (Ogawa et al., 1993; Story et al., 1993) (Figure 2-1a). We therefore consider this mutation to be a null allele of *rad-51*. The deletion strain was backcrossed five times to remove secondary mutations and the deletion was linked to *dpy-13*. Furthermore, to analyse the localization of RAD-51, a polyclonal antiserum against the first 103 amino acids of RAD-51 was generated and affinity purified. By immunoblotting, this antibody recognized a distinct band that migrates at a molecular weight of ca. M_r 39,000 and corresponds to the predicted molecular weight of RAD-51*rad-51(lg08701)* worms showed a band of reduced intensity and a size that corresponds to the N-terminal RAD-51 truncation generated by the deletion (Figure 2-1b).

7.2.2.2 Phenotypic analysis of the *rad-51* mutant

We next investigated the biological consequences of the *rad-51* deletion. As is the case with *rad-51(RNAi)* (Rinaldo et al., 1998; Takanami et al., 1998) the deletion of *rad-51* allows the survival of worms. While in *rad-51(RNAi)* animals up to ca 95% embryonic lethality and a high incidence of males had been found, we observed 100% lethality of embryos that were laid by *rad-51(lg08701)* worms. Of 1845 eggs laid by 32 different worms, no live embryos hatched after 2 days at 20°C, whereas in the *dpy13* control 370

embryos hatched from 376 eggs laid by 8 worms (1.6% lethality) under the same conditions. The complete lethality is likely due to the stronger phenotype of the genuine gene disruption as compared with the RNAi phenotype (Takanami et al., 1998). *rad-51(lg08701)* worms developed normally and at a similar pace to wild-type controls, suggesting that there is no major effect of *rad-51* on embryonic or larval cell cycle progression (data not shown).

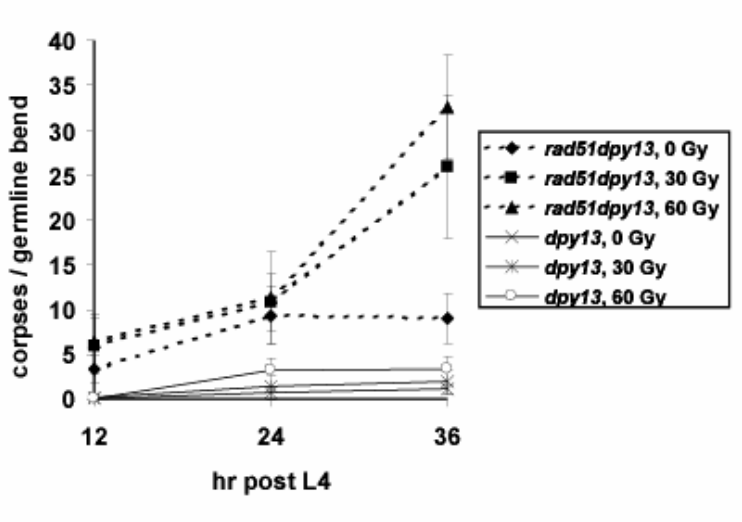

Figure 2-2 Elevated germ cell apoptosis in the *rad-5(lg08701)* disruption without and after irradiation. Late stage L4 hermaphrodites were exposed to 0, 30, and 60 Gy of γ-irradiation and apoptosis was scored 12, 24, and 36 h later as described in Gartner et al. The y-axis indicates the number of dead cells (cell corpses) per gonad arm. 15-20 gonad arms were scored for each data point; *error bars* indicate average deviation.

The *rad-51(lg08701)* disruption led to elevated germ cell apoptosis that was further enhanced by irradiation (Fig. 2-2). This enhanced level of apoptosis is due to the activation of the *C. elegans* DNA damage checkpoint response (most likely due to

unrepaired meiotic DSBs) and does not affect DNA damage-independent "physiological germ cell death" (Gartner et al., 2000; Gumienny et al., 1999). It can be completely suppressed by RNAi with *cep-1* (Schumacher et al., 2001), which encodes the *C. elegans* homolog of mammalian p53. In *rad-51 dpy-13 gfp(RNAi)* we observed 16.7±4.6 cell corpses, but in *rad-51 dpy-13 cep-1(RNAi)* only 1.3±0.8 corpses per gonad (n =10 gonads each). It should be noted that the level of germ cell death in the wild-type control upon irradiation is lower than previously described (Gartner et al., 2000), which is presumably due to the *dpy-13* background, which results in slower germ cell proliferation and hence leads to a lower level of germ cell apoptosis.

7.2.2.3 Meiosis in a *rad-51* mutant

To elucidate the role of RAD-51 in meiosis, we studied chromosome behaviour in the ovotestis of *rad-51(lg08701)* hermaphrodites. Cells at different meiotic stages can be discriminated by their nuclear morphology after staining with the DNA-specific fluorescent dye DAPI and by their presence in easily distinguishable zones along the tubular gonad. To assess meiotic chromosome pairing in *rad-51(lg08701)* worms, the association of homologous chromosomal loci, which were labelled by FISH, was investigated. We found single FISH signals (indicative of chromosome pairing) in transition zone and early and late pachytene cells at a frequency that is comparable to wild type (Figure 2-3a and b). This result indicates that homology recognition and homologous synapsis are unaffected by the absence of functional *rad-51*. In addition, immunoassaying of REC-8, a component of SCs (Pasierbek et al., 2001) revealed the

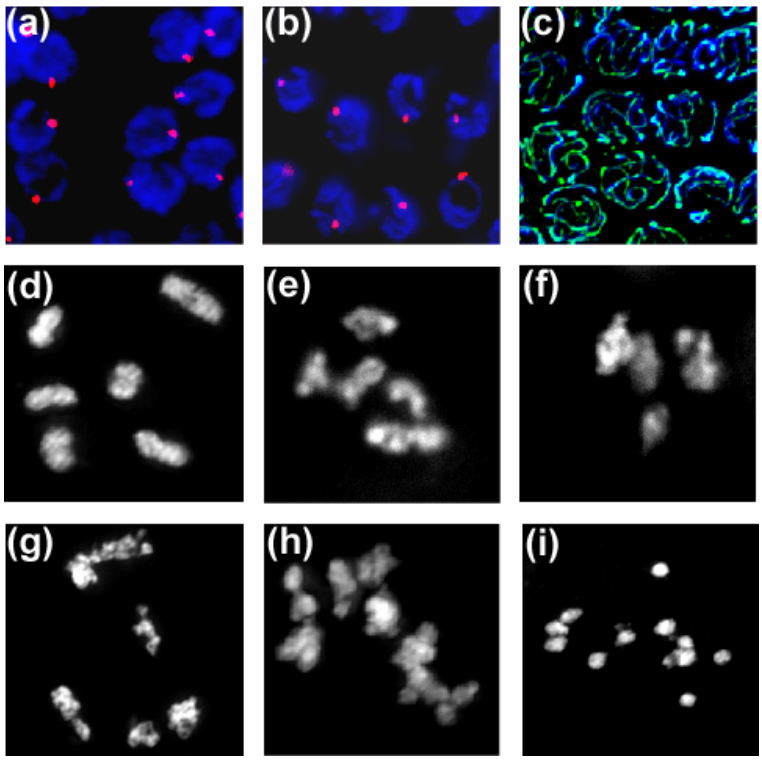

Figure 2-3 Fig. 3A–I. Meiotic phenotypes of *rad-51(lg08701)*. Meiotic chromosome pairing is normal in the mutant. Fluorescence in situ hybridisation (FISH) performed with a probe for a chromosomal region near the left end of chromosome *I*. Most pachytene nuclei show a single or tightly linked doublet FISH signals (*red*) both in the wild type **(a)** and the *rad-51* mutant **(b)** which indicate close alignment of homologous chromosomal regions. DNA was counterstained with 4´,6-diamidino-2-phenylindole (DAPI) (*blue*). **(c)** The mutant is capable of proper synaptonemal complex (SC) assembly. Immunoassaying of *rad-51(lg08701)* pachytene nuclei with the SC component REC-8 (*green*) indicates normal SC formation at pachytene. **(d-i)** Chromosome morphology in wild-type and *rad-51(lg08701)* diplotene/diakinesis (DAPI staining). Whereas in the wild type **(d)** six well-condensed bivalents are formed, in most cells of the mutant corresponding to diplotene-diakinesis, one to several chromatin masses are observed, but occasionally approximately six entities, resembling bivalents, can be resolved. In a subset of nuclei at this stage, more than six structures are present. Twelve well-condensed univalents are formed in old mutant individuals **(i)**. *Bar* represents 5 µm

Wild type appearance of this structure in the *rad-51(lg08701)* mutant (Figure 2-3c). These results suggest that *C. elegans* RAD-51 is required for neither presynaptic alignment, synapsis nor for the proper morphological appearance of the SC.

In most diakinesis nuclei of *rad-51(lg08701)*, chromosomes were clumped together and appeared diffuse. This chromosome phenotype is also elicited by RNAi depletion of RAD-51 (Rinaldo et al., 2002), and it was interpreted as a chromosome condensation defect. Whereas, in the wild type, six well-condensed bivalents are visible at this stage (Figure 2-3d), many nuclei had six weakly condensed bivalents (Figure 2-3e-g). The presence of bivalents is surprising since mutants defective in meiotic recombination are expected to form 12 univalents as chiasmata that hold homologous chromosomes together would be missing. Only a subset of diakinesis nuclei revealed more than six chromatin masses, indicating a failure of chiasma formation (Figure 2-3h). In very old *rad-51(lg08701)* worms (i.e., at the time when they had run out of sperm) we often observed 12 properly condensed univalents (Figure 2-3i), a phenotype that has been previously observed in *spo-11*, *mre-11* and *msh-5* recombination-defective worms (Chin and Villeneuve, 2001; Dernburg et al., 1998; Kelly et al., 2000b). Given the variability of diakinesis phenotypes we wondered whether a small maternally provided pool of RAD-51 might persist in *rad-51(lg08701)* worms and cause variable phenotypes. We therefore performed *rad-51* RNAi in *rad-51(lg08701)* worms. Since we observed similar phenotypes to that of the deletion only (data not shown), we conclude that *rad-51(lg08701)* displays a complete loss of function phenotype with respect to diakinesis. It is possible, however, that the aforementioned second *RecA* homolog of *C. elegans* has a partially redundant function.

7.2.2.4 Immunolocalization of RAD-51 in meiotic cells of wild-type and mutant worms

To characterize further the roles of *C. elegans* RAD-51 we examined the cytological localization of RAD-51 during meiosis. Immunoassaying of RAD-51 showed that it forms distinct round or slightly elongated dots within nuclei of the gonad. We only occasionally observed RAD-51 spots in mitotic cells. No RAD-51 staining was observed in *rad-51(lg08701)* worms or when a pre-immune serum was used (data not shown). However, RAD-51 foci were readily induced in mitotic cells upon irradiation in a dose- and time-dependent manner, similar to the situation in yeast and mammalian cells (Anton Gartner and Arno Alpi, unpublished results). The number of RAD-51 spots was very heterogeneous between cells at comparable stages within one and the same gonad. In a small fraction of nuclei in the mitotic zone 1 or 2 spots occurred (data not shown). In meiotic cells RAD-51 foci appeared in nuclei of the transition zone of the gonad, which corresponds to the leptotene to zygotene stage (Figure 2-4a, Table1). We found that many of the RAD-51 spots were bar-shaped (Figure 2-4a, and insert). This observation is in accordance with the bar-shaped or double Rad51p foci in maize (Franklin et al., 1999). They were interpreted as Rad51p nucleofilaments bridging the distance between two aligned homologs in the course of strand invasion or another recombination intermediate. In nuclei immediately adjacent to the transition zone (which correspond to late zygotene/early pachytene) up to nine RAD-51 spots were present, whereas by late pachytene they were gone (Figure 2-4a).

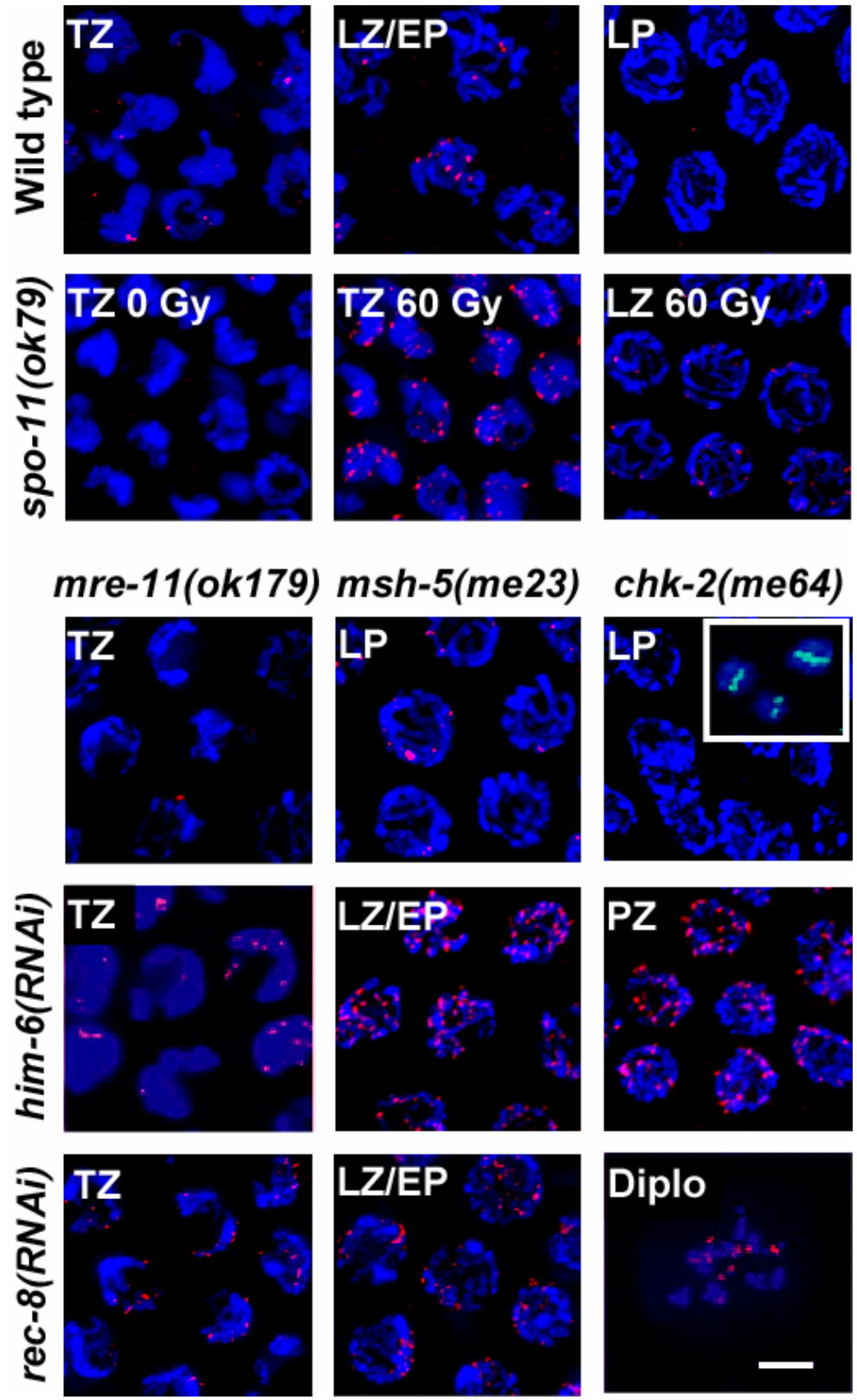
Wild type
TZ
LZ/EP
LP
spo-11(ok79)
TZ 0 Gy
TZ 60 Gy
LZ 60 Gy
mre-11(ok179)
msh-5(me23)
chk-2(me64)
TZ
LP
LP
him-6(RNAi)
TZ
LZ/EP
PZ
rec-8(RNAi)
TZ
LZ/EP
Diplo

Figure 2-4 Fig. 4A–G. Localization of RAD-51 in meiotic nuclei. (a) Immunoassaying highlights distinct chromatin-associated spots (*red*) in wild-type transition zone (*TZ*) and late zygotene/early pachytene nuclei (*LZ/EP*). They are absent from late pachytene nuclei (*LP*). Many of the RAD-51 spots are bar-shaped (*insert*). **(b)** Rad-51 staining of transition zone nuclei in unirradiated (0 Gy) and transition zone and late pachytene nuclei in irradiated (60 Gy) *spo-11* worms. **(c)** RAD-51 staining of *mre-11* transition zone nuclei. **(d)** RAD-51 staining in *msh-5* late pachytene nuclei. **(e)** Rad-51 foci do not form in *chk-2* worms. *Insert* At a later stage well condensed univalents are present whose axes contain REC-8 (*green*). **(f)** Examples of RAD-51 foci in *him-3(RNAi)* worms in transition zone, late zygotene/early pachytene and late pachytene nuclei. **(g)** RAD-51 foci in *rec-8 (RNAi)* worms occur from transition zone to diplotene (*Diplo*). For quantitative data see Table 1. *Bar* represents 5 µm

It has been demonstrated that *C. elegans spo-11* is required to generate meiotic DSBs (Dernburg et al., 1998). To determine whether *spo-11*-dependent breaks are the only targets of RAD-51 in *C. elegans* we analysed the pattern of RAD-51 foci in *spo-11* worms. We found that there were virtually no RAD-51 foci in any meiotic stage (Table 1), indicating that RAD51 associates with DSBs only. Irradiation bypasses the recombination defect of *spo-11* worms, leading to the establishment of bivalents due to

Table 1. Quantification of RAD-51 foci in several genetic backgrounds and meiotic prophase stages of *Caenorhabditis elegans*. Average numbers±SD of RAD-51 foci per nucleus are listed, and the minimum–maximum number per nucleus and the percentage of nuclei showing at least one RAD-51 focus are given in parentheses. The percentages of nuclei in which RAD-51 foci occurred in distinct clusters in the translocation strains (for examples see Figure 2-5b) are given in square brackets. Late zygotene/early pachytene nuclei were classified by their position in three to four rows of cells adjacent to the transition zone. Classification of transition and pachytene zone was according to MacQueen and Villeneuve.

	Transition zone (i.e., leptotene-zygotene)	**Late zygotene/early pachytene zone**	**Mid/late pachytene zone**
Wild type	0.9±1.0, *n* =56 (0–6, 48%)	5.2±1.7, *n* =44 (1–11, 100%)	<0.1, *n* =38 (0–1, 10%)
rad-51(lg08701)	0, *n* =40	0, *n* =44	0, *n* =41
spo-11(ok79)	<0.1, *n* =67 (0–1, 3%)	<0.1, *n* =36 (0–1, 3%)	0, *n* =42
*spo-11(ok79)*Irradiated 60 Gy	13.9±3.4, *n* =41 (6–25, 100%)	21.2±3.8, *n* =57 (12–29, 100%)	11.3±3.1, *n* =38 (3–17, 100%)
chk-2(me64)	<0.1, *n* =35 (0–1, 3%)	<0.1, *n* =60 (0–1, 3%)	0, *n* =39
mre-11(ok179)	<0.1, *n* =35 (0–1, 3%)	<0.1, *n* =50 (0–1, 3%)	0, *n* =50
msh-5(me23)	0.5±0.6, *n* =48 (1–13, 58%)	4.0±1.8, *n* =40 (1–10, 100%)	3.2±1.4, *n* =59 (1–7, 91%)
him-3(RNAi)	3.6±4.5, *n* =38 (0–20, 53%)	18.7±4.9, *n* =41 (9–35, 100%)	17.2±3.1, *n* =40 (10–33, 100%)
rec-8(RNAi)	2.6±3.0, *n* =52 (0–15, 58%)	13.9±2.8, *n* =41 (9–21, 100%)	13.0±2.8, *n* =40 (8–21, 100%)
rec-8(cosuppression)	1.6±1.5, *n* =50 (0–6, 66%)	12.7±3.4, *n* =41 (5–18, 100%)	24.5±5.7, *n* =40 (11–35, 100%)
eT1(II;V)	1.6±1.6, *n* =58 (0–10, 59%)	8.0±2.7, *n* =43 (3–16, 100%) [62%]	8.2±3.3, *n* =44 (0–20, 93%) [75%]
hT1(I;V)	1.2±1.2, *n* =47 (0–6, 63%)	8.5±3.1, *n* =42 (2–18, 100%) [65%]	10.1±4.0, *n* =56 (0–20, 96%) [74%]

the formation of functional chiasmata (Dernburg et al., 1998). As expected, this bypass of *spo-11* function likely depends on *rad-51* as irradiated *spo-11* worms displayed RAD-51 foci (Figure 2-4b).

Likewise, we scored RAD-51 in an *mre-11(ok179)* mutant. While synapsis is normal in this mutant, it shows a meiotic recombination defect. It was proposed that, similar to the situation in yeast, *C. elegans* MRE-11 may have a dual role in DSB generation and processing (Chin and Villeneuve, 2001). In accordance with the putative function of *mre-11* in the generation of meiotic DSBs or in the generation of ssDNA via the resection of DSBs, we only observed background levels of RAD-51 foci in meiotic nuclei of the mutant (Table 1, Figure 2-4c).

We next studied RAD-51 foci in the *msh-5(me23)* mutant, which has a normal SC but which is defective in chiasma formation (Kelly et al., 2000a).*msh-5* encodes the *C. elegans* MutS homolog and genetic evidence indicates that it might act after the initiation of meiotic recombination. We found wild-type levels of RAD-51 foci in transition zone nuclei and in early pachytene nuclei of *msh-5(me23)*. However, these foci persisted longer as compared with wild-type cells and could also be found in late pachytene cells (Figure 2-4d). This result suggests a defect in the processing of recombination intermediates that occurs after RAD-51 focus formation and that leads to the accumulation of RAD-51 foci in pachytene. Foci completely disappeared in diplotene, indicating that DSBs eventually become repaired or that RAD-51 dissociates from breaks.

To investigate the link between DSBs, presynaptic alignment, SC formation and RAD-51 focus formation, we performed RAD-51 immunoassaying in several meiotic

pairing mutants. First, we checked whether RAD-51 is present on chromatin in a *chk-2* mutant. In this mutant presynaptic alignment and SC formation is compromised and transition zone nuclei appear abnormal whereas other aspects of meiosis are normal and 12 well-condensed univalents are formed (MacQueen and Villeneuve, 2001). These univalents possess axes that contain the meiosis-specific cohesin REC-8 (Figure 2-4e, insert). It is not known whether meiotic recombination is initiated in the absence of presynaptic alignment in *chk-2* (MacQueen and Villeneuve, 2001). No RAD-51 foci were found in this mutant (Table 1, Figure 2-4e), suggesting that DSBs either do not occur or are not processed to a recombination intermediate that is a target of RAD-51.

We next studied the effect of HIM-3 depletion by RNAi on RAD-51 focus formation. HIM-3 localizes to chromosomal cores, and in *him-3* hypomorphs both meiotic recombination and synapsis are severely reduced (Zetka et al., 1999). Analysis by FISH confirmed that, upon dsRNA injection (which does not necessarily lead to the complete depletion of HIM-3), synapsis was abolished (data not shown). In *him-3(RNAi)* worms the incidence of RAD-51 foci was dramatically increased and a large number of RAD-51 foci persisted even in pachytene cells (Table 1, Figure 2-4f), suggesting that DSBs are formed abundantly on chromosomes that are not synapsed. Interestingly, we did not observe an elevated level of programmed cell death in *him3(RNAi)* worms. There was an average of 0.88 to 1.2 corpses per gonad in four independent *him-3* RNAi depleted worm lines, which is similar to the amount of dead cells in the wild type (Gartner et al., 2000). This result indicates that in *C. elegans* programmed pachytene cell death is not triggered by synaptic failure or by the large excess of DSBs in *him3* worms. Since RAD-51 spots disappeared in diplotene, we assume that DSBs are eventually

repaired even in the absence of synapsis or that RAD-51 protomers finally dissociate from the sites of breaks.

To corroborate further the finding that synapsis is required to remove RAD-51 spots, we analysed the cytological behaviour of RAD-51 foci in *rec-8(RNAi)* and *rec-8(cosuppression)* worms. *rec-8* encodes a meiotic cohesin that is localized at chromosomal axes and between sister chromatids. Depletion of REC-8 by RNAi leads to a defect in SC formation, whereas presynaptic alignment is maintained. Furthermore, it was suggested that meiotic DSBs remain unrepaired in *rec8* as chromosomal fragments can be detected at diplotene (Pasierbek et al., 2001). To see whether RAD-51 foci persist at unrepaired DSBs, we investigated the number of RAD-51 foci in *rec-8(RNAi)* and *rec-8(cosuppression)* worms. The number of RAD-51 spots in the transition zone was increased and a dramatically increased number of spots persisted into pachytene (Table 1). RAD-51 foci remained associated with chromatin even up to the late diplotene stage (Figure 2-4g). Only at diakinesis did the RAD-51 foci disappear, which suggests that DSBs are repaired by a mechanism that does not require the sister or the homolog as template or that they remain unrepaired but RAD-51 dissociates from these sites after some time.

To exclude the possibility that RAD-51 foci persist in the absence of HIM-3 and REC-8 owing to compromised axial element structure rather than owing to genuine defects in meiotic synapsis, we abolished synapsis by inactivating *syp-1*, which encodes a structural element of the transverse filaments of the SC (MacQueen et al., 2002). Consistent with the notion that SC formation is required for the removal of RAD-51 foci, we found that numerous RAD-51 foci persist in the nuclei of the late pachytene zone of

syp-1(RNAi) animals (data not shown). The *him-3*, *rec-8* and *syp-1* deficiency situations demonstrate that in the absence of synapsis RAD-51 remains associated with chromatin.

To test further whether SC formation is sufficient to remove RAD-51, we employed the heterozygous translocation strain *eT1 (III;V)*. In this strain, the right arm of chromosome *III* and the left arm of chromosome *V* are reciprocally exchanged (Edgley et al., 1995). Studies employing FISH probes indicated that presynaptic alignment occurs between homologous sequences even if those sequences are on separate chromosomes as is the case in the *eT1 (III;V)* translocation (Loidl et al) (for illustration see Figure 2-5a). Subsequently SC formation is initiated from the non-translocated part of homologous chromosomes and non-homologous SCs are possibly formed at the translocated areas of the affected chromosomes (Loidl, 1990). Consequently, two unsynapsed or non-homologous SC tracts are present in pachytene nuclei within the reciprocally translocated areas of chromosomes *III* and *V*. Immunostaining with RAD-51 revealed the presence of numerous RAD-51 foci (Table 1), which tended to be arranged in a string-like or clustered arrangement in two distinct areas of the nucleus (Figure 2-5b). These results suggest that RAD-51 foci persist in unsynapsed or in non-homologously synapsed regions of the genome. The results obtained with the analysis of *eT1 (III;V)* were also confirmed by the analysis of another reciprocal translocation, *hT1(I;V)* (Table 1).

7.2.3 Discussion

RAD-51 protein accumulates in spots in nuclei undergoing DSB repair

We found that ~0–11 distinct RAD-51 foci occur in transition zone nuclei (corresponding to leptotene/zygotene) and in early pachytene nuclei of wild-type worms. By late

pachytene, all RAD-51 foci were gone (Table 1). The presence of RAD-51 in early meiotic prophase nuclei is in agreement with the established role of the protein in the processing of meiotic DSBs (Paques and Haber, 1999) that occurs around the zygotene

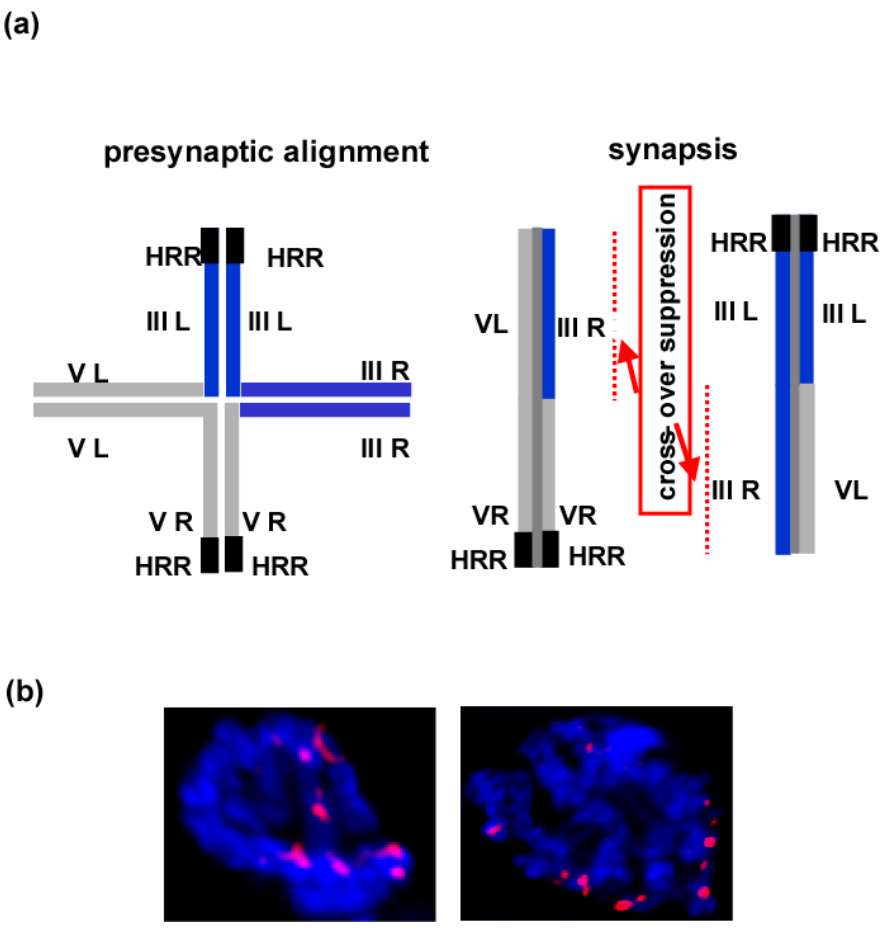

Figure 2-5 RAD-51 foci persist in heterozygous translocation strains. (a) Model of chromosome pairing during presynaptic alignment and synapsis in the *eT1* translocation. During presynaptic alignment homologous DNAs associate irrespective of whether they are on homologous chromosomes or not. Synapsis starts from homologous recognition regions (*HRR*) and extends into non-homologous regions that are crossover suppressed. **(b)** Two examples of late pachytene cells in worms bearing heterozygous *eT1* translocations. RAD-51 foci are indicated as *red dots*.

stage in yeast (Allers and Lichten, 2001; Hunter and Kleckner, 2001). No RAD-51 spots were present in DSB-deficient *spo-11* mutant worms, confirming evidence from other organisms that RAD-51 protein is associated with meiotic DSBs only (for review see (Masson and West, 2001). Similarly, we did not find RAD-51 spots in *mre-11* mutants, confirming that *C. elegans* MRE-11 is required to produce or to process meiotic DSBs. The timing of RAD-51 focus formation resembles the situation in budding yeast where Rad51 dissociates from chromosome axes during incipient SC formation (Bishop, 1994). Similarly, immunolabeling of RAD-51 in a variety of organisms has in general revealed similar dynamics: appearance in leptotene or zygotene, maximal abundance in zygotene, and reduction in pachytene (Ashley et al., 1995; Barlow et al., 1997a; Franklin et al., 1999; Moens et al., 1997; Plug et al., 1996; Tarsounas et al., 1999; Terasawa et al., 1995).

RAD-51 foci are remarkably rare in *C. elegans* wild-type meiosis

In budding yeast, mouse, lily and maize, several tens to hundreds of RAD-51 foci were counted in leptotene to early pachytene nuclei where they decorate the axes of unsynapsed chromosomes (Ashley et al., 1995; Bishop, 1994; Franklin et al., 1999; Tarsounas et al., 1999; Terasawa et al., 1995). In lily and mouse it was shown that RAD-51 foci colocalize with early nodules (Anderson et al., 1997; Tarsounas et al., 1999) that mark the sites of first convergence of homologs undergoing presynaptic alignment . In *Saccharomyces cerevisiae* it has been proposed that the axial elements of homologs converge and synapsis initiates at the sites of interchromosomal recombination(Agarwal and Roeder, 2000; Chua and Roeder, 1998). The observed number of these sites (~57 as scored by the localization of Zip3p; (Agarwal and Roeder, 2000) corresponds well with

the maximum number (64) of RAD-51/Dmc1p foci (Bishop, 1994) although both are less frequent than the estimated mean number of 75–90 crossovers per nucleus (Agarwal and Roeder, 2000; Jacobson et al., 1975), not to speak of recombination events if non-crossover outcomes are included. However, this difference could be explained by the tendency of RAD-51 foci to fuse and/or by the asynchronous occurrence of RAD-51 foci. Compared with the organisms mentioned, the number of meiotic RAD-51 foci per nucleus (0–11) is remarkably low in *C. elegans,* and on average there may be less than one focus per chromosome that can be observed at any given time. Asynchronous formation or conglomeration of DSBs/RAD-51 foci may only partially explain their sparseness. It is tempting to speculate that in *C. elegans,* since there is no requirement for DSBs to promote SC formation, only relatively few DSBs occur in addition to those that are resolved as crossovers and result in the six chiasmata per cell. On the other hand, we observed up to 35 RAD-51 spots in synapsis-defective mutants and up to 20 RAD-51 spots in translocation strains where approximately 20% of the genome does not form homologous SCs. This increased number of RAD-51 foci might be due to the accumulation of RAD-51 foci in the continued absence of synapsis (see below).

RAD-51 foci are removed from homologously synapsed chromosomes

RAD-51 foci accumulate in pachytene cells that are incapable of homologous synapsis due to the depletion of *him-3, rec-8* and *syp-1* (MacQueen et al., 2002; Pasierbek et al., 2001; Zetka et al., 1999). In addition, it has been shown for *him-3* and *syp-1* hypomorphs that they are severely defective in meiotic recombination(MacQueen et al., 2002; Zetka et al., 1999). These results are in accord with previous experiments from budding yeast

where RAD-51 foci persist in mutants devoid of an SC (Bishop, 1994). Our data also demonstrate that meiotic DSBs originate independently of SC formation and they are compatible with the evidence derived from other organisms that in the wild type DSB formation and processing by a RAD-51-dependent pathway precede synapsis (Bishop, 1994). In addition, the appearance of RAD-51 foci in leptotene/zygotene nuclei in wild-type *C. elegans* confirms that DSB formation occurs prior to chromosome synapsis, although it is not a precondition for the latter in this organism (Dernburg et al., 1998).

RAD-51 spots, mostly arranged in clusters, also persisted into pachytene in the two heterozygous translocation strains investigated. Crossing over does not occur in the translocated chromosome regions, for which reason they are widely used as genetic balancers (Edgley et al., 1995). We suspect that RAD-51 spots remain attached to the affected arms because they do not synapse homologously. There is evidence from electron microscopy that synapsis, which is initiated in the homologous (homology recognition region-bearing) portions of translocation chromosomes, continues into the adjacent non-homologous regions, since Goldstein 1986 reported the presence of six linear, unforked SCs in a heterozygous translocation strain. This raises the possibility that some of the regions where RAD-51 foci persist are non-homologously synapsed, which would mean that synapsis needs to be homologous for RAD-51 foci to disappear. Thus, our experiments suggest that within the framework of homologous SCs, DSBs are subject to recombinational repair and are no longer a substrate of RAD-51.

While RAD-51 foci form in mutants that do not initiate synapsis, we did not observe RAD-51 foci in the *chk-2* mutant where initial homology recognition (as indicated by presynaptic alignment) fails (MacQueen and Villeneuve, 2001). Thus, unlike

in budding yeast where the initiation of recombination is independent of the interaction of homologs (de Massy et al., 1994; Gilbertson and Stahl, 1994) successful homology recognition might be a precondition for DSB formation or RAD-51 recruitment to DSBs in *C. elegans*.

Double-strand breaks do not necessarily trigger apoptosis

Our *rad-51* deletion mutant displayed an elevated level of germ cell death, which triggers the DNA damage-dependent, p53-suppressible apoptotic pathway, presumably as a consequence of unrepaired meiotic DSBs. Thus, similar to mammalian systems, meiotic failure can trigger a DNA damage checkpoint pathway that requires p53 for the activation of programmed cell death (Barlow et al., 1997b). On the other hand, in *him-3(RNAi)* and *rec-8(RNAi)* synapsis-defective worms and in worms bearing translocation chromosomes, where RAD-51 foci accumulate, programmed cell death is not elicited. These results imply that the *C. elegans* pachytene checkpoint does not respond to all DSBs. Furthermore, our results suggest that the pachytene checkpoint does not sense the failure to synapse homologous chromosomes properly.

Depletion of RAD-51 causes diffuse chromatin and univalent formation in diakinesis

Analysis of diakinesis nuclei of *rad-51* mutants revealed a variable phenotype mostly comprising diffuse masses of chromatin that were difficult to tell apart. This phenotype was similarly observed by the depletion of *rad-51* by RNAi (Rinaldo et al., 2002; Takanami et al., 1998). Quite often six diffuse masses of chromatin could be discerned, indicating the formation of bivalents. This result is remarkable, because the *rad-*

51(lg08701) allele has to be considered a null mutation and the phenotype of *rad-51(lg08701)* could not be enhanced by *rad-51(RNAi)*. After the disappearance of the SC at the end of pachytene, homologous contacts are believed to rely on the exchange of DNA strands at incipient chiasmata. The occurrence of bivalent-like structures in *C. elegans* suggests that, whatever kind of DNA interactions are taking place in the absence of RAD-51, they are sufficiently robust to maintain the physical association between the majority of homologs. Although the diffuse appearance of diakinesis chromatin has been interpreted as a condensation defect, it possibly could also arise due to massive DNA fragmentation that occurs due to the generation of many meiotic DSBs that cannot be repaired in *rad-51* mutants. This notion is supported by the recent finding of Rinaldo et al. 2002 according to which the diffuse appearance of pachytene chromatin is suppressed in *rad51(RNAi) spo-11* and *rad51(RNAi) mre-11* strains, which contain nicely condensed univalents, presumably because they fail to generate meiotic DSBs. Furthermore, irradiated diakinesis nuclei of *mre-11* worms look similar to *rad-51*, likely because breaks that are generated upon irradiation cannot be repaired (Chin and Villeneuve, 2001). If one assumes that many *spo-11*-dependent DSBs per chromosome are generated during meiosis, one can also explain the 100% lethality we observed in the progeny of *rad-51* worms. In this case, embryonic lethality would not only be caused by aneuploidy due to random meiotic chromosome segregation (that would by chance result in rare surviving embryos with a correct chromosome set), but also by abundant chromosome breaks that are generated by SPO-11 but cannot be repaired properly in the absence of RAD-51. Since we occasionally observed 12 nicely formed univalents in very old *rad-51* worms, we speculate that in old worms where oocytes are not fertilized anyway, the

incidence of SPO-11-generated DSBs is reduced.

7.3 "Multiple genetic pathways involving the *C. elegans* Bloom's syndrome gene *him-6, mre-11, rad-51* and *top-3* are needed to maintain genome stability in the germ line."

7.3.1 Introduction

Mutations in three genes encoding human recQ helicases BLM, WRN and recQ4 are associated with distinct clinical disorders namely Bloom's syndrome (BS), Werner's syndrome (WS) and Rothmund-Thomson syndrome (RTS) (Ellis et al., 1995; Kitao et al., 1999; Yu et al., 1996), respectively. BS is characterized by an elevated risk for a wide variety of cancers, immunodeficiency, slow growth, male sterility and female sub-fertility (German, 1993). Furthermore, BS cells exhibit a hyper recombination phenotype, greatly enhanced reciprocal exchanges between sister chromatids, as well as chromatid gaps and breaks. These phenotypes are consistent with recent evidence from *Drosophila* that BLM might be required for synthesis dependent double strand annealing (SDSA) (Adams et al., 2003). WS and RTS are both associated with cancer predisposition, and WS with premature aging (Shen and Loeb, 2000; Vennos and James, 1995). The fact that patients suffering from these syndromes are prone to develop cancers shows the importance of the role played by the RecQ family of helicases in the maintenance of genome stability and the prevention of tumorogenesis.

The prototypic recQ helicase is *E. coli* RecQ. RecQ is a component of the RecF pathway, which is a pathway required for recombinational repair, essential for nearly all non-double strand break recombination in *E. coli* (Nakayama et al., 1985; Smith, 1991). Because of its helicase activity that can unwind DNA at broken ends, the RecQ protein

together with the RecJ 5′-3′ nuclease was proposed to act as functional analogs of the RecBCD helicase/nuclease in the RecBCD pathway during recombination repair (Harmon and Kowalczykowski, 1998).

In budding yeast, Sgs1p plays a key role in regulating mitotic recombination and functions in the S-phase checkpoint response (Frei and Gasser, 2000a; Watt et al., 1996). When expressed in yeast, the human BLM and WRN proteins are able to partially suppress the mitotic recombination defects of *sgs1* mutants (Yamagata et al., 1998), suggesting that the function of Sgs1p and its human counterparts are evolutionarily conserved. The phenotype of *sgs1* mutants includes a slight reduction in growth rate, a 10-fold increase in chromosome missegregation, an elevated mitotic recombination frequency, a high sensitivity to methyl methanesulfonate (MMS) and hydroxyurea (HU) (Frei and Gasser, 2000b; Yamagata et al., 1998) and premature aging as a consequence of an increased number of extrachromosomal rDNA circles in the cell (Gangloff et al., 1994; Sinclair and Guarente, 1997; Watt et al., 1995; Watt et al., 1996). More recently, it was found that *sgs1* mutants display defects related to meiotic recombination (Gangloff et al., 1999). In addition, Sgs1p acts redundantly with the budding yeast helicase Srs2p, which has been shown to inhibit loading of Rad51p onto ssDNA *in vitro* (Krejci et al., 2003). *In vitro*, Sgs1p interacts physically with Top3p (Gangloff et al., 1994). Top3p is a type I topoisomerase that catalyses passage of two DNA double strands through each other for two consecutive break and rejoining cycles, one single strand at a time (Wang, 2002). In humans, an association between BLM and topoisomerase IIIα was observed in somatic and meiotic cells. The importance of this association was corroborated by their interaction *in vitro* (Johnson et al., 2000; Wu et al., 2000). In budding and fission yeast

mutations in *sgs1* act as suppressors of the slow growth phenotype of *top3* (Gangloff et al., 1994; Laursen et al., 2003). It has been proposed that Top3p acts on substrates created by Sgs1p. Similarly to Sgs1p, Top3p is involved in regulating the levels of mitotic recombination(Gangloff et al., 1994).

To better understand the *in vivo* function of the Blooms syndrome gene as well as its genetic interactions with *top-3*, *mre-11* and *rad-51* in a multicellular system we undertook a comprehensive analysis of the mitotic and meiotic roles of the *C. elegans* ortholog of the human Blooms syndrome RecQ-like helicase. *C. elegans* provides several advantages to study the function of the BLM ortholog. It is a multicellular animal that circumvents intrinsic complications of mammalian systems including phenotypes associated with gene disruptions of recombination genes like early embryonic lethality or programmed cell death at early meiotic stages both of which confound a detailed cytological analysis in the respective mutants (Hirao et al., 2000; Lim and Hasty, 1996; Luo et al., 2000; Tsuzuki et al., 1996; Yamaguchi-Iwai et al., 1999). Several features of the adult *C. elegans* germ line make it a powerful system for the cytological and genetic dissection of meiotic recombination and DNA damage responses. Within the *C. elegans* gonad cells are organized in a highly polarized way. The distal end of the ovotestes contains a mitotic stem cell compartment that is followed by cells in different stages of meiotic prophase. Within a dissected gonad both mitotic cells as well as distinct stages of meiotic chromosome pairing can be observed. In response to DNA damage, checkpoint pathways cause cell cycle arrest of mitotic germ cells and apoptotic death of meiotic pachytene cells (Ahmed et al., 2001; Gartner et al., 2000; Hofmann et al., 2002; Schumacher et al., 2001).

There are four recQ-like helicases encoded by the *C. elegans* genome. Here we show that *him-6* (for high incidence of males) encode the worm ortholog of the human Bloom's syndrome protein. Homozygous *him-6* loss-of-function mutants are radiation sensitive and are partially defective in S-phase-checkpoint function and ionising radiation-induced apoptotic checkpoint response. *him-6* mutants exhibit a decrease in the levels of meiotic crossover recombination and an altered pattern of RAD-51 recombination-foci, suggesting defects in the progression of meiotic crossover recombination. *him-6*, *mre-11*, and *top-3* act redundantly to maintain genome stability in mitotic germ cells and, in contrast to the situation in yeast, mutations in both *him-6* and *top-3* lead to mitotic catastrophe during division of the germ cells. Mitotic catastrophe and massive accumulation of RAD-51 foci in *top-3(RNAi)him-6* worms depend on *rad-51* but not on *mre-11* or *spo-11*. These data as well as the presence of RAD-51 foci in irradiated *mre-11* worm cells further suggests that *mre-11* acts in parallel or downstream of *rad-51* in repairing double strand breaks. Besides, we also show that topoisomerase IIIα by itself acts during meiotic recombination at a step after the initiation of meiotic recombination.

7.3.2 Results

7.3.2.1 *him-6* encodes the *C. elegans* homolog of the human Bloom's syndrome protein

The two alleles of the *him-6*, *e1423* and *e1104,* cause phenotypes indicative of meiotic defects including a high percentage of males among the viable progeny (10 % and 4.2 % respectively) and reduced viability (47 % and 83.4 % viable embryos respectively). A

high incidence of XO males among the self-fertilization progeny of XX hermaphrodites (known as the Him phenotype) and an increased embryonic lethality can indicate a defect in meiotic chromosome segregation. *him-6* maps close to the genomic sequence (T04A11.6) encoding a RecQ-type of DNA helicase. Since recQ helicases have been implicated in genome stability we tested whether or not T04A11.6 corresponds to the *him-6* locus. Sequence analysis revealed that each of the two alleles *e1423* and *e1104* had a point mutation within the sequence of T04A11.6 (Figure 3-1a). The mutation associated with the strong allele, *e1423,* is a T to A transversion resulting in a premature termination of translation at codon 479, half way through the helicase domain, whereas the weaker allele, *e1104,* contains a G to A transition causing G to Q substitution at codon 561, a highly conserved position in the helicase domain. Furthermore, a 1687bp deletion in the *him-6* locus *(ok412)*, recovered by the International *C. elegans* Gene Knockout Consortium (Figure 3-1a), removes 5 exons encoding the entire helicase domain and causes reduced viability and a high incidence of males (54 % viable embryos, 11.7 % males), comparable to the phenotype of the *e1423* allele (47 % viable embryos, 10 % males). Altogether these data confirm that T04A11.6 corresponds to *him-6*. Furthermore, they suggest that the severe alleles *e1423* and *ok412* are null alleles and that the amino acid substitution in the *e1104* mutant leads to a partial loss of function of the *him-6* gene. Using RACE (5' rapid amplification of cDNA ends) and EST sequencing (Kohara, 1996) we characterized a 3.1 kb *him-6* cDNA trans-spliced to the SL1 splice leader (Blumenthal, 1995)(Figure 3-1a). The helicase domain of HIM-6 (accession number AY095296) is most similar to that of the human Bloom's syndrome protein, a member of the recQ family of DNA helicases (53% of identical amino acids) and is also closely

related to other members of the BLM subgroup of recQ helicases including the *D. melanogaster* Dmblm, the *S. cerevisiae* Sgs1p, the *S. pombe* RQH1 and the *E. coli* RecQ proteins (Figure 3-1b). Outside the helicase region, HIM-6 show little sequence similarity with the Bloom's syndrome protein except for conserved features, such as an enrichment in charged and polar amino acids, especially serines, and patches of acidic residues

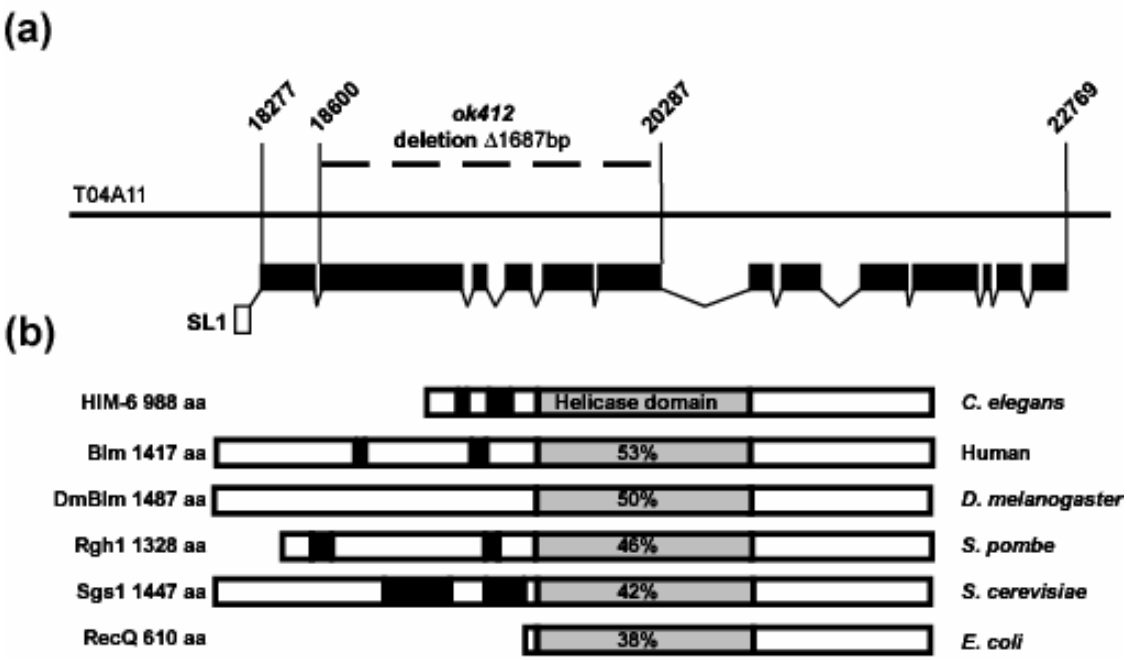

Figure 3-1 *him-6* encodes a recQ-like helicase. **(a)** *him-6* gene structure. The mutation *him-6(ok412)* is a 1687 bp deletion of 5 exons. The numbers indicate the nucleotide position in the cosmid T04A11. **(b)** Schematic representation of the members of the BLM subgroup of recQ-like DNA helicase; the name of the gene product and the length in aa. is shown on the left and the organism on the right. Helicase domains are shown as grey boxes; acidic domains are shown as black boxes. The proteins were arranged by aligning the helicase domains. The % values indicate the level of conservation throughout the helicase domain between HIM-6 and its counterparts in other organisms. Arrowheads indicate residues mutated in *him-6* alleles: K479Stop in e1423 and G561Q in e1104. HIM-6 accession number: AY095296.

(Figure 3-1b) present in the N-terminus. Furthermore domains with low levels of amino acid conservation are found at the C-terminus (Morozov et al., 1997), including a putative nuclear localization signal (aa 939-954) (Kaneko et al., 1997). In summary, the data indicate that *him-6* is the *C.elegans* ortholog of the Blooms syndrome gene.

7.3.2.2 *him-6* is required for normal levels of recombination during meiosis

A Him phenotype coupled to reduced viability is characteristic for mutations causing an increased level of chromosome nondisjunction. We have examined whether chromosome nondysjunction was due to a decrease in the number of chiasmata, which are the consequences of meiotic recombination. In wild-type worms, germ cells proliferate in the distal portion of the gonad. After passing through a transition zone marking the onset of meiotic prophase, they progress through an extended pachytene region and enter diplotene/diakinesis, staying in diakinesis until oocyte maturation is induced (Figure 3-2a). At the final stage of meiotic prophase six DAPI-stained bodies, corresponding to desynapsed homologous chromosomes physically linked by chiasmata are visible (Figure 3-2b). In *him-6* mutants the nuclei contained a mixture of bivalents and achiasmatic chromosomes (univalents) that formed smaller stained bodies (Figure 3-2b). The average number of DAPI-stained bodies was 6.01±0.01 (n=78) in wild type, 7.36 ± 0.14 (n=50) in *e1423*, 7.22±0.12 (n=60) in *ok412* and 6.35 ± 0.09 (n=45) in *e1104*. This result indicated that the high percentage of male and non-viable progeny in the *him-6* mutant was caused by a reduced number of chiasmata, which are necessary for proper chromosome segregation. The reduced number of chiasmata in *him-6* mutants suggested a defect in the meiotic recombination process. Indeed, a general decrease in the level of meiotic

recombination was suggested by previous experiments measuring recombination on chromosome I using the severe allele *e1423 (Zetka and Rose, 1995b).* To further examine levels of recombination, we analysed two intervals on chromosomes I and X using the *e1423* and *e1104* alleles (Table 1). In *e1104* animals, crossing-over was reduced in only one of the four intervals tested. However, for the allele *e1423,* a 25 % to 50% decrease in crossing-over frequency was observed in all intervals tested. The reduction in crossing-over frequency was consistent with the number of univalents observed in the two alleles and with the idea that the loss of function of *him-6* causes decreases in the level of meiotic crossing-over.

A second approach to analyse meiotic recombination was used. We dissected intact germ lines from worms and stained the germ cells with an antibody against RAD-51. RAD51 is a member of the recA-strand exchange protein family and catalyses the invasion of DNA single-strand overhangs into a recipient double-stranded DNA initiating recombination (Bishop et al., 1992; Rinaldo et al., 2002; Roeder, 1997; Takanami et al., 1998). RAD-51 foci are indicative of ongoing meiotic recombination in *C. elegans* (Alpi et al., 2003). They start to appear in transition zone nuclei and reach their maximal abundance in early pachytene nuclei in wild type and *him-6* animals carrying the mutations *e1423* and *ok412* (Figure 3-2c). However, unlike in wild-type worms RAD-51 foci often persist in late pachytene in *him-6* mutant worms and accumulate prominently in *him-6* worms containing two or more univalent in diakinesis (Figure 3-2c). To test whether defects in chromosome pairing and SC formation may be responsible for the persisting RAD-51 foci in *him-6* mutants, we stained the germ line nuclei with an antibody against HIM-3, a meiotic chromosome core component (Zetka et al., 1999).

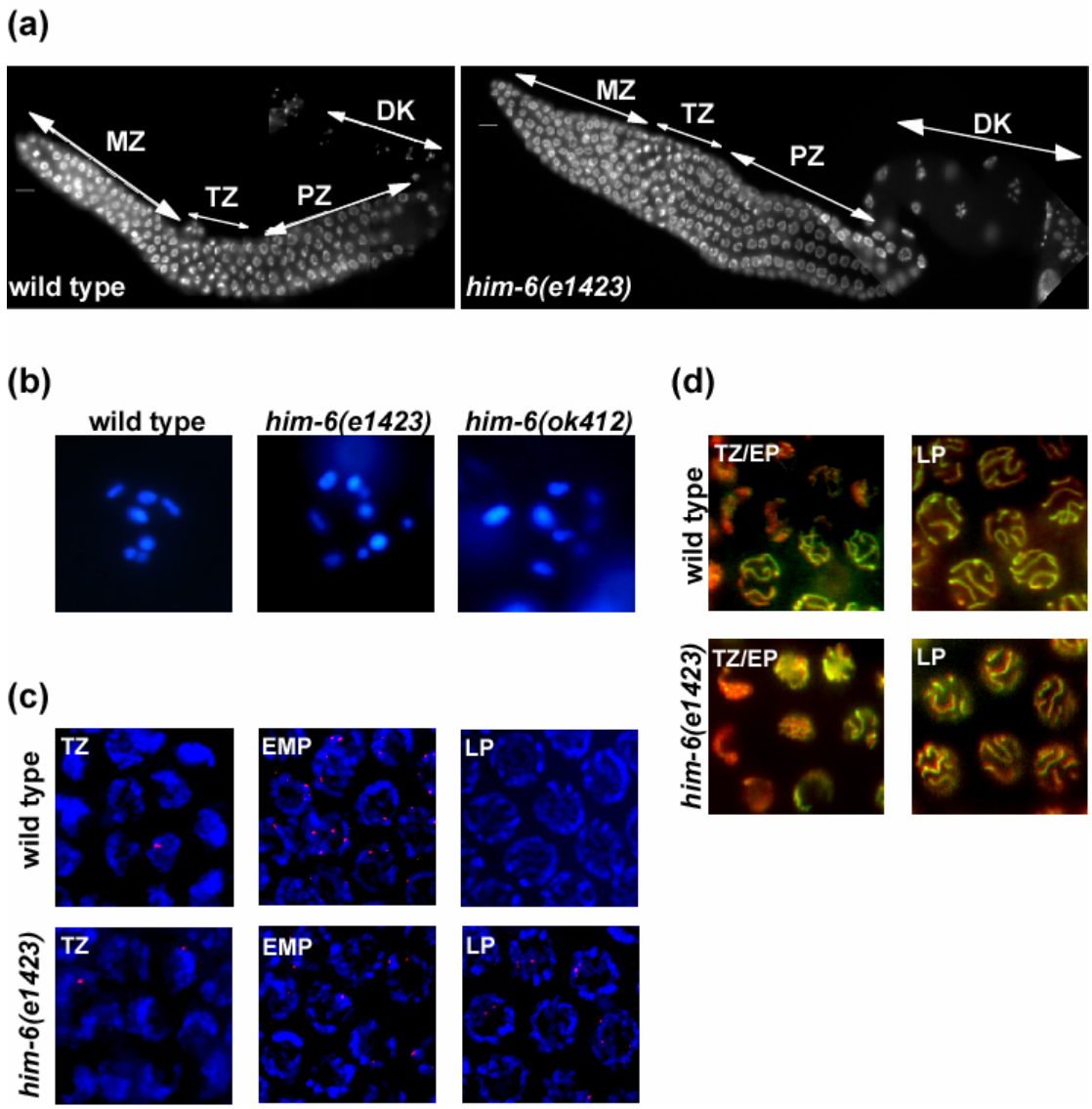

Figure 3-2 Meiotic phenotypes of *him-6*. (a) Wild type gonad (left panel) and *him-6(e1423)* gonad (right panel) stained with DAPI, which show a normal progression of the germ cells through meiotic prophase. **(b)** Wild type oocyte at diakinesis stained with DAPI: six stained bodies can be observed corresponding to the six sets of homologous chromosomes attached by chiasmata, *him-6(e1423)* oocyte and *him-6 (ok412)* oocyte: more than six structures are present, which correspond to a mix of bivalents and univalents. **(c)** Meiotic prophase nuclei stained with anti-RAD-51 antibody (red) and DAPI (blue) The RAD-51 immunostaining reveals similar foci pattern in wild type and *him-6(e1423)* transition zone and early-mid pachytene nuclei. Foci are absent from late pachytene nuclei in wild type, but persist in the *him-6(e1423)* mutant. **(d)** Meiotic prophase nuclei stained with anti-HIM-3 antibody (green) and DAPI (red). The

staining revealed no pairing defects in the transition zone and pachytene nuclei of the *him-6* mutant. MZ: mitotic zone, TZ: transition zone, EMP: early-mid pachytene, LP: late pachytene, P: pachytene, DK: diakinesis. Scale bars: 10 µm.

We observed no obvious abnormalities in the transition zone or pachytene nuclei of the *him-6* mutant (Figure 3-2d). To distinguish, whether the RAD-51 foci observed during meiosis in *him-6* animals are dependent on the SPO-11 nuclease or if they were inherited as double strand breaks generated in premeiotic S-phase, we analysed the distribution of RAD-51 foci in *spo-11(ok79)him-6(e1423)* worms. The absence of SPO-11 specifically blocks the initiation of meiotic recombination and causes extensive meiotic chromosome missegregation (Dernburg et al., 1998; Roeder, 1997) resulting in almost no viable progeny. In wild-type animals, RAD-51 recruitment depends on meiotic DSBs and virtually no RAD-51 foci are detected during meiosis in *spo-11* mutant animals (Alpi et al., 2003). Likewise, in *spo-11 him-6* double mutants, no RAD-51 staining was observed (data not shown), suggesting that RAD-51 foci in *him-6* worms are *spo-11* dependent and that meiotic double strand breaks occur in *him-6* mutants. Altogether our observations suggest that *him-6* is necessary for normal levels of crossing-over recombination and functions during a late step in this process.

7.3.2.3 *him-6* has defects in response to DNA damage

The budding yeast Sgs1p was shown to function during the S-phase checkpoint whereas in fission yeast Sgs1p homolog has no S-phase checkpoint function (Frei and Gasser, 2000b; Stewart et al., 1997). The role of BLM in this process in mammalian cells is still unclear (Bjergbaek et al., 2002). To determine whether HIM-6 is needed in response to

DNA damage we exposed L4 larvae to increasing levels of γ-irradiation and scored the survival rate of the progeny as described previously (Gartner et al., 2000). We found that *him-6* mutants show an enhanced sensitivity to irradiation (Figure 3-3a). In addition, we tested whether germ cell apoptosis (of meiotic pachytene cells) and mitotic germ cell cycle arrest are induced in response to genotoxic stress in *him-6* mutants (Gartner et al., 2000). *him-6(e1423)* and *him-6(ok412)* animals showed attenuated levels of programmed cell death within 6 hours after irradiation (Figure 3-3b and data not shown). However, programmed cell death reached almost wild-type levels 36 hours after irradiation (data not shown).

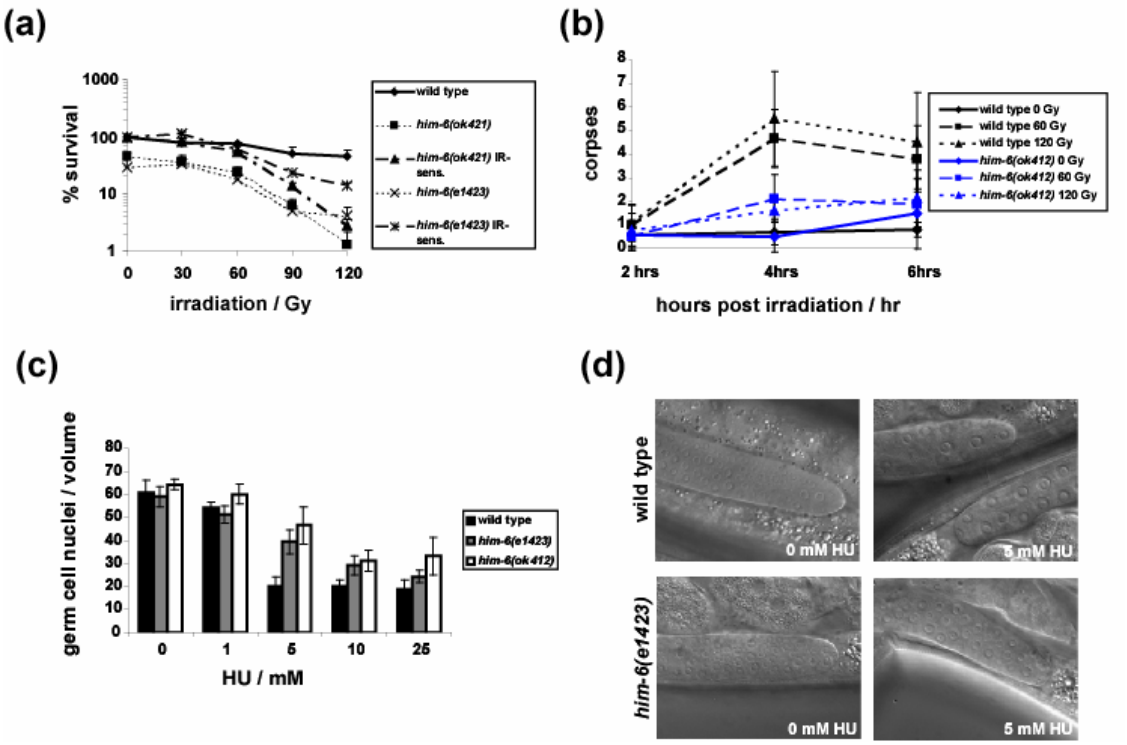

Figure 3-3 Figure 3. *him-6* mutants are defective in responding to DNA damage. (a) *him-6* germ cells are more sensitive to γ-irradiation. To compare the irradiation sensitivity (IR-sensitivity curve) of the mutant the survival rate of N2, *him-6(e1423)* and *him-6(ok412)* are set to 100 at 0 Gy, although the survival rate of the *him-6(e1423)* and *him-6(ok412)* progenies is only 21 % and 36 % respectively. **(b)** *him-6(e1423)*

mutant show decreased germ cell apoptosis. Late stage L4 hermaphrodites were exposed to 0, 60 and 120 Gy of γ-irradiation and apoptosis was scored after 2, 4 and 6 hr later as described in Gartner et al. (Gartner et al., 2000). The y-axis indicates the number of dead cells (cell corpses) per gonad arm. **(c)** *him-6* germ lines are sensitive to hydroxyurea (HU). *him-6* and wild type worms were grown on plates containing 0 mM, 1 mM, 5 mM, 10 mM or 25 mM of HU. Cell cycle arrest was measured by counting the average number of cells in a defined volume of the germ line. The *him-6* mutants show a higher number of germ cells upon HU treatment compared to wild type. **(d)** Normaski pictures of wild type and *him-6(e1423)* mitotic zones exposed to 0 mM and 5 mM HU. *him-6(e1423)* has more mitotic nuclei when exposed to 5 mM HU due to a defect in cell cycle arrest.

We did not observe any defects in cell cycle arrest in response to radiation by mitotic germ cells (data not shown). We tested whether *him-6* worms were defective in the S-phase checkpoint by growing them on plates containing hydroxyurea (HU), a drug that leads to the depletion of dNTP pools (Dasika et al., 1999)**.** Cell cycle arrest was measured by counting the average cell number in a defined volume of the germ line, which is indicative of cell cycle progression (wild type cells transiently stop dividing in response to HU but S-phase checkpoint defective cells continue to proliferate) (Ahmed and Hodgkin, 2000; Alpi et al., 2003; Gartner et al., 2000). Both *him-6(ok412)* and *him-6(e1423)* mutants showed a partially defective cell cycle arrest in response to HU treatment as revealed by the elevated number of mitotic germ cells and their smaller size upon HU (Figuress 3-3c and 3-3d). To test whether *him-6* is also required to repair double strand breaks in normally proliferating mitotic germ cells we scored for the number of RAD-51 foci in untreated animals. The average number of RAD-51 foci was 2.3±0.3 in wild type, 6.6±1.0 in *him-6(e1423)* and 7.6±0.9 in *him-6(ok412)* per hundred mitotic germ cells. Thus, RAD-51 is already recruited during the proliferation of the

germ line in *him-6* mutants suggestive of elevated levels of double strand breaks, or the failure to process double strand breaks. Taken together, these results indicate that *him-6* is needed for efficient DNA repair and that *him-6* mutants are partially defective in activating DNA damage checkpoint responses.

7.3.2.4 Combined depletion of HIM-6 and TOP-3 leads to mitotic catastrophe, which is suppressed by the loss-of-function of *rad-51*

Since HIM-6 was shown to interact genetically and physically with topoisomerase IIIα, we were interested to further analyse the genetic interaction (Kim et al., 2002). Kim et al. (2002) had demonstrated that *top-3(RNAi);him-6(e1104)* germ cells showed severe chromosome abnormalities and were arrested during mitosis. We observed a similar phenotype for *top-3(RNAi);him-6(e1423)* animals (Figure 3-4a). In *top-3(RNAi);him-6(e1423)* using RAD-51 antibody, we detected a dramatic increase of RAD-51 foci as well as intense nuclear staining (Figure 3-4b). The increased number of RAD-51 foci in the mitotic zone of *him-6(e1423)* (6.6±1.0 foci per 100 nuclei) and *top-3(RNAi)* (47.8±6.7 foci per 100 nuclei) worms compared to wild-type animals (2.3±0.3 foci per 100 nuclei) suggested elevated levels of DSBs in mitotic germ cells of the respective single mutants (Figure 3-4c). We tested if the DSBs were the result of SPO-11 or RAD-51 activity by comparing *top-3(RNAi);spo-11(ok79)him-6(e1423)* and *top-3(RNAi);rad-51(lg08701)him-6(e1423)* worms. Mutation in *rad-51* but not *spo-11* completely suppressed the *top-3(RNAi);him-6(e1423*) phenotype (Figure 3-4d and data not shown). The data indicate that the severe defects observed in the *top-3(RNAi);him-6(e1423)* worms result from RAD-51 function and not on SPO-11 activity. Thus, we propose that

RAD-51 is involved in the generation of toxic recombination intermediates that form in the combined absence of HIM-6 and TOP-3 during the proliferation of mitotic germ cells.

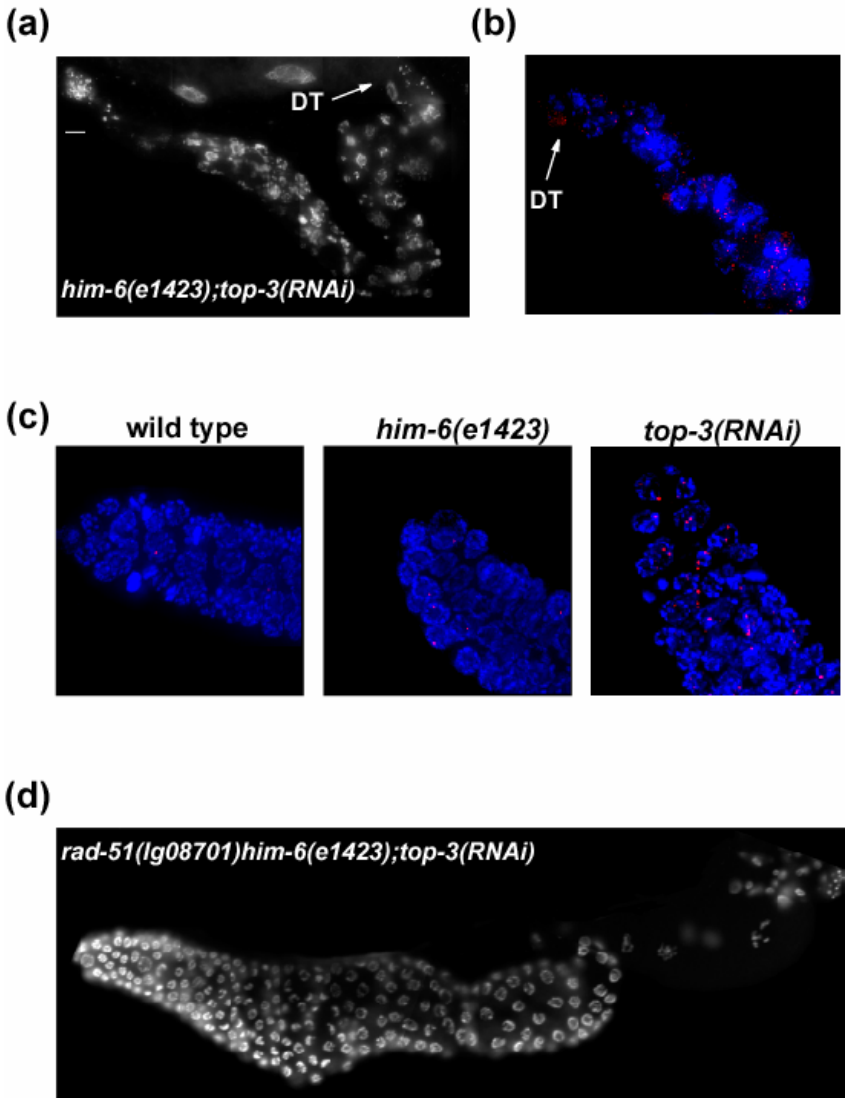

Figure 3-4 ***top-3(RNAi);him-6(e1423)*** **worms show mitotic catastrophe and massive RAD-51 recruitment in the germ line.** The defects are suppressed by mutation in *rad-51*. **(a)** *top-3(RNAi);him-6(e1423)* gonad stained with DAPI, which shows germ line nuclei with severe chromosomal abnormalities. **(b)** *top-3(RNAi);him-(ok412)* gonad stained with DAPI (blue) and anti-RAD-51 antibody (red). **(c)** Mitotic

germ nuclei of wild-type, *him-6(e1423)* and *top-3(RNAi)* worms stained with DAPI (blue) and anti-RAD-51 antibody (red), which revealed a higher number of RAD-51 foci compared to wild type. **(d)** *top-3(RNAi);rad-51(lg08701)him-6(e1423)* gonad stained with DAPI, which shows a normal proliferation of the germ line nuclei and a normal progression through meiotic prophase. Scale bars: 10 μm.

7.3.2.5 *mre-11* acts downstream or in parallel of *rad-51* in the processing of double strand breaks

The suppression of the *top-3(RNAi);him-6* mitotic catastrophe by mutant *rad-51* prompted us to analyse whether or not mutation in *mre-11* would suppress the *top-3(RNAi);him-6(e1423)* phenotype. Studies in *C. elegans* and other organisms have shown that the MRE-11 nuclease is required for generating double strand breaks during meiotic recombination and for an early step of mitotic DNA repair (Chin and Villeneuve, 2001; D'Amours and Jackson, 2002a; Haber, 1998). In yeast, Mre11p promotes genome stability through several pathways, including homologous recombination dependent repair and non-homologous end joining (Haber, 1998). It is not however required for repair of HO-induced double strand breaks as *mre-11* mutants defective in nuclease activity are able to repair these (Furuse et al., 1998; Moreau et al., 2001; Tsubouchi and Ogawa, 2000). We examined the gonads of *top-3(RNAi);him-6(e1423);mre-11(me41)* animals and observed severe defects comparable to those observed in *top-3(RNAi);him-6(e1423)* animals (Figure 3-5a). These data suggested that MRE-11, unlike RAD-51, cannot suppress the mitotic catastrophe of *top-3 (RNAi);him-6(e1423)* worms. The data are consistent with the suggestion that the MRE-11 nuclease functions in a pathway distinct from, or downstream of RAD-51. To seek independent confirmation of this hypothesis we generated double strand breaks in mitotic germ cells by ionising radiation

and analysed the effect of MRE-11. 12 hours after ionising radiation we scored for RAD-51 foci, which are indicative of processed double strand breaks, and observed that the number grew with increasing doses of radiation. RAD-51 foci

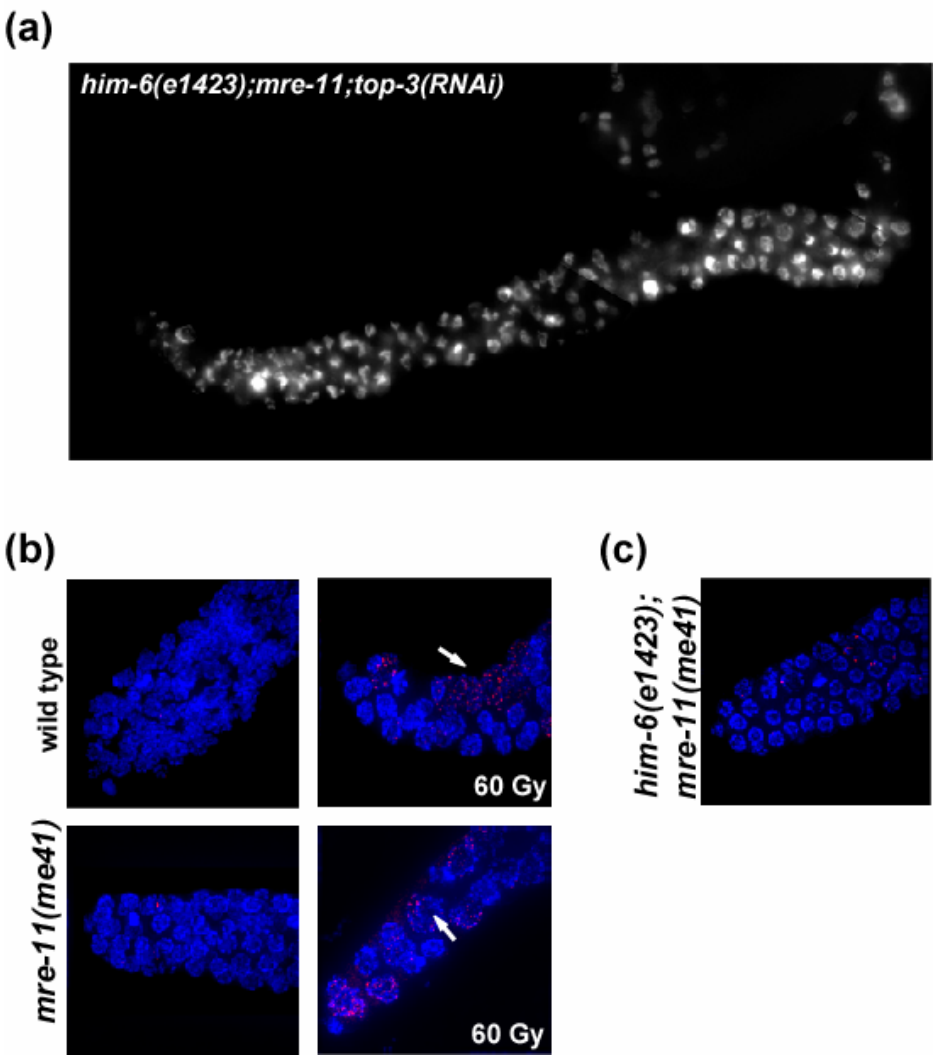

Figure 3-5 Loss-of-function of *mre-11(me41)* does not suppress mitotic catastrophe in *top-3(RNAi);him-6(e1423)* worms. (a) DAPI stained *top-3(RNAi);him-6(e1423) mre-11(me41)* gonad. **(b)** Mitotic zone nuclei of irradiated wild-type and *mre-11(me41)* animals show similar number of RAD-51 foci **(c)** Mitotic zone of *him-6(e1423);mre-11(me41)* worms. Scale bars: 10 µm.

accumulated in cell cycle arrested nuclei but disappeared in cells that resumed cell cycle

progression (Figure 3-5b). When we analysed RAD-51 foci in *mre-11* mutant worms we found a slightly higher number of RAD-51 foci as compared to wild type worms (see below), indicating that MRE-11 processing is not required for the formation of RAD-51 foci once a break occurs. These results suggest that MRE-11 acts in parallel or downstream of RAD-51 in repairing double strand breaks. To test whether MRE-11 is required in concert with HIM-6 to repair double strand breaks in normally proliferating mitotic germ cells we scored for the number of RAD-51 foci in *him-6(e1423);mre-11(me41)* worms in comparison to *him-6(e1423)* and *mre-11(me41)* single mutant worms. While *him-6(e1423);mre-11(me41)* mutant animals exhibited a phenotype similar to that of *mre-11(me41)* single mutant animals (Chin and Villeneuve, 2001) (normal cell proliferation and subsequent progression through meiotic prophase, with 12 univalents at diakinesis, data not shown), *him-6 mre-11* double mutants had more RAD-51 foci than either single mutant or wild type animals (wild type 2.3±0.3 foci, *him-6(e1423)*: 6.6±1.0 foci, and *mre-11(me41)*: 8.7±2.1 foci per 100 nuclei) and (*him-6(e1423); mre-11(me41)*: 26.6±2.6 foci per 100 nuclei) (Figure 3-5c). These results indicate that *mre-11* and *him-6* contribute to genome stability in proliferating germ cells by different pathways as their combined depletion leads to increased levels of double strand breaks.

7.3.2.6 Topoisomerase IIIα also acts at a late stage of meiotic recombination

In *C. elegans* TOP-3 is required for fertility. *top-3(RNAi)* worms had a variable phenotype ranging from normal to completely sterile worms (Kim et al., 2000). In gonads of *top-3(RNAi)* animals, the prophase nuclei persist in a transition and/or early pachytene zone-like morphology and only reach full pachytene morphology late during meiotic

prophase (Figure 3-6a) (Kim et al., 2000). We studied the RAD-51 staining pattern in nuclei of the transition zone in *top-3(RNAi)* worms and found a large number of RAD-51 foci (Figure 3-6b). The increased number of RAD-51 foci in the transition zone indicated that DSBs are accumulating in *top-3(RNAi)* worms early in meiotic prophase. The data are consistent with the suggestion that *top-3(RNAi)* worms are defective in processing meiotic recombination intermediates.

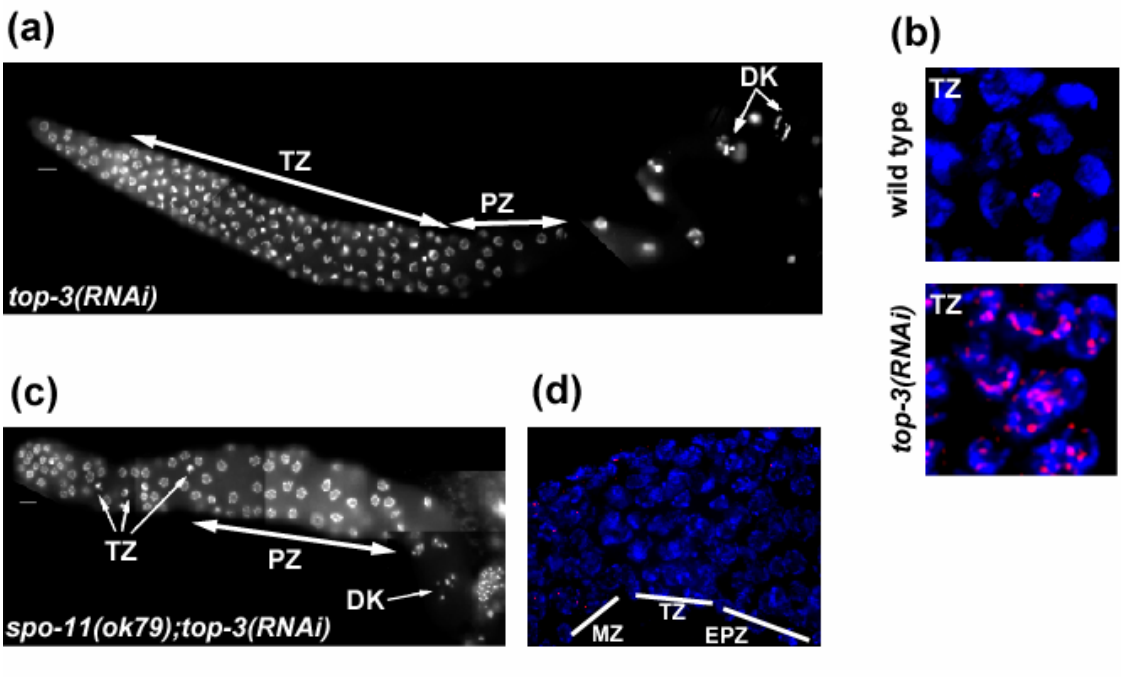

Figure 3-6: *top-3(RNAi)* worms show defects, which depend on meiotic recombination. **(a)** *top-3(RNAi)* gonad stained with DAPI, which revealed an extended transition zone. **(b)** Transition zone nuclei stained with an anti-RAD-51 antibody (red) and DAPI (blue). *top-3(RNAi)* nuclei show a increased number of RAD-51 foci compared to wild type. **(c)** *top-3(RNAi);spo-11(ok79);* gonad stained with DAPI, which show a normal progression of the germ nuclei through meiotic prophase. **(d)** RAD-51 foci are absent from *top-3(RNAi);spo-11(ok79);* nuclei in the transition zone and in early pachytene. **(e)** *top-3(RNAi);rad-51(lg08701)* gonad stained with DAPI, which shows a normal proliferation of the germ line nuclei and a normal progression through meiotic prophase. Scale bars: 10 µm.

The hypothesis is supported by the finding that nuclei in *top-3(RNAi);spo-11(ok79)* double mutants progress normally through meiotic prophase, but in fewer numbers (Figure 3-6c). Furthermore, the large amount of RAD-51 foci observed at the transition zone of *top-3(RNAi)* worms were absent from *top-3(RNAi*);*spo-11(ok79)* worms, indicating that the accumulation of DSBs at the transition zone was dependent on *spo-11*. *rad-51* acts after *spo-11*. In the absence of RAD-51 function, we found that *top-3(RNAi);rad-51(lg08701)* animals had a normal progression through meiotic prophase (Figure 3-6d). Based on these results we concluded that RAD-51 activity is responsible for the top-3 mutant delayed progression through prophase and that TOP-3 acts after SPO-11 and RAD-51. The reduced number of germ line nuclei in *top-3(RNAi);spo-11(ok79)* worms may result from a further role for TOP-3 in the (mitotic) proliferation of the germ line (see above)

7.3.3 Discussion

In this paper, we show that *him-6* encodes for the *C. elegans* homolog of the mammalian Blooms syndrome gene. *him-6* partially contributes to DNA damage checkpoint signalling in response to ionising radiation and in S-phase checkpoint regulation in the germ line. We propose that during mitotic cell divisions *him-6* acts redundantly with *top-3,* downstream of *rad-51* to process lesions generated during normal mitotic germ cell divisions (Figure 3-7). Furthermore, *mre-11* is likely to act in parallel to-, or downstream of *rad-51* to process double strand breaks (Figure 3-7). During meiotic recombination *him-6* together with *top-3* act downstream of *spo-11*, *mre-11* and *rad-51* (see below) during the initiation of meiotic recombination (Figure 3-7).

HIM-6 has checkpoint function in the germ line

him-6 mutant worms show an enhanced sensitivity to ionising radiation indicating that it plays a role in DNA repair. In addition, we observed a partial checkpoint defect in responding to HU and to ionising irradiation induced germ cell death in *him-6* worms. A function of recQ helicases in the DNA damage response pathway was already suggested in other organisms but was not observed universally. *sgs1* deficient budding yeast cells are partially defective to arrest S-phase progression in response to hydroxyurea (Frei and Gasser, 2000b; Yamagata et al., 1998). Human Bloom's -/- cells on the other hand respond normally to HU (Ababou et al., 2002). Similarly, *S. pombe* cells lacking the recQ-like helicase Rqh1p react normally to hydroxyurea but are defective in the recovery from S-phase arrest when exposed to HU (Stewart et al., 1997). It is likely that recQ-dependent damage checkpoint responses are mediated by functionally redundant or overlapping pathways. In *C. elegans* we observe only partial checkpoint defects in *him-6* worms. Similarly, irradiation induced apoptosis and G2/M cell cycle arrest is only partially compromised in human Bloom´s -/- cells (Ababou et al., 2002; Wang et al., 2001). It was recently shown that HIM-6 physically interacts with the *C. elegans* ATR homologue whose inactivation by RNAi leads to defective checkpoint processes in response to ionising radiation (Boulton et al., 2002) as well as to hydroxyurea (Anton Gartner, unpublished observation). Therefore, it is conceivable that HIM-6 acts together with the ATM/ATR-like kinases to affect DNA damage checkpoint responses.

TOP-3 and HIM-6 act together to prevent deleterious recombination during the mitotic cell proliferation in the germ line

top-3(RNAi);him-6(e1423) germ lines display some profound defects, including a reduced number of germ line nuclei. The chromatin of these nuclei appears to be disorganized and sometimes fragmented, and RAD-51 foci massively accumulate, a strong phenotype that is suppressed by the absence of RAD-51 but not by the absence of MRE-11 or SPO-11. The results suggest that HIM-6 and TOP-3 act redundantly downstream of RAD-51 but not of MRE-11 to process recombination intermediates that result from double strand breaks occurring spontaneously in normally proliferating mitotic germ cells (Figure 3-7b). The presence of an increased number of RAD-51 foci in the mitotic zone of *him-6* and *top-3* single mutant worms suggests that HIM-6 and TOP-3 are involved the processing of recombination intermediates. In the absence of HIM-6 and TOP-3 recombination intermediates may be formed that can not be processed and therefore result in massive genomic instability and that could lead to the defects observed in *top-3(RNAi);him-6(e1423)* germ line nuclei. Once double stand breaks are generated and processed by RAD-51, we propose that cells path through a "point of no return" that precludes alternative repair pathways (Figure 3-7b). Accordingly, in the absence of RAD-51, toxic recombination intermediates cannot be formed and double strand breaks that form in the absence of RAD-51 may be processed by alternative repair pathways such as, e.g., end joining.

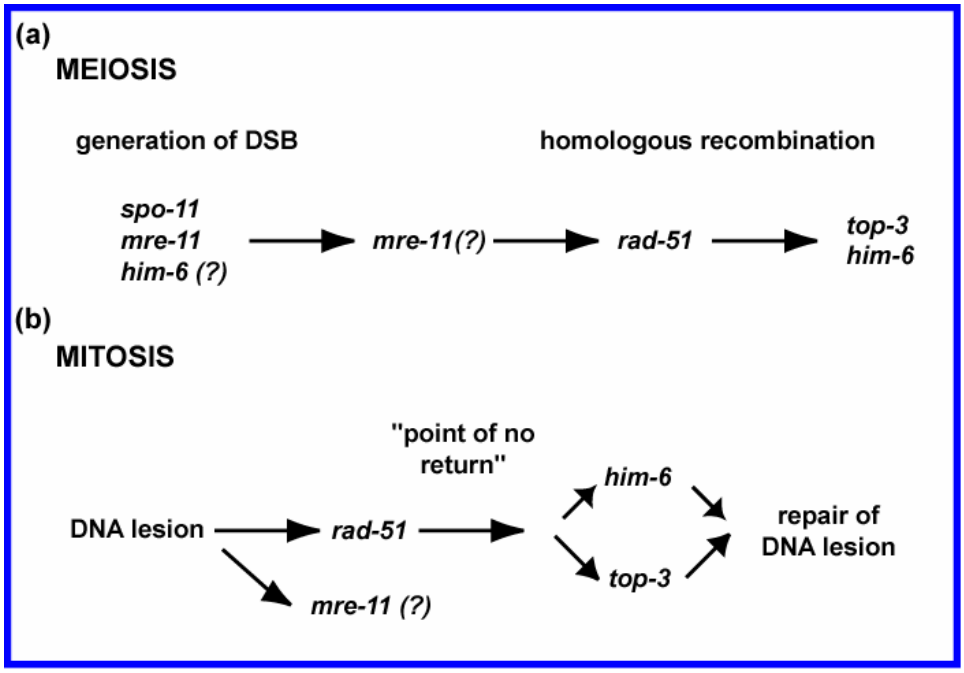

Figure 3-7 Genetic model for him-6 in meiotic (a) and mitotic (b) homologous recombination. See discussion for details.

The genetic interactions between *him-6 top3* and *rad-51* differ from those observed with the corresponding mutations in *S. cerevisiae* and *S. pombe*. In yeast it was shown that Sgs1p as well as other recombination proteins suppress the slow growth phenotype and the retarded cell cycle progression of *top3* mutants (Gangloff et al., 1994). It is assumed that Sgs1p generates DNA structures during replication or repair that need TOP-3 or other recombination proteins to be resolved. In *C. elegans top-3(RNAi);him-6(e1423)* mutants display synergistic defects. What might be the reason for the differences observed in the yeast and worm system? It is likely that *him-6* and *top-3* act redundantly to prevent the illegitimate accumulation of toxic recombination intermediates that occur as a consequence of mistakes happening during normal S-phase progression. According to this model, inactivation of *rad-51* function would bypass the combined

defects of *top-3;him-6* worms by preventing the accumulation of toxic recombination intermediates (Figure 3-7b).

MRE-11 might act downstream or in parallel of RAD-51

The mitotic catastrophe observed in *top-3(RNAi);him-6(e1423)* worms cannot be suppressed by the absence of *mre-11*. Furthermore, we found that that RAD-51 foci accumulate in mitotic germ cells of irradiated *mre-11* worms similar to wild type worms. We therefore suggest that *mre-11* acts downstream or in parallel to *rad-51* to process double stand breaks that have been generated by ionising irradiation or in the *top3(RNAi);him-6(e1423)* mutant situation (Figure 3-7b). Alternatively, this result could also suggest that *mre-11* has no role in double strand break repair. We think, however, that this is not the case because irradiation of *mre-11* worms leads to massive and persistent chromosome breakage as indicated by the fragmentation of univalents (Chin and Villeneuve, 2001) (and our unpublished observations). The situation is different during *C. elegans* meiosis, where *mre-11* plays an essential role in the generation of meiotic double strand breaks (Alpi et al., 2003; Chin and Villeneuve, 2001) and budding yeast (Cao et al., 1990). The finding that *mre-11* acts downstream or in parallel to *rad-51* in recombinational repair is also supported by the finding that RAD-51 foci accumulate in irradiated chicken DT40 *mre-11*$^{-}$*/mre-11*$^{-}$ cell lines. Furthermore, it was recently reported that in *S. pombe* cells defective for *rad-50*, which acts in the same epistasis group as *mre-11*, RAD-51 foci accumulate upon irradiation, albeit at reduced rates (Caspari et al., 2002)

him-6 is required for normal levels of meiotic recombination

What might be the function of HIM-6 during meiotic recombination? HIM-6 may play a role at the resolution step. In *him-6* mutants the rate of meiotic recombination is reduced and RAD-51 foci persist in late pachytene, whereas in wild type nuclei of the same stage virtually no RAD-51 foci are observed. This phenotype is reminiscent to that of *msh-5* mutants. Genetic and cytological evidence indicated that MSH-5 acts after the initiation of recombination. Like MSH-5, HIM-6 could act after the initiation of recombination and might be necessary for the resolution of recombination intermediates (Figure 3-7a). Additionally, HIM-6 could also play a role at the initiation step of recombination (Figure 3-7a). In *E. coli*, it has been shown that recQ can initiate recombination in concert with recA and SSB proteins *in vitro*. It can also initiate recombination *in vivo*, when the recBCD enzyme is rendered non-functional, reviewed in (Kowalczykowski, 2000). According to the possibility that *him-6* may play an additional role in the initiation of meiotic recombination we find a partial rescue of the *him-6* meiotic defect upon irradiation with low doses of irradiation (Figure 3-3a). In *spo-11* worms, where no meiotic double strand breaks occur the generation of double strand breaks by ionising irradiation partially bypasses the meiotic defects of *spo-11* (Dernburg et al., 1998). At high radiation doses *him-6* worms are more irradiation sensitive than wild type animals, whereas at low doses they are equally or even less sensitive (Figure 3-3a). According to the idea that *him-6* plays a role in the initiation of meiosis, the number of RAD-51 foci in the transition zone of *him-6* worms often appeared to be reduced. Due to the low base line of RAD-51 foci in transition zone nuclei, however, we failed to detect a statistically significant difference in RAD-51 foci in wild type and *him-6* worms.

Whereas the role of eukaryotic RecQ proteins in regulating mitotic recombination has been well established, only indirect evidence exists so far implicating RecQ proteins in the regulation of meiotic recombination (Wu and Hickson, 2001). The Bloom's syndrome is characterized by male sterility and female sub-fertility and BLM and RAD51 co-localize in mouse spermatocytes during meiotic prophase (Moens et al., 2000). However, unlike in the *him-6* mutant, the frequency of meiotic crossing over seems not to be affected in *blm* knockout mice (Luo et al., 2000). In *S. cerevisiae*, the single RECQ homolog (Sgs1p) is not required for the initiation of double strand breaks but seems to be needed for the processing of recombination intermediates during meiosis. The first meiotic division in *sgs1* mutant is delayed and this delay is alleviated in a *spo11* minus background (Gangloff et al., 1999). As in *Blm*-deficient mice, however, the frequency of meiotic recombination seems to be unchanged in yeast (Gangloff et al., 1999; Watt et al., 1996), possibly because the meiotic prophase delay compensates for the recombination-processing deficit.

TOP-3 is required for meiotic recombination

While studying a possible interaction between HIM-6 and TOP-3, we observed that *top-3* single mutant displayed an interesting phenotype, which was distinct from those resulting from the lack of recombination machinery components such as RAD-51 and SPO-11. Absence of TOP-3 lead to an accumulation of nuclei at the so-called transition stage and this defect was dependent on meiotic recombination, since it was suppressed by mutations in *spo-11* and *rad-51*. Furthermore, RAD-51 foci were very abundant in transition zone nuclei of *top-3* worms, indicating that an increased number of

recombination events were initiated but not resolved. These results are consistent with the notion that TOP-3 might act downstream of RAD-51 during meiotic recombination (Figure 3-7a). Since due to excessive mitotic defects *top-3;him-6* worms do not enter meiosis we could not study that the effect of this double mutant in meiotic recombination. The accumulation of unprocessed double strand breaks in *top-3* worms could cause a severe delay or even an arrest in the progression through the transition zone. It remains to be seen whether the accumulation of transition zone nuclei in *top-3* worms depends on the DNA damage checkpoint. Since these defects and the abundant RAD-51 foci in the transition zone are alleviated by mutation in *spo-11,* the *top-3* mutant phenotype depends on the generation of double strand breaks. Indeed, we also observe a similar defect in irradiated *rad-51* and *mre-11* worms where massive levels of double strand breaks are generated but can not be repaired (Anton Gartner and Arno Alpi, unpublished observation). Our finding thus generalize observations made in yeast suggesting that *top-3* might be required during meiosis in a stage acting after the initiation of meiotic double strand breaks (Gangloff et al., 1999).

C. elegans and Bloom's syndrome

Bloom's syndrome is mainly associated with somatic phenotypes, such as short stature, skin disorders, predisposition to cancer, although the germ line is also affected (German, 1993). Similarly, we have shown here a role for *him-6* during both mitotic division and meiosis. The *him-6* gene is predominantly expressed in the germ line of *C. elegans* (Reinke et al., 2000) and its loss-of-function has no apparent effect in the soma. However, during *C. elegans* somatic development cells only go through a very limited

number of cell divisions before becoming terminally differentiated. This is in contrast to the massive proliferation needed in mammalian systems to expand rare stem cells into terminally differentiated tissues. Thus, it is not surprising that mechanisms to maintain genome stability are more active in the *C. elegans* germ line, which is continuously proliferating. This developmental setting in *C. elegans* allows for the unique possibility to analyse the combined effect of multiple DNA repair associated mutations. Our study defined synthetic interactions between *C. elegans* repair proteins that were not anticipated from previous studies in yeasts. Synthetic phenotypes, like those we uncovered for *top-3;him-6* double and *top-3;rad-51him-6* triple mutants, might indeed in the long run be useful for cancer therapy. For example, in cases where single genes like *blm* are lost due to genomic instability associated with cancer progression, drugs against TOP-3 might selectively target cancer cells.

8. Materials and methods

8.1 Worm strains

Strains were cultured as described by Brenner (Brenner, 1974). The wild-type strain background was Bristool *N2*. For **PART 1** following mutant strains and chromosome rearrangements were used: *mrt-2(e2664)* is described in (Ahmed and Hodgkin, 2000), *hus-1(op241)* in (Hofmann et al., 2002), *clk-1(2519), clk-2(qm37), clk-3(qm38),* and *gro-1(e2400)* are described in detail in (Lakowski and Hekimi, 1996). Mapping of *rad-5(mn159)*: *rad-5-(mn159),* whose map position was previously reported near –2 on chromosome III, was mapped more precisely using a multifactor cross with the strain *WS711 dpy-17(e164)ced-6(n1813)mec-14(u55)ncl-1(e1865)unc-36(e251).* Dpy-non-Unc and Unc-non-Dpy animals were picked in the F2 generation and scored for temperature sensitive (ts) lethality at 25°C associated with *rad-5(mn159).* The number of recombinations revealed the approximate map position of *rad-5(mn159)* between –0.6 and –0.76. We continued with a refined three factor cross with an *unc-36 rad-5 sma-3* strain that was crossed with the polymorphic CB4854 strain and analysed single nucleotide polymorphisms between N2 and CB4854. The two most informative polymorphisms were ACA (N2)/T (CB4854) TTTTTTTTTAc on cosmid T21D11 and ATAACGTA (N2)/G (CB4854) ATAA on cosmid C03B8 hat allowed placing *rad-5(mn159)* between T21D11 and C03B8. Cosmids (provided by the Caenorhabditis Genetics Center) were prepared using a QIAGEN plasmid isolation kit followed by a Phenol/Chloroform extraction and Ethanol precipitation step. These purified cosmids

were injected at ~2.5 ng/µl together with 50 ng/µl pRF-4*(rol-6(su1006)*). One line transformed with a cosmid pool R13A5, C07H6, K07D8 rescued the ts lethal phenotype at 25°C. By injections of the single cosmid C07H6 out of this pool and subsequently a long PCR product encompassing C07H6.6 and C07H6.8 we rescued the checkpoint phenotypes of *rad-5(mn159)* and *clk-2(qm37)*. Sequence analysis revealed a single point mutation in C07H6.6: in *rad-5(mn159)* a TA to GC transversion, and in *clk-2(qm37)* a CG to TA transition. The *rad-5/clk-2* cDNA sequence was determined by analysing the apparently full-length EST yk447b4 (kindly provided by Yuji Kohara).

PART 2: The *rad-51* deletion (lg08701) (nucleotides 15810 to 14871 of Y43C5A.6) was isolated from a *C. elegans* deletion library and was kindly provided by Elegene (Munich, Germany). *rad-51(lg08701*) was back-crossed five times with Bristol N2 and marked with *dpy-13(e184)* and balanced by *nT1*. Balancer strains containing *eT1(III;V) (BC2200,dpy-18(e364)/eT1 III; unc-46(e177)/eT1 V)* and *hT1(I;V) (KR1037, unc-13(e51)/hT1; dpy-11(e224)/hT1(unc-42(e270))V)* were provided by the *Caenorhabditis* Genetics Center (Universisty of Minnesota, St. Paul, Minn.). AV112, *mre-11(ok179) IV/nT1(unc-?(n754)let-?)(IV;V), DR787, dpy-13(e184)ama-1(m118)let-276(m240)/nT1 IV; +/nT1 V* and MT5734, *nDf41 IV/nT1(unc-?8n754)let-?)(IV;V)* were also obtained *Caenorhabditis* Genetics Center. AV115, *msh-5(me23)*, AV106, *spo-11(ok79),* and AV146, *chk-2(me64)* strains were kindly provided by A.M. Villeneuve (Stanford University, California).

PART 3: The mutations used in this study were obtained from the *Caenorhabditis* Genetic Centre. LG I: *dpy-5(e61), unc-101(m1), unc-54(e190).* LG III; *glp-1(q224ts*). LG IV: *him-6(e1423), him-6 (e1104), spo-11(ok79), rad-51(lg08701).* LG V: *mre-11(me41).*

LG X: *unc-1(e719), dpy-3(e27), lon-2(e678), dpy-7(e88), unc-3(e151).* The *him-6* gene has been mapped to linkage group IV, between *unc-22* and *unc-31*. To map *him-6* more precisely, we used deficiencies in the region to do complementation tests. *him-6* failed to complement *sDf62* but complemented *sDf61(Clark and Baillie, 1992)*. This placed *him-6* between *let-93* and *let-99*, to the right of *unc-22*. General molecular manipulations followed standard protocols (Sambrook et al., 1989). The sequence of the *him-6* genomic region was established by the *C. elegans* Sequencing Consortium(Wilson et al., 1994). A partial cDNA clone was obtained from Yuji Kohara (National Institute of Genetics, Mishima, Japan). The 5' end of the cDNA was isolated by RT-PCR using the Perkin Elmer Cetus kit and the conditions described by the manufacturer. The sequence of the primers used for amplification were SL1 (5'-GGTTTAATTACCCA-AGTTTGAG-3') and RQ-3 (5'-GCTGGCAA-TTGGTAGCAC-3'). Molecular changes in the *him-6* alleles were identified by sequencing PCR amplified products. All sequence analyses were performed with the GCG sequence analysis software package (Genetic Computer Group, 1991).

8.2. DNA damage response assays

Apoptotic response: The quantification of the apoptotic response in meiotic pachytene cells has been described recently in detail by Gartner et al.(Gartner et al., 2000) In brief, a synchronize population of L4 worms was treated with different doses of X-rays ranging from 0 Gy to 120 Gy and the number of cell corpse in were counted after 12, 24, and 36 hr after irradiation using Nomarski optics. In an alternative assay synchronous adult

animals (24 hr post L4) were irradiated with X-rays and scored for cell corpse after 0, 1.5, 3 and 6 hr post irradiation.

Cell cycle arrest response: Radiation induced cell cycle arrest of mitotic germ cell was determined as described previously by Gartner et al.(Gartner et al., 2000). In brief, worms were irradiated at the L4 stage and analysed 12 hr after irradiation for the appearance of enlarged, arrested germ cells in the distal part of the gonad. To quantify the cell cycle arrest the number of mitotic germ cell nuclei was scored as follows. We used a grid (net-microm 12.5 from ZEISS, Germany), which was placed in the ocular of the microscope. The number of mitotic germ cells was counted within two square fields screening from the top focal plane to the bottom focal plane of the particular region of the gonad. A drop in the number of mitotic germ cells within this defined volume was indicative for a cell cycle arrest.

Quantification of S-phase defects: Worms were grown on NGM plates containing hydroxyurea (HU) with different concentrations (0, 1, 5, 10, 25 mM HU) starting from the L4 stage at 25°C. After 14 hr, the extend of the cell cycle arrest was determined as described for the irradiation induced cell cycle arrest by scoring for the number of mitotic germ cells in a defined volume.

Irradiation sensitivity: To score for the X-ray hypersensitivity of single and double mutant combinations, young L4´s (grown at 20°C) were irradiated with 30, 60, 90, or 120 Gy and allowed to lay eggs over a period of 24 hr before they were removed from the plate. Survival rate of the offspring was determined by counting hatched versus dead embryos.

8.3 Determination of the telomere length

To measure telomere length of single out-crossed F2 animals they were allowed to produce progeny needed for genomic DNA preparation using a Puregene DNA isolation kit (Gentra). *Hin*FI-digested genomic DNA was separated on 0.6% agarose gels at $1.5Vcm^{-1}$, and Southern blotting was carried out using a dioxygenin-dUTP-labelled PCR probe according to the manufacturer´s protocols (Boehringer Mannheim). The probe was made using T3 and Te12 (5´-GAATAATGAAGAATTTTCAGGC-3´) primers to amplify telomeric repeats from the cTel55X plasmid using PCR.

8.4 RNAi

The RAD-51, HIM-3 and SYP-1 proteins were depleted by double-stranded RNA interference (RNAi). RNAi mediated depletion of *rad-51* was performed as described in Gartner et al. by dsRNA injection (Fire et al., 1998). For *him-3* RNAi a PCR fragment was amplified out of cDNA of N2 worms using the primers 5´-TAATACGACTCACTATAGGGGCGGCCGCGGCGACGAAA-GAGCAGATTG-3´and 5´-TAATACGACTCACT-ATAGGGCGGCCGCTCTTCTTCGTAATGCCCT-GAC-3´, which contains the targeted sequence flanked by the T7 promoter (underlined sequence). For *syp-1* (F26D2.2) RNAi by injection, dsRNA was produced using the primers given by MacQueen et al. (MacQueen et al., 2002) The dsRNA was prepared using a Promega kit (Madison, Wis.) *in vitro* transcription kit. The dsRNA was delivered

by injection (~200 µg/ml) into gonads or intestines of young adults as described in Fire et al.

For REC-8 depletion a cosuppression line was constructed as described by Dernburg et al. (Dernburg et al., 2000). In brief, a 3.4 kb PCR product comprising the W02A2.6 sequence was amplified from genomic DNA of N2 worms using the following primers: 5′-TCTTGAATAGGCTCCTGGGGTGCT-3′and 5′-ACCGTGCGGCACGAATCGTTTCAT-3′. This fragment was gel-purified, purified by phenol/chloroform extraction, and co-injected with *rol-6(su1006)* marker gene. Offspring showing the "roler" phenotype were selected and lines with the *rec-8* deficiency phenotype were established. The lines used for further experiments were checked each time by 4′,6-diamidino-2-phenylindole (DAPI) staining for the preservation of the phenotype. Topoisomerase IIIα fragment was amplified from a cDNA clone, which was constructed by RT-PCR, using the primers 5'-GAAAAGAGCCTTATTTGTGGCCG-3' and 5'-CCCATTTAAAGAAATTACATTTTTCAG-3' and cloned into a pGEM-T-Easy vector (Promega). This vector was used to synthesize dRNA as described above.

8.5 Production of anti-RAD-51 antibodies

A polymerase chain reaction (PCR) fragment encoding the N-terminal 103 amino acids of *C. elegans* RAD-51 was cloned in frame as a glutathione S-transferase (GST) fusion into pGEX-4T-1 (Amersham, Uppsala, Sweden) and as a maltose binding protein (MBP) fusion into pMAL-2c (New England BioLabs, Beverly, Mass.). Recombinant GST and MBP fusions were expressed in *Escherichia coli* BL21 CodonPlus (Stratagene, La Jolla,

Calif.), purified under native conditions (lysis buffer: 1xPBS, 5 mM DTT, 20 µg/ml DNAse,1 mg/ml lysozyme, and protease-inhibitor mix (complete, Mini, EDTA-free, ROCHE) by affinity chromatography using Glutathione-Sepharose 4B (Amersham, Uppsala, Sweden) and by amylose resin affinity chromatography (New England BioLabs, Beverly, Mass.) respectively. The purified GST protein fusion was dialyzed against 1x PBS and used for immunization of rabbits (Eurogentech, Seraing, Belgium). For anti-RAD-51 antibody affinity purification MBP-RAD-51 fusion protein was used. The MBP fusion was dialysed against 1xPBS and 2 mg of total protein was covalently bound to an Affi-Gel 15 matrix (BioRad, Hercules, Calif.). Crude serum was diluted 1:1 in 20 mM TRIS-HCl pH7.5 and pre-cleaned by centrifugation and applied to the column to allow for the binding of the antibody. After washing with 10 mM TRIS-HCl, ph7.5 and 10 mM TRIS-HCl, ph7.5, 0.5 M NaCl, antibodies were eluted with 100 mM glycin, pH2.5 and the eluates were fractionated and immediately neutralized with 1.5 M TRIS-HCl, pH8.0.

8.6 Cytology

Cytological preparations: To prepare whole gonads for fluorescence in situ hybridisation (FISH) analysis, hermaphrodites were transferred to a drop (~10 µl) of M9 buffer (0.3% KH_2PO4, 0.6% Na2HPO4, 0.5% NaCl, 1mM MgSO4) placed on a poly-L-lysine-coated microscope slide (for coating, 3 µl of a 0.1% solution of poly-L-lysine were spread out on a clean slide and left to dry at 37°C). The gonads were released by cutting worms with a fine injection needle behind the pharynx or in the tail region. An equal volume of 7.4% formaldehyde was added, and the material was gently squashed under a

cover slip to remove the excess fixative. Slides were then immediately frozen in liquid nitrogen for at least 10 min, cover slip was cracked off, and the slides were transferred to 96% ethanol at –20°C for 5 min and then placed in 1xPBS at room temperature. Slides were then dehydrated in an ethanol series (40%, 70%, 96%, 2 min each), air dried, and stored in the refrigerator until use for conventional chromosome staining or FISH. For subsequent immunostaining, worms were prepared as above. After removal of the cover slip, preparations were fixed in a series of methanol, methanol/acetone 1:1, and acetone for 5 min at –20°C, and immediately transferred to 1xPBS at room temperature without drying.

Immunostaining: Immunostaining was performed according to the standard protocol described in Pasierbek et al. (Pasierbek et al., 2001) Briefly, preparations were washed three times for 5 min in 1xPBS and blocked with 3% BSA in 1xPBS for 30 min at room temperature in a humid chamber. The primary antibody was applied and the specimen was incubated overnight at 4°C in a humid chamber. Antibodies were diluted in 1xPBS containing 3% BSA as follows: 1:100 anti-REC-8, 1:50 anti-RAD-51. After washing three times in 1xPBS, 0.1% Tween20 secondary antibodies were applied with following dilutions: anti-rabbit Cy3 (1:250), anti-rabbit fluorescein isothiocyanate (FITC) (1:500) or anti-rat-FITC (1:500) (all from Molecular Probes, Oregon, USA). After 30 min incubation at room temperature, slides were washed and mounted in Vectashield anti-fading medium (Vector Laboratories, Burlingame, Calif., USA) containing DAPI (2 µg/nl).

Fluorescence in situ hybridisation (FISH): Cosmid F56C11 (~42 kb) from near the left end of chromosome I (obtained from Alan Coulson, Nematode functional Genomics

Group, Sanger Centre) was used as a FISH probe. The cosmid was labelled with digoxigenin-11-dUTP using the BioNick Labelling System (Life Technologies, Rockville, Md.) according to the instructions of the manufacturer. FISH was performed on conventional preparations according to Dernberg et al. with some modifications. Briefly, air-dried slides were permeabilized by applying 20 µl of 1 M (Sodiumthiocyanate) NaSCN under a cover slip for 4 min at 90°C. The slides were then washed three times for 5 min in 2xSSC (20x stock: 3M NaCl, 0.3M Sodium citrate (pH7.0) (and the specimens were subjected to RNAse treatment (30 µg per slide) at 37°C for 40 min followed by formaldehyde treatment (3.7% in 2xSSC) for 10 min at room temperature to stop enzymatic reactions. Slides were washed three times for 5 min in 2xSSC, dehydrated in an ethanol series (2x 70%, 1x 96%, 2 min each) and air-dried. Labelled probe DNA (60 ng) mixed with salmon sperm (20 ng) was vacuum-dried and resuspended in 6 µl of formamide (100%) and 6 µl of hybridisation mix (4xSSC, 20% dextransulfate). The probe was denaturated at 95°C for 5 min and placed on ice for 1 min. After spinning down, it was dropped onto the slide and a coverslip was sealed with rubber cement (Fixogum, Marabuwerke GmbH, Tamm, Germany). DNA on slides was then denaturated at 80°C for 10 min, and left up to 48 hr at 37°C in a humid chamber to hybridise. Coverslip were rinsed off by incubation of slides in 2xSSC containing 50% formamide in a copling jar at 42°C. The slides were transferred to 1xSSC, 0.2xSSC, and 0.1xSSC for 5 min at 42°C. Excess liquid was drained and blocking solution (3% BSA, 0.1% Tween 20, 4xSSC) was applied for 30 min at 37°C. Digoxigenin-labelled probes were detected with rhodamine-conjugated anti-digoxigenin and biotinylated probes with FITC-conjugated streptavidin in detection solution (1% BSA, 0.1% Tween 20, 4xSSC) at

37°C for 50 min. Finally, slides were washed three times for 5 min in washing solution (4xSSC, 0.1% Tween 20) and mounted in Vectashield supplemented with DAPI (2 µg/ml).

Cytological studies were performed with a Zeiss Axioskope epifluoresscence microscope. For the quantification of RAD-51 immunofluorescence signals, images were taken using a DeltaVision setup (Applied Precision LLC, Issaquah, Wash.). Immunostained gonads were serially scanned with a scan depth of 0.2 µm using a 100x objective to generate a three-dimensional image. Stacks of images (50-60) were deconvoluted with up to 10 interations with the softWoRx software (applied Precision LLC, Issaquah, Wash.) and finally projected to generate a single image. To allow a comparable quantification of the RAD-51 foci on different immunological samples, we mathematically subtracted the background (background intensity was defined as less than 5% of the maximal intensity of RAD-51 foci) resulting in an image with distinct foci. Images were processed using Adobe Photoshop (Adobe Systems, Mountain View, Calif., USA)

8.7 Recombination analysis

Recombination frequencies in the hermaphrodite were measured by scoring the number of recombinant progeny of a *cis*-heterozygote under the conditions described by(Rose and Baillie, 1979). The recombination frequency p between two genetic markers was calculated using the formula $p = 1 - (1 - 2R)^{1/2}$, where R was the number of visible recombinant individuals divided by the total progeny number(Brenner, 1974). Since the

double homozygote class was not scored because of its reduced viability, the total progeny number was estimated by 4/3 (number of wild types + one recombinant class). In some intervals, recovery of only one recombinant class was possible and in these instances, R = 2 X (one recombinant class) divided by the total progeny number. The 95% confidence intervals were estimated using the statistics of (Crow and Gardner, 1959).

8.8 *cdc-7(RNAi)* and *rad-5(RNAi)*

PCR fragment of the *C. elegans cdc-7* (C34G6.5) with flanking T/ primers was amplified out of cDNA (home made) using the primer set "CeCDC7-T7s" 5´-TAATACGACTCACTATAGGGATGTCCATAAAATCGTCACGG and "CeCDC7-T7a" 5´ TAATACGACTCACTATAGGGTTAGAATGGATCTTGATTCGAC (underlined the sequence of T7). The ssRNA was prepared using a Promega kit (Madison, Wis.) *in vitro* transcription kit. The ssRNA was phenol/chloroform purified, incubated for 10 min at 68°C followed by an incubation at 37°C for 30 min to anneal dRNA. To get very concentrated RNA solution, the dRNA was precipitated with ethanol and dissolved in 10 µl of nuclease free water. *dRNA(cdc-7)* was delivered by injection (~ 4mg/ml) into gonads or intestines of young adults as described in (Fire et al., 1998). The dRNA for *rad-5/clk-2* was generated in the same way as for *cdc-7* using the primer set "RAD5-T7s" 5´-TAATACGACTCACTATAGGGATGAATTTACGAAGTCGCCTG and "RAD5-T7as bp1179" 5´-TAATACGACTCACTATAGGGTTGATTAACA-AAAATACCACT. 20 hrs after injection, animals were put on new plates and the offspring was analyses for embryonic lethality and developmental arrest at L1 larval stage.

8.9 4D Microscopy

The experiments were performed in the lab of Ralf Schnabel, University of Braunschweig, Germany. Wildtype*,* *rad-5(mn159)* and *clk-2(qm37)* animals were transferred as young L4´s to 25°C (restrictive temperature). After 24 hrs animals were prepared for 4D microscopy as described in (Schnabel et al., 1997)

8.10 Far Western Blot

PCR fragment encoding the full length of *C. elegans* RAD-5/CLK-2 was cloned in frame as a glutathione S-transferase (GST) fusion into pGEX-4T-1 (Amersham, Uppsala, Sweden) and *C. elegans* CDC-7 was cloned as a maltose binding protein (MBP) fusion into pMAL-2c (New England BioLabs, Beverly, Mass.). Recombinant GST-RAD-5 fusion was expressed in *E. coli* BL21 CodonPlus (Stratagene, La Jolla, Calif.), purified under native conditions (lysis buffer: 1xPBS, 5 mM DTT, 20 µg/ml DNAse,1 mg/ml lysozyme, and protease-inhibitor mix (Complete,Mini,EDTA-free, ROCHE) by affinity chromatography using Glutathione-Sepharose 4B (Amersham, Uppsala, Sweden). The GST-RAD-5, bound to the column, was cleaved off enzymatically with Thrombin (10U/ml). MBP-CDC-7 was expressed in *E. coli* BL21 CodonPlus (Stratagene, La Jolla, Calif.) Bacterial lysates were separated on a SDS-PAGE and transferred to nitrocellulose membrane according to standard techniques. Subsequently, the membrane was incubated with basic buffer (BB, 20 mM HEPES-pH7.5, 50 mM KCl, 10 mM $MgCl_2$, 1 mM

dithiothreitol and 0.1% NP40) for 10 min at 4°C followed by incubation with blocking buffer (BB plus 5% nonfat dry milk) for 4 hrs at 4°C. Recombinant RAD-5 was diluted in incubation buffer (BB plus 1% nonfat dry milk) to a final concentration of ~2nM and used to probe the membrane for 5 hrs at 4°C. Afterwards, the membrane was washed four times with 1xPBS(+0.2% Triton X100) and twice with 1xPBS (0.2% TritonX100, 100 mM KCl) and final proceeded to Western blot analysis using an polyclonal antiRAD-5 antibody (generated by Simon Boulton, Clare Hall, South Mimms, UK).

8.11 Yeast two-hybrid interaction

Standard molecular biology techniques were used for all constructs; The *S. cerevisiae* cDNA of *cdc-7* was cloned as a GAL4 DNA binding fusion and GAL4 activation domain fusion into the EcoRI/PstI sites of pGBDΩC1 (CLONTECH) and NcoI/EcoRI sites of pACT2c (CLONTECH), respectively. *tel-2* cDNA was cloned into EcoRI/BglII of pGBDΩC1 and NcoI/EcoRI of pACT2c; *C. elegans cdc-7* into XmaI/ClaI of pGBDΩC1 and NcoI/XhoI of pACT2c; *rad-5/clk-2* into XmaI/PstI of pGBDΩC1 and NcoI/XhoI of pACT2c; These constructs (in various combinations, see 7.1.4.2) were transformed in the reporter strain PJ69-4A according to the CLONTECH Laboratories yeast protocol handbook. Growth of these transformed yeast strains plated on synthetic media lacking leucine, tryptophan, and histidine or adenine with 2% glucose as the carbon source indicated a positive interaction between given constructs. (list of primer sets:

S.c. cdc-7: CDC7-BD5: 5′ TCGAATTCATGACAAGCAAAACGAAGAA

CDC7-BD3: 5′ AGACTGCAGCTATTCAGATATTAGGAGAA

CDC7-AD5: 5′ TGGCCATGGAGATGACAAGCAAAACGAAGAA

CDC7-AD3: 5′ TCGAATTCGCTATTCAGATATTAGGAGAA

S.c. tel-2: TEL2-AD5: 5′ TGGCCATGGAGATGGTTTTAGAAACGCTGAA

TEL2-AD3: 5′ TCGAATTCGCTAACCTTTATTGAGAGAAA

TEL2-BD5: 5′ CGGAATTCATGGTTTTAGAAACGCTGAA

TEL2-BD3: 5′ GAAGATCTCTAACCTTTATTGAGAGAAA

cdc-7: CeCDC7-BD5: 5′ TCCCCCGGGATGTCCATAAAATCGTCACG

CeCDC7-BD3: 5′ CCATCGATTTAGAATGGATCTTGATTCG

CeCDC7-AD5: 5′ TGGCCATGGAGATGTCCATAAAATCGTCACG

CeCDC7-AD3: 5′ CCGCTCGAGGTTAGAATGGATCTTGATTCG

rad-5: RAD5-BD5: 5′ TCCCCCGGGATGAATTTACGAAGTGGCCT

RAD5-BD3: 5′ AACTGCAGTTAAACGTCTTGGTGTTGCA

RAD5-AD5: 5′ TGGCCATGGAGATGAATTTACGAAGTCGGCT

RAD5-AD3: 5′ CCGCTCGAGGTTAAACGTCTTGGTGTTGCA)

8.12 Cell cycle profiling

Gonads are prepared like it is described in section 8.6. and propidiumiodide staining performed according the protocol in (Feng et al., 1999). Briefly, samples were fixed and permeabilised in Methanol for 30 min at –20°C followed by 30 min in acetone, -20°C and three times washing with 1x PBS at RT for 5 min. RNA was degraded by RNAse treatment (40 µg/ml in 1x PBS) for 2 hr at 37°C, followed by three washing steps (5 min with 1x PBS at RT). For the propidiumiodide staining propidiumiodide with a final

concentration of 50 µg/ml (dissolved in 1xPBS) was applied to the samples and incubate for 2 hr at RT in a humidity chamber. Samples were washed three times with 1x PBS at RT and mounted for microscopic analysis as described in 8.6. Microscopy and signal quantification was done as described in Feng et al. (Feng et al., 1999). For normalization of the DNA content we use the DNA content of the distal tip cell (or the sheet cells) with 2N and meiotic nuclei with 4N DNA content.

9. List of Publications

Ahmed S, **Alpi A**, Hengartner MO, Gartner A

C. elegans RAD-5/CLK-2 defines a new DNA damage checkpoint gene.

Curr Biol. 2001 Dec, 11, 1934-1944

Alpi A., Pasierbek P., Gartner A., Loidl J

Genetic and cytological characterisation of the recombination protein RAD-51 in *C .elegans*.

Chromosoma, 2003, Jul, 112, 6-16.

Gartner A, **Alpi A**, Schumacher B

Promgramed cell death in *C. elegans*

Genetics of Apoptosis, Grimm S (ed.), BIOS Scientific Publishers Limited, 2003, 155-175

Schumacher B, **Alpi A**, Gartner A

Cell cycle: check for asynchrony.

Curr Biol. 2003 Jul 15;13(14):R560-2.

Wunderlich W, Fialka I, Teiss D, **Alpi A**, Pfeifer A, Parton GP, Lottspeich F, Huber LA

A novel 14-kilodalton protein interacts with the mitogen-activated protein kinase scaffold MP1 on a late endosomal/lysosomal compartment.

JCB, 2001, Feb, 152,765-776

Wicky C, **Alpi A**, Passannante M, Rose A, Gartner A, Müller F

Multiple genetic pathways involving the *C. elegans* Bloom´s syndrome gene *him-6, mre-11, rad-51* and *top-3* are needed to maintain genome stability in germ line.

Submitted to MCB journal

10. Curriculum Vitae

Name: Arno Friedrich Alpi
Date and place of birth: 13 April 1973, Klagenfurt, Austria
Address: Dachauerstrasse 95/4, 80335 Munich, Germany
Telephone: 0049-89-8578-3120
e-mail: alpi@biochem.mpg.de
Academic status: PhD student
Academic title: Mag. rer. nat
Nationality: Austria
Marital status: single, no child

Scientific Education

Since May 2000: PhD thesis in the laboratory of Dr Anton Gartner, Department of Cell Biology, Max-Planck-Institute for Biochemistry, Martinsried, Germany; PhD project: "DNA damage checkpoint pathways in the nematode *C. elegans"*

February – May 2000: Guest student in the laboratory of Dr KJ Patel, MRC Laboratory of Molecular Biology, Protein and Nucleic Acid Chemistry, Cambridge, UK;

January 2000: Diploma Exam, Department of Biochemistry, University of Vienna, Austria; grade: 1.0

April 1998- September 1999: Diploma thesis at the Institute of Molecular Pathology (IMP), Supervisor Univ. Prof Dr Lukas A. Huber; topic: " Biochemical characterisation and Analysis of the compartimental association of a newly identified Golgi-associated protein", grade: 1.0

October 1991-January 2000: Studies in Chemistry/Biochemistry (including three terms in Human Medicine), University of Vienna;

Intermediate Examination (Vordiplom) in Chemistry/Biochemistry, November 1996, grade: 1.3

June 1991: Matura (University entrance qualification), grade: 2.2

Teaching activity:

Teaching assistant (Tutor) in Chemistry, winter term 1996 and summer term 1997, University of Vienna;

Meeting abstracts:

European Worm Meeting 2002, Paestum, Italy;
Arno Alpi, Pawel Pasierbek, Verena Jantsch, Josef Loidl, Anton Gartner
Poster. "Cytological characterization of RAD-51 in DNA damage response and in meiosis"

GRC on Genetic Toxicology, 2003, Oxford, UK
Arno Alpi and Anton Gartner
Poster: "RAD-5/CLK-2 maintains genome stability in the germline of *C. elegans*"

Workshop on Recombination, October 2003, GSF-Garching, Munich, Germany;
Arno Alpi, Chantal Wicky, Fritz Müller, Anton Gartner
Talk: „Recombination in *C.elegans*: RAD-51 and Bloom´s"

11. Acknowledgements

First of all I would like to thank my advisor Toni Gartner for scientific guidance and friendship. I had a very good time in his lab and it has been a fun to do science together with him. I would also like to thank Erich Nigg for support.

Furthermore, I would like to thank all my lab members, in particular Björn Schumacher, Volker Stucke, Thomas Kufer, Ingvar Ferby, Tim Holmström and Ulli Grüneberg for friendship and scientific support. Special thanks to Christoph Baumann, who became a real good friend over the last year.

I would like to thank my collaborator Shawn Ahmed, for the generation of the DNA damage checkpoint double mutants; Pawel Pasierbek and Sepp Loidl for introducing me in cytological techniques and for sharing reagents; Chantal Wicky and Fritz Müller for the fruitful teamwork on the study of *him-6/blm*, and Simon Boulton, not only for kindly providing reagents, but also for scientific discussions and technical advise. Finally, I would like to acknowledge Ingo Büsing and Ralf Schnabel, who were instrumental for the 4-D microscopic analysis of *rad-5* mutants.

12. Bibliography

Ababou,M., Dumaire,V., Lecluse,Y., and Amor-Gueret,M. (2002). Cleavage of BLM and sensitivity of Bloom's syndrome cells to hydroxurea and UV-C radiation. Cell Cycle *1*, 262-266.

Abraham,R.T. (2001). Cell cycle checkpoint signaling through the ATM and ATR kinases. Genes Dev. *15*, 2177-2196.

Adams,M.D., McVey,M., and Sekelsky,J.J. (2003). Drosophila BLM in double-strand break repair by synthesis-dependent strand annealing. Science *299*, 265-267.

Agarwal,S. and Roeder,G.S. (2000). Zip3 provides a link between recombination enzymes and synaptonemal complex proteins. Cell *102*, 245-255.

Ahmed,S., Alpi,A., Hengartner,M.O., and Gartner,A. (2001). C. elegans RAD-5/CLK-2 defines a new DNA damage checkpoint protein. Curr. Biol. *11*, 1934-1944.

Ahmed,S. and Hodgkin,J. (2000). MRT-2 checkpoint protein is required for germline immortality and telomere replication in C. elegans. Nature *403*, 159-164.

Allers,T. and Lichten,M. (2001). Differential timing and control of noncrossover and crossover recombination during meiosis. Cell *106*, 47-57.

Alpi,A., Pasierbek,P., Gartner,A., and Loidl,J. (2003). Genetic and cytological characterization of the recombination protein RAD-51 in Caenorhabditis elegans. Chromosoma *112*, 6-16.

Anderson,L.K., Offenberg,H.H., Verkuijlen,W.M., and Heyting,C. (1997). RecA-like proteins are components of early meiotic nodules in lily. Proc. Natl. Acad. Sci. U. S. A *94*, 6868-6873.

Ashley,T., Plug,A.W., Xu,J., Solari,A.J., Reddy,G., Golub,E.I., and Ward,D.C. (1995). Dynamic changes in Rad51 distribution on chromatin during meiosis in male and female vertebrates. Chromosoma *104*, 19-28.

Barlow,A.L., Benson,F.E., West,S.C., and Hulten,M.A. (1997a). Distribution of the Rad51 recombinase in human and mouse spermatocytes. EMBO J. *16*, 5207-5215.

Barlow,C., Liyanage,M., Moens,P.B., Deng,C.X., Ried,T., and Wynshaw-Boris,A. (1997b). Partial rescue of the prophase I defects of Atm-deficient mice by p53 and p21 null alleles. Nat. Genet. *17*, 462-466.

Bartek,J., Falck,J., and Lukas,J. (2001). CHK2 kinase--a busy messenger. Nat. Rev. Mol. Cell Biol. *2*, 877-886.

Benard,C., McCright,B., Zhang,Y., Felkai,S., Lakowski,B., and Hekimi,S. (2001). The C. elegans maternal-effect gene clk-2 is essential for embryonic development, encodes a protein homologous to yeast Tel2p and affects telomere length. Development *128*, 4045-4055.

Bergerat,A., de Massy,B., Gadelle,D., Varoutas,P.C., Nicolas,A., and Forterre,P. (1997). An atypical topoisomerase II from Archaea with implications for meiotic recombination. Nature *386*, 414-417.

Berry,L.W., Westlund,B., and Schedl,T. (1997). Germ-line tumor formation caused by activation of glp-1, a Caenorhabditis elegans member of the Notch family of receptors. Development *124*, 925-936.

Bishop,D.K. (1994). RecA homologs Dmc1 and Rad51 interact to form multiple nuclear complexes prior to meiotic chromosome synapsis. Cell *79*, 1081-1092.

Bishop,D.K., Park,D., Xu,L., and Kleckner,N. (1992). DMC1: a meiosis-specific yeast homolog of E. coli recA required for recombination, synaptonemal complex formation, and cell cycle progression. Cell *69*, 439-456.

Bjergbaek,L., Cobb,J.A., and Gasser,S.M. (2002). RecQ helicases and genome stability: lessons from model organisms and human disease. Swiss. Med. Wkly. *132*, 433-442.

Blumenthal,T. (1995). Trans-splicing and polycistronic transcription in Caenorhabditis elegans. Trends Genet. *11*, 132-136.

Boulton,S.J., Gartner,A., Reboul,J., Vaglio,P., Dyson,N., Hill,D.E., and Vidal,M. (2002). Combined functional genomic maps of the C. elegans DNA damage response. Science *295*, 127-131.

Bousset,K. and Diffley,J.F. (1998). The Cdc7 protein kinase is required for origin firing during S phase. Genes Dev. *12*, 480-490.

Brauchle,M., Baumer,K., and Gonczy,P. (2003). Differential activation of the DNA replication checkpoint contributes to asynchrony of cell division in C. elegans embryos. Curr. Biol. *13*, 819-827.

Brenner,S. (1974). The genetics of Caenorhabditis elegans. Genetics *77*, 71-94.

Brown,A.L., Lee,C.H., Schwarz,J.K., Mitiku,N., Piwnica-Worms,H., and Chung,J.H. (1999). A human Cds1-related kinase that functions downstream of ATM protein in the cellular response to DNA damage. Proc. Natl. Acad. Sci. U. S. A *96*, 3745-3750.

Brown,E.J. and Baltimore,D. (2000). ATR disruption leads to chromosomal fragmentation and early embryonic lethality. Genes Dev. *14*, 397-402.

Burtelow,M.A., Roos-Mattjus,P.M., Rauen,M., Babendure,J.R., and Karnitz,L.M. (2001). Reconstitution and molecular analysis of the hRad9-hHus1-hRad1 (9-1-1) DNA damage responsive checkpoint complex. J. Biol. Chem. *276*, 25903-25909.

Cao,L., Alani,E., and Kleckner,N. (1990). A pathway for generation and processing of double-strand breaks during meiotic recombination in S. cerevisiae. Cell *61*, 1089-1101.

Carney,J.P., Maser,R.S., Olivares,H., Davis,E.M., Le Beau,M., Yates,J.R., III, Hays,L., Morgan,W.F., and Petrini,J.H. (1998). The hMre11/hRad50 protein complex and Nijmegen breakage syndrome: linkage of double-strand break repair to the cellular DNA damage response. Cell *93*, 477-486.

Caspari,T., Dahlen,M., Kanter-Smoler,G., Lindsay,H.D., Hofmann,K., Papadimitriou,K., Sunnerhagen,P., and Carr,A.M. (2000a). Characterization of Schizosaccharomyces pombe Hus1: a PCNA-related protein that associates with Rad1 and Rad9. Mol. Cell Biol. *20*, 1254-1262.

Caspari,T., Davies,C., and Carr,A.M. (2000b). Analysis of the fission yeast checkpoint Rad proteins. Cold Spring Harb. Symp. Quant. Biol. *65:451-6.*, 451-456.

Caspari,T., Murray,J.M., and Carr,A.M. (2002). Cdc2-cyclin B kinase activity links Crb2 and Rqh1-topoisomerase III. Genes Dev. *16*, 1195-1208.

Cervantes,M.D., Farah,J.A., and Smith,G.R. (2000). Meiotic DNA breaks associated with recombination in S. pombe. Mol. Cell *5* , 883-888.

Chaturvedi,P., Eng,W.K., Zhu,Y., Mattern,M.R., Mishra,R., Hurle,M.R., Zhang,X., Annan,R.S., Lu,Q., Faucette,L.F., Scott,G.F., Li,X., Carr,S.A., Johnson,R.K., Winkler,J.D., and Zhou,B.B. (1999). Mammalian Chk2 is a downstream effector of the ATM-dependent DNA damage checkpoint pathway. Oncogene *18*, 4047-4054.

Chen,C.Y., Oliner,J.D., Zhan,Q., Fornace,A.J., Jr., Vogelstein,B., and Kastan,M.B. (1994). Interactions between p53 and MDM2 in a mammalian cell cycle checkpoint pathway. Proc. Natl. Acad. Sci. U. S. A *91* , 2684-2688.

Chen,F., Hersh,B.M., Conradt,B., Zhou,Z., Riemer,D., Gruenbaum,Y., and Horvitz,H.R. (2000). Translocation of C. elegans CED-4 to nuclear membranes during programmed cell death. Science *287*, 1485-1489.

Chin,G.M. and Villeneuve,A.M. (2001). C. elegans mre-11 is required for meiotic recombination and DNA repair but is dispensable for the meiotic G(2) DNA damage checkpoint. Genes Dev. *15*, 522-534.

Chua,P.R. and Roeder,G.S. (1998). Zip2, a meiosis-specific protein required for the initiation of chromosome synapsis. Cell *93*, 349-359.

Clark,D.V. and Baillie,D.L. (1992). Genetic analysis and complementation by germ-line transformation of lethal mutations in the unc-22 IV region of Caenorhabditis elegans. Mol. Gen. Genet. *232*, 97-105.

Conradt,B. and Horvitz,H.R. (1998). The C. elegans protein EGL-1 is required for programmed cell death and interacts with the Bcl-2-like protein CED-9. Cell *93*, 519-529.

Costanzo,V., Shechter,D., Lupardus,P.J., Cimprich,K.A., Gottesman,M., and Gautier,J. (2003). An ATR- and Cdc7-dependent DNA damage checkpoint that inhibits initiation of DNA replication. Mol. Cell *11*, 203-213.

D'Amours,D. and Jackson,S.P. (2001). The yeast Xrs2 complex functions in S phase checkpoint regulation. Genes Dev. *15*, 2238-2249.

D'Amours,D. and Jackson,S.P. (2002b). The Mre11 complex: at the crossroads of dna repair and checkpoint signalling. Nat. Rev. Mol. Cell Biol. *3*, 317-327.

D'Amours,D. and Jackson,S.P. (2002a). The Mre11 complex: at the crossroads of dna repair and checkpoint signalling. Nat. Rev. Mol. Cell Biol. *3*, 317-327.

Dalal,S.N., Schweitzer,C.M., Gan,J., and DeCaprio,J.A. (1999). Cytoplasmic localization of human cdc25C during interphase requires an intact 14-3-3 binding site. Mol. Cell Biol. *19*, 4465-4479.

Dasika,G.K., Lin,S.C., Zhao,S., Sung,P., Tomkinson,A., and Lee,E.Y. (1999). DNA damage-induced cell cycle checkpoints and DNA strand break repair in development and tumorigenesis. Oncogene *%20;18*, 7883-7899.

de Massy,B., Baudat,F., and Nicolas,A. (1994). Initiation of recombination in Saccharomyces cerevisiae haploid meiosis. Proc. Natl. Acad. Sci. U. S. A *91*, 11929-11933.

del Peso,L., Gonzalez,V.M., Inohara,N., Ellis,R.E., and Nunez,G. (2000). Disruption of the CED-9.CED-4 complex by EGL-1 is a critical step for programmed cell death in Caenorhabditis elegans. J. Biol. Chem. *275*, 27205-27211.

Dernburg,A.F., McDonald,K., Moulder,G., Barstead,R., Dresser,M., and Villeneuve,A.M. (1998). Meiotic recombination in C. elegans initiates by a conserved mechanism and is dispensable for homologous chromosome synapsis. Cell *94*, 387-398.

Dernburg,A.F., Zalevsky,J., Colaiacovo,M.P., and Villeneuve,A.M. (2000). Transgene-mediated cosuppression in the C. elegans germ line. Genes Dev. *14*, 1578-1583.

Dierick,H. and Bejsovec,A. (1999). Cellular mechanisms of wingless/Wnt signal transduction. Curr. Top. Dev. Biol. *43:153-90.* , 153-190.

Donaldson,A.D., Fangman,W.L., and Brewer,B.J. (1998). Cdc7 is required throughout the yeast S phase to activate replication origins. Genes Dev. *12*, 491-501.

Edgley,M.L., Baillie,D.L., Riddle,D.L., and Rose,A.M. (1995). Genetic balancers. Methods Cell Biol. *48:147-84.*, 147-184.

Edwards,R.J., Bentley,N.J., and Carr,A.M. (1999). A Rad3-Rad26 complex responds to DNA damage independently of other checkpoint proteins. Nat. Cell Biol. *1*, 393-398.

Ellis,H.M. and Horvitz,H.R. (1986). Genetic control of programmed cell death in the nematode C. elegans. Cell *44*, 817-829.

Ellis,N.A., Groden,J., Ye,T.Z., Straughen,J., Lennon,D.J., Ciocci,S., Proytcheva,M., and German,J. (1995). The Bloom's syndrome gene product is homologous to RecQ helicases. Cell *83*, 655-666.

Ellis,R.E. and Horvitz,H.R. (1991). Two C. elegans genes control the programmed deaths of specific cells in the pharynx. Development *112*, 591-603.

Ellis,R.E., Jacobson,D.M., and Horvitz,H.R. (1991). Genes required for the engulfment of cell corpses during programmed cell death in Caenorhabditis elegans. Genetics *129*, 79-94.

Encalada,S.E., Martin,P.R., Phillips,J.B., Lyczak,R., Hamill,D.R., Swan,K.A., and Bowerman,B. (2000). DNA replication defects delay cell division and disrupt cell polarity in early Caenorhabditis elegans embryos. Dev. Biol. *228*, 225-238.

Enoch,T., Carr,A., and Nurse,P. (1993). Checkpoint check. Nature *361*, 26.

Feng,H., Zhong,W., Punkosdy,G., Gu,S., Zhou,L., Seabolt,E.K., and Kipreos,E.T. (1999). CUL-2 is required for the G1-to-S-phase transition and mitotic chromosome condensation in Caenorhabditis elegans. Nat. Cell Biol. *1*, 486-492.

Feng,W. and D'Urso,G. (2001). Schizosaccharomyces pombe cells lacking the amino-terminal catalytic domains of DNA polymerase epsilon are viable but require the DNA damage checkpoint control. Mol. Cell Biol. *21*, 4495-4504.

Fire,A., Xu,S., Montgomery,M.K., Kostas,S.A., Driver,S.E., and Mello,C.C. (1998). Potent and specific genetic interference by double-stranded RNA in Caenorhabditis elegans. Nature *%19;391*, 806-811.

Franklin,A.E., McElver,J., Sunjevaric,I., Rothstein,R., Bowen,B., and Cande,W.Z. (1999). Three-dimensional microscopy of the Rad51 recombination protein during meiotic prophase. Plant Cell *11*, 809-824.

Fraser,A. and James,C. (1998). Fermenting debate: do yeast undergo apoptosis? Trends Cell Biol. *8*, 219-221.

Frei,C. and Gasser,S.M. (2000a). RecQ-like helicases: the DNA replication checkpoint connection. J. Cell Sci. *113*, 2641-2646.

Frei,C. and Gasser,S.M. (2000b). The yeast Sgs1p helicase acts upstream of Rad53p in the DNA replication checkpoint and colocalizes with Rad53p in S-phase-specific foci. Genes Dev. *14*, 81-96.

Furuse,M., Nagase,Y., Tsubouchi,H., Murakami-Murofushi,K., Shibata,T., and Ohta,K. (1998). Distinct roles of two separable in vitro activities of yeast Mre11 in mitotic and meiotic recombination. EMBO J. *17*, 6412-6425.

Gangloff,S., de Massy,B., Arthur,L., Rothstein,R., and Fabre,F. (1999). The essential role of yeast topoisomerase III in meiosis depends on recombination. EMBO J. *18*, 1701-1711.

Gangloff,S., McDonald,J.P., Bendixen,C., Arthur,L., and Rothstein,R. (1994). The yeast type I topoisomerase Top3 interacts with Sgs1, a DNA helicase homolog: a potential eukaryotic reverse gyrase. Mol. Cell Biol. *14*, 8391-8398.

Gartner,A., Milstein,S., Ahmed,S., Hodgkin,J., and Hengartner,M.O. (2000). A conserved checkpoint pathway mediates DNA damage--induced apoptosis and cell cycle arrest in C. elegans. Mol. Cell *5*, 435-443.

Gatei,M., Young,D., Cerosaletti,K.M., Desai-Mehta,A., Spring,K., Kozlov,S., Lavin,M.F., Gatti,R.A., Concannon,P., and Khanna,K. (2000). ATM-dependent phosphorylation of nibrin in response to radiation exposure. Nat. Genet. *25*, 115-119.

German,J. (1993). Bloom syndrome: a mendelian prototype of somatic mutational disease. Medicine (Baltimore) *72*, 393-406.

Gilbertson,L.A. and Stahl,F.W. (1994). Initiation of meiotic recombination is independent of interhomologue interactions. Proc. Natl. Acad. Sci. U. S. A *91*, 11934-11937.

Gonczy,P., Echeverri,C., Oegema,K., Coulson,A., Jones,S.J., Copley,R.R., Duperon,J., Oegema,J., Brehm,M., Cassin,E., Hannak,E., Kirkham,M., Pichler,S., Flohrs,K., Goessen,A., Leidel,S., Alleaume,A.M., Martin,C., Ozlu,N., Bork,P., and Hyman,A.A. (2000). Functional genomic analysis of cell division in C. elegans using RNAi of genes on chromosome III. Nature *408*, 331-336.

Gottifredi,V., Shieh,S.Y., and Prives,C. (2000). Regulation of p53 after different forms of stress and at different cell cycle stages. Cold Spring Harb. Symp. Quant. Biol. *65:483-8.*, 483-488.

Green,C.M., Erdjument-Bromage,H., Tempst,P., and Lowndes,N.F. (2000). A novel Rad24 checkpoint protein complex closely related to replication factor C. Curr. Biol. *10*, 39-42.

Greenwell,P.W., Kronmal,S.L., Porter,S.E., Gassenhuber,J., Obermaier,B., and Petes,T.D. (1995). TEL1, a gene involved in controlling telomere length in S. cerevisiae, is homologous to the human ataxia telangiectasia gene. Cell *82*, 823-829.

Grelon,M., Vezon,D., Gendrot,G., and Pelletier,G. (2001). AtSPO11-1 is necessary for efficient meiotic recombination in plants. EMBO J. *20*, 589-600.

Grenon,M., Gilbert,C., and Lowndes,N.F. (2001). Checkpoint activation in response to double-strand breaks requires the Mre11/Rad50/Xrs2 complex. Nat. Cell Biol. *3*, 844-847.

Gumienny,T.L., Lambie,E., Hartwieg,E., Horvitz,H.R., and Hengartner,M.O. (1999). Genetic control of programmed cell death in the Caenorhabditis elegans hermaphrodite germline. Development *126*, 1011-1022.

Haber,J.E. (1998). The many interfaces of Mre11. Cell *95*, 583-586.

Hall,D.H., Winfrey,V.P., Blaeuer,G., Hoffman,L.H., Furuta,T., Rose,K.L., Hobert,O., and Greenstein,D. (1999). Ultrastructural features of the adult hermaphrodite gonad of Caenorhabditis elegans: relations between the germ line and soma. Dev. Biol. *212*, 101-123.

Harmon,F.G. and Kowalczykowski,S.C. (1998). RecQ helicase, in concert with RecA and SSB proteins, initiates and disrupts DNA recombination. Genes Dev. *12*, 1134-1144.

Hartman,P.S. and Herman,R.K. (1982). Radiation-sensitive mutants of Caenorhabditis elegans. Genetics *102*, 159-178.

Hedgecock,E.M., Sulston,J.E., and Thomson,J.N. (1983). Mutations affecting programmed cell deaths in the nematode Caenorhabditis elegans. Science *220*, 1277-1279.

Hengartner,M.O., Ellis,R.E., and Horvitz,H.R. (1992). Caenorhabditis elegans gene ced-9 protects cells from programmed cell death. Nature *356*, 494-499.

Hengartner,M.O. and Horvitz,H.R. (1994a). Activation of C. elegans cell death protein CED-9 by an amino-acid substitution in a domain conserved in Bcl-2. Nature *369*, 318-320.

Hengartner,M.O. and Horvitz,H.R. (1994b). Programmed cell death in Caenorhabditis elegans. Curr. Opin. Genet. Dev. *4*, 581-586.

Hill,A.A., Hunter,C.P., Tsung,B.T., Tucker-Kellogg,G., and Brown,E.L. (2000). Genomic analysis of gene expression in C. elegans. Science *290*, 809-812.

Hirao,A., Kong,Y.Y., Matsuoka,S., Wakeham,A., Ruland,J., Yoshida,H., Liu,D., Elledge,S.J., and Mak,T.W. (2000). DNA damage-induced activation of p53 by the checkpoint kinase Chk2. Science *287*, 1824-1827.

Hofmann,E.R., Milstein,S., Boulton,S.J., Ye,M., Hofmann,J.J., Stergiou,L., Gartner,A., Vidal,M., and Hengartner,M.O. (2002). Caenorhabditis elegans HUS-1 is a DNA damage checkpoint protein required for genome stability and EGL-1-mediated apoptosis. Curr. Biol. *%19;12*, 1908-1918.

Hofmann,E.R., Milstein,S., and Hengartner,M.O. (2000). DNA-damage-induced checkpoint pathways in the nematode Caenorhabditis elegans. Cold Spring Harb. Symp. Quant. Biol. *65:467-73.*, 467-473.

Horvitz,H.R., Shaham,S., and Hengartner,M.O. (1994). The genetics of programmed cell death in the nematode Caenorhabditis elegans. Cold Spring Harb. Symp. Quant. Biol. *59:377-85.*, 377-385.

Hunter,N. and Kleckner,N. (2001). The single-end invasion: an asymmetric intermediate at the double-strand break to double-holliday junction transition of meiotic recombination. Cell *106*, 59-70.

Hwang,B.J., Ford,J.M., Hanawalt,P.C., and Chu,G. (1999). Expression of the p48 xeroderma pigmentosum gene is p53-dependent and is involved in global genomic repair. Proc. Natl. Acad. Sci. U. S. A *%19;96*, 424-428.

Jackson,A.L., Pahl,P.M., Harrison,K., Rosamond,J., and Sclafani,R.A. (1993). Cell cycle regulation of the yeast Cdc7 protein kinase by association with the Dbf4 protein. Mol. Cell Biol. *13*, 2899-2908.

Jacobson,G.K., Pinon,R., Esposito,R.E., and Esposito,M.S. (1975). Single-strand scissions of chromosomal DNA during commitment to recombination at meiosis. Proc. Natl. Acad. Sci. U. S. A *72*, 1887-1891.

Jiang,N., Benard,C.Y., Kebir,H., Shoubridge,E.A., and Hekimi,S. (2003). Human CLK2 links cell cycle progression, apoptosis, and telomere length regulation. J. Biol. Chem. *278*, 21678-21684.

Jiang,W., McDonald,D., Hope,T.J., and Hunter,T. (1999). Mammalian Cdc7-Dbf4 protein kinase complex is essential for initiation of DNA replication. EMBO J. *18*, 5703-5713.

Johnson,F.B., Lombard,D.B., Neff,N.F., Mastrangelo,M.A., Dewolf,W., Ellis,N.A., Marciniak,R.A., Yin,Y., Jaenisch,R., and Guarente,L. (2000). Association of the Bloom syndrome protein with topoisomerase IIIalpha in somatic and meiotic cells. Cancer Res. *60*, 1162-1167.

Kaneko,H., Orii,K.O., Matsui,E., Shimozawa,N., Fukao,T., Matsumoto,T., Shimamoto,A., Furuichi,Y., Hayakawa,S., Kasahara,K., and Kondo,N. (1997). BLM (the causative gene of Bloom syndrome) protein translocation into the nucleus by a nuclear localization signal. Biochem. Biophys. Res. Commun. *240*, 348-353.

Kastan,M.B., Onyekwere,O., Sidransky,D., Vogelstein,B., and Craig,R.W. (1991). Participation of p53 protein in the cellular response to DNA damage. Cancer Res. *51*, 6304-6311.

Keeney,S., Baudat,F., Angeles,M., Zhou,Z.H., Copeland,N.G., Jenkins,N.A., Manova,K., and Jasin,M. (1999). A mouse homolog of the Saccharomyces cerevisiae meiotic recombination DNA transesterase Spo11p. Genomics *61*, 170-182.

Keeney,S., Giroux,C.N., and Kleckner,N. (1997). Meiosis-specific DNA double-strand breaks are catalyzed by Spo11, a member of a widely conserved protein family. Cell *88*, 375-384.

Kelly,K.O., Dernburg,A.F., Stanfield,G.M., and Villeneuve,A.M. (2000a). Caenorhabditis elegans msh-5 is required for both normal and radiation-induced meiotic crossing over but not for completion of meiosis. Genetics *156*, 617-630.

Kelly,K.O., Dernburg,A.F., Stanfield,G.M., and Villeneuve,A.M. (2000b). Caenorhabditis elegans msh-5 is required for both normal and radiation-induced meiotic crossing over but not for completion of meiosis. Genetics *156*, 617-630.

Ketting,R.F. and Plasterk,R.H. (2000). A genetic link between co-suppression and RNA interference in C. elegans. Nature *404*, 296-298.

Kim,H.S. and Brill,S.J. (2001). Rfc4 interacts with Rpa1 and is required for both DNA replication and DNA damage checkpoints in Saccharomyces cerevisiae. Mol. Cell Biol. *21*, 3725-3737.

Kim,Y.C., Lee,J., and Koo,H.S. (2000). Functional characterization of Caenorhabditis elegans DNA topoisomerase IIIalpha. Nucleic Acids Res. *28*, 2012-2017.

Kim,Y.C., Lee,M.H., Ryu,S.S., Kim,J.H., and Koo,H.S. (2002). Coaction of DNA topoisomerase IIIalpha and a RecQ homologue during the germ-line mitosis in Caenorhabditis elegans. Genes Cells *7*, 19-27.

Kimble,J. and Hirsh,D. (1979). The postembryonic cell lineages of the hermaphrodite and male gonads in Caenorhabditis elegans. Dev. Biol. *70*, 396-417.

Kitao,S., Shimamoto,A., Goto,M., Miller,R.W., Smithson,W.A., Lindor,N.M., and Furuichi,Y. (1999). Mutations in RECQL4 cause a subset of cases of Rothmund-Thomson syndrome. Nat. Genet. *22*, 82-84.

Klein,H.L. (2001). Mutations in recombinational repair and in checkpoint control genes suppress the lethal combination of srs2Delta with other DNA repair genes in Saccharomyces cerevisiae. Genetics *157*, 557-565.

Kohara,Y. (1996). [Large scale analysis of C. elegans cDNA]. Tanpakushitsu Kakusan Koso *41*, 715-720.

Kondo,T., Matsumoto,K., and Sugimoto,K. (1999). Role of a complex containing Rad17, Mec3, and Ddc1 in the yeast DNA damage checkpoint pathway. Mol. Cell Biol. *19*, 1136-1143.

Kondo,T., Wakayama,T., Naiki,T., Matsumoto,K., and Sugimoto,K. (2001). Recruitment of Mec1 and Ddc1 checkpoint proteins to double-strand breaks through distinct mechanisms. Science *294*, 867-870.

Kota,R.S. and Runge,K.W. (1998). The yeast telomere length regulator TEL2 encodes a protein that binds to telomeric DNA. Nucleic Acids Res. *26*, 1528-1535.

Kota,R.S. and Runge,K.W. (1999). Tel2p, a regulator of yeast telomeric length in vivo, binds to single-stranded telomeric DNA in vitro. Chromosoma *108*, 278-290.

Kowalczykowski,S.C. (2000). Initiation of genetic recombination and recombination-dependent replication. Trends Biochem. Sci. *25*, 156-165.

Krause,S.A., Loupart,M.L., Vass,S., Schoenfelder,S., Harrison,S., and Heck,M.M. (2001). Loss of cell cycle checkpoint control in Drosophila Rfc4 mutants. Mol. Cell Biol. *21*, 5156-5168.

Krejci,L., Van Komen,S., Li,Y., Villemain,J., Reddy,M.S., Klein,H., Ellenberger,T., and Sung,P. (2003). DNA helicase Srs2 disrupts the Rad51 presynaptic filament. Nature *423*, 305-309.

Lakowski,B. and Hekimi,S. (1996). Determination of life-span in Caenorhabditis elegans by four clock genes. Science *272*, 1010-1013.

Laursen,L.V., Ampatzidou,E., Andersen,A.H., and Murray,J.M. (2003). Role for the fission yeast RecQ helicase in DNA repair in G2. Mol. Cell Biol. *23*, 3692-3705.

Lee,S.H. and Kim,C.H. (2002). DNA-dependent protein kinase complex: a multifunctional protein in DNA repair and damage checkpoint. Mol. Cells *13*, 159-166.

Levine,A.J. (1997). p53, the cellular gatekeeper for growth and division. Cell *88*, 323-331.

Li,P., Nijhawan,D., Budihardjo,I., Srinivasula,S.M., Ahmad,M., Alnemri,E.S., and Wang,X. (1997). Cytochrome c and dATP-dependent formation of Apaf-1/caspase-9 complex initiates an apoptotic protease cascade. Cell *91*, 479-489.

Lim,C.S., Mian,I.S., Dernburg,A.F., and Campisi,J. (2001). C. elegans clk-2, a gene that limits life span, encodes a telomere length regulator similar to yeast telomere binding protein Tel2p. Curr. Biol. *11*, 1706-1710.

Lim,D.S. and Hasty,P. (1996). A mutation in mouse rad51 results in an early embryonic lethal that is suppressed by a mutation in p53. Mol. Cell Biol. *16*, 7133-7143.

Lim,D.S., Kim,S.T., Xu,B., Maser,R.S., Lin,J., Petrini,J.H., and Kastan,M.B. (2000). ATM phosphorylates p95/nbs1 in an S-phase checkpoint pathway. Nature *404*, 613-617.

Lindsey-Boltz,L.A., Bermudez,V.P., Hurwitz,J., and Sancar,A. (2001). Purification and characterization of human DNA damage checkpoint Rad complexes. Proc. Natl. Acad. Sci. U. S. A *98*, 11236-11241.

Liu,Q., Guntuku,S., Cui,X.S., Matsuoka,S., Cortez,D., Tamai,K., Luo,G., Carattini-Rivera,S., DeMayo,F., Bradley,A., Donehower,L.A., and Elledge,S.J. (2000). Chk1 is an essential kinase that is regulated by Atr and required for the G(2)/M DNA damage checkpoint. Genes Dev. *14*, 1448-1459.

Liu,Q.A. and Hengartner,M.O. (1999). The molecular mechanism of programmed cell death in C. elegans. Ann. N. Y. Acad. Sci. *887:92-104.*, 92-104.

Loidl,J. (1990). The initiation of meiotic chromosome pairing: the cytological view. Genome *33*, 759-778.

Lowe,S.W., Schmitt,E.M., Smith,S.W., Osborne,B.A., and Jacks,T. (1993). p53 is required for radiation-induced apoptosis in mouse thymocytes. Nature *362*, 847-849.

Luo,G., Santoro,I.M., McDaniel,L.D., Nishijima,I., Mills,M., Youssoufian,H., Vogel,H., Schultz,R.A., and Bradley,A. (2000). Cancer predisposition caused by elevated mitotic recombination in Bloom mice. Nat. Genet. *26*, 424-429.

Luo,G., Yao,M.S., Bender,C.F., Mills,M., Bladl,A.R., Bradley,A., and Petrini,J.H. (1999). Disruption of mRad50 causes embryonic stem cell lethality, abnormal embryonic development, and sensitivity to ionizing radiation. Proc. Natl. Acad. Sci. U. S. A *96*, 7376-7381.

Lustig,A.J. and Petes,T.D. (1986). Identification of yeast mutants with altered telomere structure. Proc. Natl. Acad. Sci. U. S. A *83*, 1398-1402.

Lydall,D. and Weinert,T. (1997). G2/M checkpoint genes of Saccharomyces cerevisiae: further evidence for roles in DNA replication and/or repair. Mol. Gen. Genet. *256*, 638-651.

MacQueen,A.J., Colaiacovo,M.P., McDonald,K., and Villeneuve,A.M. (2002). Synapsis-dependent and -independent mechanisms stabilize homolog pairing during meiotic prophase in C. elegans. Genes Dev. *16*, 2428-2442.

MacQueen,A.J. and Villeneuve,A.M. (2001). Nuclear reorganization and homologous chromosome pairing during meiotic prophase require C. elegans chk-2. Genes Dev. *15*, 1674-1687.

Mahadevaiah,S.K., Turner,J.M., Baudat,F., Rogakou,E.P., de Boer,P., Blanco-Rodriguez,J., Jasin,M., Keeney,S., Bonner,W.M., and Burgoyne,P.S. (2001). Recombinational DNA double-strand breaks in mice precede synapsis. Nat. Genet. *27*, 271-276.

Masson,J.Y. and West,S.C. (2001). The Rad51 and Dmc1 recombinases: a non-identical twin relationship. Trends Biochem. Sci. *26*, 131-136.

Matsuoka,S., Huang,M., and Elledge,S.J. (1998). Linkage of ATM to cell cycle regulation by the Chk2 protein kinase. Science *282*, 1893-1897.

Maya,R., Balass,M., Kim,S.T., Shkedy,D., Leal,J.F., Shifman,O., Moas,M., Buschmann,T., Ronai,Z., Shiloh,Y., Kastan,M.B., Katzir,E., and Oren,M. (2001). ATM-dependent phosphorylation of Mdm2 on serine 395: role in p53 activation by DNA damage. Genes Dev. *15*, 1067-1077.

Melo,J.A., Cohen,J., and Toczyski,D.P. (2001). Two checkpoint complexes are independently recruited to sites of DNA damage in vivo. Genes Dev. *15*, 2809-2821.

Moens,P.B., Chen,D.J., Shen,Z., Kolas,N., Tarsounas,M., Heng,H.H., and Spyropoulos,B. (1997). Rad51 immunocytology in rat and mouse spermatocytes and oocytes. Chromosoma *106*, 207-215.

Moens,P.B., Freire,R., Tarsounas,M., Spyropoulos,B., and Jackson,S.P. (2000). Expression and nuclear localization of BLM, a chromosome stability protein mutated in Bloom's syndrome, suggest a role in recombination during meiotic prophase. J. Cell Sci. *113*, 663-672.

Moreau,S., Morgan,E.A., and Symington,L.S. (2001). Overlapping functions of the Saccharomyces cerevisiae Mre11, Exo1 and Rad27 nucleases in DNA metabolism. Genetics *159*, 1423-1433.

Morgan,D.O. (1995). Principles of CDK regulation. Nature *374*, 131-134.

Morozov,V., Mushegian,A.R., Koonin,E.V., and Bork,P. (1997). A putative nucleic acid-binding domain in Bloom's and Werner's syndrome helicases. Trends Biochem. Sci. *22*, 417-418.

Morrow,D.M., Tagle,D.A., Shiloh,Y., Collins,F.S., and Hieter,P. (1995). TEL1, an S. cerevisiae homolog of the human gene mutated in ataxia telangiectasia, is functionally related to the yeast checkpoint gene MEC1. Cell *82*, 831-840.

Moynahan,M.E., Chiu,J.W., Koller,B.H., and Jasin,M. (1999). Brca1 controls homology-directed DNA repair. Mol. Cell *4*, 511-518.

Naiki,T., Shimomura,T., Kondo,T., Matsumoto,K., and Sugimoto,K. (2000). Rfc5, in cooperation with rad24, controls DNA damage checkpoints throughout the cell cycle in Saccharomyces cerevisiae. Mol. Cell Biol. *20*, 5888-5896.

Nakano,K. and Vousden,K.H. (2001). PUMA, a novel proapoptotic gene, is induced by p53. Mol. Cell *7*, 683-694.

Nakayama,K., Irino,N., and Nakayama,H. (1985). The recQ gene of Escherichia coli K12: molecular cloning and isolation of insertion mutants. Mol. Gen. Genet. *200*, 266-271.

Nasmyth,K., Peters,J.M., and Uhlmann,F. (2000). Splitting the chromosome: cutting the ties that bind sister chromatids. Science *288*, 1379-1385.

Navas,T.A., Sanchez,Y., and Elledge,S.J. (1996). RAD9 and DNA polymerase epsilon form parallel sensory branches for transducing the DNA damage checkpoint signal in Saccharomyces cerevisiae. Genes Dev. *10*, 2632-2643.

Navas,T.A., Zhou,Z., and Elledge,S.J. (1995). DNA polymerase epsilon links the DNA replication machinery to the S phase checkpoint. Cell *80*, 29-39.

Nurse,P. (1997). Checkpoint pathways come of age. Cell *91*, 865-867.

O'Connell,M.J., Walworth,N.C., and Carr,A.M. (2000). The G2-phase DNA-damage checkpoint. Trends Cell Biol. *10*, 296-303.

O'Connor,L., Strasser,A., O'Reilly,L.A., Hausmann,G., Adams,J.M., Cory,S., and Huang,D.C. (1998). Bim: a novel member of the Bcl-2 family that promotes apoptosis. EMBO J. *17*, 384-395.

Ogawa,T., Yu,X., Shinohara,A., and Egelman,E.H. (1993). Similarity of the yeast RAD51 filament to the bacterial RecA filament. Science *259*, 1896-1899.

Osborn,A.J., Elledge,S.J., and Zou,L. (2002). Checking on the fork: the DNA-replication stress-response pathway. Trends Cell Biol. *12*, 509-516.

Paques,F. and Haber,J.E. (1999). Multiple pathways of recombination induced by double-strand breaks in Saccharomyces cerevisiae. Microbiol. Mol. Biol. Rev. *63*, 349-404.

Parrish,J., Metters,H., Chen,L., and Xue,D. (2000). Demonstration of the in vivo interaction of key cell death regulators by structure-based design of second-site suppressors. Proc. Natl. Acad. Sci. U. S. A *97*, 11916-11921.

Pasierbek,P., Jantsch,M., Melcher,M., Schleiffer,A., Schweizer,D., and Loidl,J. (2001). A Caenorhabditis elegans cohesion protein with functions in meiotic chromosome pairing and disjunction. Genes Dev. *15*, 1349-1360.

Paulovich,A.G., Margulies,R.U., Garvik,B.M., and Hartwell,L.H. (1997). RAD9, RAD17, and RAD24 are required for S phase regulation in Saccharomyces cerevisiae in response to DNA damage. Genetics *145*, 45-62.

Peifer,M. (1993). The product of the Drosophila segment polarity gene armadillo is part of a multi-protein complex resembling the vertebrate adherens junction. J. Cell Sci. *105*, 993-1000.

Peifer,M. (1995). Cell adhesion and signal transduction: the Armadillo connection. Trends Cell Biol. *5*, 224-229.

Peng,C.Y., Graves,P.R., Thoma,R.S., Wu,Z., Shaw,A.S., and Piwnica-Worms,H. (1997). Mitotic and G2 checkpoint control: regulation of 14-3-3 protein binding by phosphorylation of Cdc25C on serine-216. Science *277*, 1501-1505.

Plug,A.W., Xu,J., Reddy,G., Golub,E.I., and Ashley,T. (1996). Presynaptic association of Rad51 protein with selected sites in meiotic chromatin. Proc. Natl. Acad. Sci. U. S. A *93*, 5920-5924.

Rauen,M., Burtelow,M.A., Dufault,V.M., and Karnitz,L.M. (2000). The human checkpoint protein hRad17 interacts with the PCNA-like proteins hRad1, hHus1, and hRad9. J. Biol. Chem. *275*, 29767-29771.

Reinke,V., Smith,H.E., Nance,J., Wang,J., Van Doren,C., Begley,R., Jones,S.J., Davis,E.B., Scherer,S., Ward,S., and Kim,S.K. (2000). A global profile of germline gene expression in C. elegans. Mol. Cell *6* , 605-616.

Rhind,N., Baber-Furnari,B.A., Lopez-Girona,A., Boddy,M.N., Brondello,J.M., Moser,B., Shanahan,P., Blasina,A., McGowan,C., and Russell,P. (2000). DNA damage checkpoint control of mitosis in fission yeast. Cold Spring Harb. Symp. Quant. Biol. *65:353-9.*, 353-359.

Rich,T., Allen,R.L., and Wyllie,A.H. (2000). Defying death after DNA damage. Nature *407*, 777-783.

Riha,K., McKnight,T.D., Griffing,L.R., and Shippen,D.E. (2001). Living with genome instability: plant responses to telomere dysfunction. Science *291*, 1797-1800.

Rinaldo,C., Bazzicalupo,P., Ederle,S., Hilliard,M., and La Volpe,A. (2002). Roles for Caenorhabditis elegans rad-51 in meiosis and in resistance to ionizing radiation during development. Genetics *160*, 471-479.

Rinaldo,C., Ederle,S., Rocco,V., and La Volpe,A. (1998). The Caenorhabditis elegans RAD51 homolog is transcribed into two alternative mRNAs potentially encoding proteins of different sizes. Mol. Gen. Genet. *260*, 289-294.

Roeder,G.S. (1997). Meiotic chromosomes: it takes two to tango. Genes Dev. *11*, 2600-2621.

Romanienko,P.J. and Camerini-Otero,R.D. (2000). The mouse Spo11 gene is required for meiotic chromosome synapsis. Mol. Cell *6*, 975-987.

Rose,A.M. and Baillie,D.L. (1979). A mutation in Caenorhabditis elegans that increases recombination frequency more than threefold. Nature *281*, 599-600.

Runge,K.W. and Zakian,V.A. (1996). TEL2, an essential gene required for telomere length regulation and telomere position effect in Saccharomyces cerevisiae. Mol. Cell Biol. *16*, 3094-3105.

Schnabel,R., Hutter,H., Moerman,D., and Schnabel,H. (1997). Assessing normal embryogenesis in Caenorhabditis elegans using a 4D microscope: variability of development and regional specification. Dev. Biol. *184*, 234-265.

Schumacher,B., Alpi,A., and Garter,A. (2003). Cell cycle: check for asynchrony. Curr. Biol. *13*, R560-R562.

Schumacher,B., Hofmann,K., Boulton,S., and Gartner,A. (2001). The C. elegans homolog of the p53 tumor suppressor is required for DNA damage-induced apoptosis. Curr. Biol. *11*, 1722-1727.

Seydoux,G. and Schedl,T. (2001). The germline in C. elegans: origins, proliferation, and silencing. Int. Rev. Cytol. *203:139-85.*, 139-185.

Shen,J.C. and Loeb,L.A. (2000). The Werner syndrome gene: the molecular basis of RecQ helicase-deficiency diseases. Trends Genet. *16*, 213-220.

Shimada,M., Okuzaki,D., Tanaka,S., Tougan,T., Tamai,K.K., Shimoda,C., and Nojima,H. (1999). Replication factor C3 of Schizosaccharomyces pombe, a small subunit of replication factor C complex, plays a role in both replication and damage checkpoints. Mol. Biol. Cell *10*, 3991-4003.

Shinohara,A., Ogawa,H., and Ogawa,T. (1992). Rad51 protein involved in repair and recombination in S. cerevisiae is a RecA-like protein. Cell *69*, 457-470.

Sibon,O.C., Laurencon,A., Hawley,R., and Theurkauf,W.E. (1999). The Drosophila ATM homologue Mei-41 has an essential checkpoint function at the midblastula transition. Curr. Biol. *9*, 302-312.

Sibon,O.C., Stevenson,V.A., and Theurkauf,W.E. (1997). DNA-replication checkpoint control at the Drosophila midblastula transition. Nature *388*, 93-97.

Sinclair,D.A. and Guarente,L. (1997). Extrachromosomal rDNA circles--a cause of aging in yeast. Cell *91*, 1033-1042.

Smith,G.R. (1991). Conjugational recombination in E. coli: myths and mechanisms. Cell *64*, 19-27.

Stewart,E., Chapman,C.R., Al Khodairy,F., Carr,A.M., and Enoch,T. (1997). rqh1+, a fission yeast gene related to the Bloom's and Werner's syndrome genes, is required for reversible S phase arrest. EMBO J. *16*, 2682-2692.

Story,R.M., Bishop,D.K., Kleckner,N., and Steitz,T.A. (1993). Structural relationship of bacterial RecA proteins to recombination proteins from bacteriophage T4 and yeast. Science *259*, 1892-1896.

Sulston,J.E. (1983). Neuronal cell lineages in the nematode Caenorhabditis elegans. Cold Spring Harb. Symp. Quant. Biol. *48 Pt 2:443-52.*, 443-452.

Sulston,J.E. and Horvitz,H.R. (1977). Post-embryonic cell lineages of the nematode, Caenorhabditis elegans. Dev. Biol. *56*, 110-156.

Takanami,T., Sato,S., Ishihara,T., Katsura,I., Takahashi,H., and Higashitani,A. (1998). Characterization of a Caenorhabditis elegans recA-like gene Ce-rdh-1 involved in meiotic recombination. DNA Res. *5*, 373-377.

Takeda,T., Ogino,K., Matsui,E., Cho,M.K., Kumagai,H., Miyake,T., Arai,K., and Masai,H. (1999). A fission yeast gene, him1(+)/dfp1(+), encoding a regulatory subunit for Hsk1 kinase, plays essential roles in S-phase initiation as well as in S-phase checkpoint control and recovery from DNA damage. Mol. Cell Biol. *19*, 5535-5547.

Tarsounas,M., Morita,T., Pearlman,R.E., and Moens,P.B. (1999). RAD51 and DMC1 form mixed complexes associated with mouse meiotic chromosome cores and synaptonemal complexes. J. Cell Biol. *147*, 207-220.

Terasawa,M., Shinohara,A., Hotta,Y., Ogawa,H., and Ogawa,T. (1995). Localization of RecA-like recombination proteins on chromosomes of the lily at various meiotic stages. Genes Dev. *9*, 925-934.

Tercero,J.A., Longhese,M.P., and Diffley,J.F. (2003). A central role for DNA replication forks in checkpoint activation and response. Mol. Cell *11*, 1323-1336.

Tsubouchi,H. and Ogawa,H. (2000). Exo1 roles for repair of DNA double-strand breaks and meiotic crossing over in Saccharomyces cerevisiae. Mol. Biol. Cell *11*, 2221-2233.

Tsuzuki,T., Fujii,Y., Sakumi,K., Tominaga,Y., Nakao,K., Sekiguchi,M., Matsushiro,A., Yoshimura,Y., and MoritaT (1996). Targeted disruption of the Rad51 gene leads to lethality in embryonic mice. Proc. Natl. Acad. Sci. U. S. A *93*, 6236-6240.

Uetz,P., Giot,L., Cagney,G., Mansfield,T.A., Judson,R.S., Knight,J.R., Lockshon,D., Narayan,V., Srinivasan,M., Pochart,P., Qureshi-Emili,A., Li,Y., Godwin,B., Conover,D., Kalbfleisch,T., Vijayadamodar,G., Yang,M., Johnston,M., Fields,S., and Rothberg,J.M. (2000). A comprehensive analysis of protein-protein interactions in Saccharomyces cerevisiae. Nature *403*, 623-627.

Usui,T., Ogawa,H., and Petrini,J.H. (2001). A DNA damage response pathway controlled by Tel1 and the Mre11 complex. Mol. Cell *7*, 1255-1266.

van Gent,D.C., Hoeijmakers,J.H., and Kanaar,R. (2001). Chromosomal stability and the DNA double-stranded break connection. Nat. Rev. Genet. *2*, 196-206.

Venclovas,C. and Thelen,M.P. (2000). Structure-based predictions of Rad1, Rad9, Hus1 and Rad17 participation in sliding clamp and clamp-loading complexes. Nucleic Acids Res. *28*, 2481-2493.

Venkitaraman,A.R. (2002). Cancer susceptibility and the functions of BRCA1 and BRCA2. Cell *108*, 171-182.

Vennos,E.M. and James,W.D. (1995). Rothmund-Thomson syndrome. Dermatol. Clin. *13*, 143-150.

Vogelstein,B., Lane,D., and Levine,A.J. (2000). Surfing the p53 network. Nature *408*, 307-310.

Wahl,G.M., Linke,S.P., Paulson,T.G., and Huang,L.C. (1997). Maintaining genetic stability through TP53 mediated checkpoint control. Cancer Surv. *29:183-219.*, 183-219.

Wang,J.C. (2002). Cellular roles of DNA topoisomerases: a molecular perspective. Nat. Rev. Mol. Cell Biol. *3*, 430-440.

Wang,K., Gross,A., Waksman,G., and Korsmeyer,S.J. (1998). Mutagenesis of the BH3 domain of BAX identifies residues critical for dimerization and killing. Mol. Cell Biol. *18*, 6083-6089.

Wang,X.W., Tseng,A., Ellis,N.A., Spillare,E.A., Linke,S.P., Robles,A.I., Seker,H., Yang,Q., Hu,P., Beresten,S., Bemmels,N.A., Garfield,S., and Harris,C.C. (2001). Functional interaction of p53 and BLM DNA helicase in apoptosis. J. Biol. Chem. *276*, 32948-32955.

Wang,Y., Cortez,D., Yazdi,P., Neff,N., Elledge,S.J., and Qin,J. (2000). BASC, a super complex of BRCA1-associated proteins involved in the recognition and repair of aberrant DNA structures. Genes Dev. *14*, 927-939.

Watt,P.M., Hickson,I.D., Borts,R.H., and Louis,E.J. (1996). SGS1, a homologue of the Bloom's and Werner's syndrome genes, is required for maintenance of genome stability in Saccharomyces cerevisiae. Genetics *144*, 935-945.

Watt,P.M., Louis,E.J., Borts,R.H., and Hickson,I.D. (1995). Sgs1: a eukaryotic homolog of E. coli RecQ that interacts with topoisomerase II in vivo and is required for faithful chromosome segregation. Cell *81*, 253-260.

Weinert,T., Little,E., Shanks,L., Admire,A., Gardner,R., Putnam,C., Michelson,R., Nyberg,K., and Sundareshan,P. (2000). Details and concerns regarding the G2/M DNA damage checkpoint in budding yeast. Cold Spring Harb. Symp. Quant. Biol. *65:433-41.*, 433-441.

Weinreich,M. and Stillman,B. (1999). Cdc7p-Dbf4p kinase binds to chromatin during S phase and is regulated by both the APC and the RAD53 checkpoint pathway. EMBO J. *18*, 5334-5346.

Weiss,R.S., Leder,P., and Enoch,T. (2000). A conserved role for the Hus1 checkpoint protein in eukaryotic genome maintenance. Cold Spring Harb. Symp. Quant. Biol. *65:457-66.*, 457-466.

West,S.C. (2003). Molecular views of recombination proteins and their control. Nat. Rev. Mol. Cell Biol. *4*, 435-445.

Wicky,C., Villeneuve,A.M., Lauper,N., Codourey,L., Tobler,H., and Muller,F. (1996). Telomeric repeats (TTAGGC)n are sufficient for chromosome capping function in Caenorhabditis elegans. Proc. Natl. Acad. Sci. U. S. A *%20;93*, 8983-8988.

Wilson,R., Ainscough,R., Anderson,K., Baynes,C., Berks,M., Bonfield,J., Burton,J., Connell,M., Copsey,T., Cooper,J., and . (1994). 2.2 Mb of contiguous nucleotide sequence from chromosome III of C. elegans. Nature *368*, 32-38.

Wood,W.B. (1991). Evidence from reversal of handedness in C. elegans embryos for early cell interactions determining cell fates. Nature *349*, 536-538.

Wu,L., Davies,S.L., North,P.S., Goulaouic,H., Riou,J.F., Turley,H., Gatter,K.C., and Hickson,I.D. (2000). The Bloom's syndrome gene product interacts with topoisomerase III. J. Biol. Chem. *275*, 9636-9644.

Wu,L. and Hickson,I.D. (2001). RecQ helicases and topoisomerases: components of a conserved complex for the regulation of genetic recombination. Cell Mol. Life Sci. *58*, 894-901.

Wu,X. and Deng,Y. (2002). Bax and BH3-domain-only proteins in p53-mediated apoptosis. Front Biosci. *7:d151-6.*, d151-d156.

Yamagata,K., Kato,J., Shimamoto,A., Goto,M., Furuichi,Y., and Ikeda,H. (1998). Bloom's and Werner's syndrome genes suppress hyperrecombination in yeast sgs1 mutant: implication for genomic instability in human diseases. Proc. Natl. Acad. Sci. U. S. A *95*, 8733-8738.

Yamaguchi-Iwai,Y., Sonoda,E., Sasaki,M.S., Morrison,C., Haraguchi,T., Hiraoka,Y., Yamashita,Y.M., Yagi,T., Takata,M., Price,C., Kakazu,N., and Takeda,S. (1999). Mre11 is essential for the maintenance of chromosomal DNA in vertebrate cells. EMBO J. *18*, 6619-6629.

Yang,E., Zha,J., Jockel,J., Boise,L.H., Thompson,C.B., and Korsmeyer,S.J. (1995). Bad, a heterodimeric partner for Bcl-XL and Bcl-2, displaces Bax and promotes cell death. Cell *80*, 285-291.

Yang,J., Winkler,K., Yoshida,M., and Kornbluth,S. (1999). Maintenance of G2 arrest in the Xenopus oocyte: a role for 14-3-3-mediated inhibition of Cdc25 nuclear import. EMBO J. *18*, 2174-2183.

Yang,X., Chang,H.Y., and Baltimore,D. (1998). Essential role of CED-4 oligomerization in CED-3 activation and apoptosis. Science *281*, 1355-1357.

Yoon,H.J., Loo,S., and Campbell,J.L. (1993). Regulation of Saccharomyces cerevisiae CDC7 function during the cell cycle. Mol. Biol. Cell *4*, 195-208.

Yu,C.E., Oshima,J., Fu,Y.H., Wijsman,E.M., Hisama,F., Alisch,R., Matthews,S., Nakura,J., Miki,T., Ouais,S., Martin,G.M., Mulligan,J., and Schellenberg,G.D. (1996). Positional cloning of the Werner's syndrome gene. Science *272*, 258-262.

Yu,J., Zhang,L., Hwang,P.M., Kinzler,K.W., and Vogelstein,B. (2001). PUMA induces the rapid apoptosis of colorectal cancer cells. Mol. Cell *7*, 673-682.

Yuan,J. and Horvitz,H.R. (1992). The Caenorhabditis elegans cell death gene ced-4 encodes a novel protein and is expressed during the period of extensive programmed cell death. Development *116*, 309-320.

Yuan,J., Shaham,S., Ledoux,S., Ellis,H.M., and Horvitz,H.R. (1993). The C. elegans cell death gene ced-3 encodes a protein similar to mammalian interleukin-1 beta-converting enzyme. Cell *%19;75*, 641-652.

Zetka,M. and Rose,A. (1995a). The genetics of meiosis in Caenorhabditis elegans. Trends Genet. *11*, 27-31.

Zetka,M.C., Kawasaki,I., Strome,S., and Muller,F. (1999). Synapsis and chiasma formation in Caenorhabditis elegans require HIM-3, a meiotic chromosome core component that functions in chromosome segregation. Genes Dev. *13*, 2258-2270.

Zetka,M.C. and Rose,A.M. (1995b). Mutant rec-1 eliminates the meiotic pattern of crossing over in Caenorhabditis elegans. Genetics *141*, 1339-1349.

Zhao,S., Weng,Y.C., Yuan,S.S., Lin,Y.T., Hsu,H.C., Lin,S.C., Gerbino,E., Song,M.H., Zdzienicka,M.Z., Gatti,R.A., Shay,J.W., Ziv,Y., Shiloh,Y., and Lee,E.Y. (2000). Functional link between ataxia-telangiectasia and Nijmegen breakage syndrome gene products. Nature *405*, 473-477.

Zhou,B.B. and Elledge,S.J. (2000). The DNA damage response: putting checkpoints in perspective. Nature *408*, 433-439.

Zickler,D. and Kleckner,N. (1999). Meiotic chromosomes: integrating structure and function. Annu. Rev. Genet. *33:603-754.*, 603-754.

Zou,H., Henzel,W.J., Liu,X., Lutschg,A., and Wang,X. (1997). Apaf-1, a human protein homologous to C. elegans CED-4, participates in cytochrome c-dependent activation of caspase-3. Cell *90*, 405-413.